Networked control system design and parameter estimation

A Thesis Submitted to the

College of Graduate Studies and Research

in Partial Fulfillment of the Requirements

for the degree of Master of Science

in the Department of Mechanical Engineering

University of Saskatchewan

Saskatoon

By

Bo Yu

Permission to Use

In presenting this thesis in partial fulfilment of the requirements for a Postgraduate degree from the University of Saskatchewan, I agree that the Libraries of this University may make it freely available for inspection. I further agree that permission for copying of this thesis in any manner, in whole or in part, for scholarly purposes may be granted by the professor or professors who supervised my thesis work or, in their absence, by the Head of the Department or the Dean of the College in which my thesis work was done. It is understood that any copying or publication or use of this thesis or parts thereof for financial gain shall not be allowed without my written permission. It is also understood that due recognition shall be given to me and to the University of Saskatchewan in any scholarly use which may be made of any material in my thesis.

Requests for permission to copy or to make other use of material in this thesis in whole or part should be addressed to:

Head of the Department of Mechanical Engineering

57 Campus Drive

University of Saskatchewan

Saskatoon, Saskatchewan

Canada

S7N 5A9

ABSTRACT

Networked control systems (NCSs) are a kind of distributed control systems in which the data between control components are exchanged via communication networks. Because of the attractive advantages of NCSs such as reduced system wiring, low weight, and ease of system diagnosis and maintenance, the research on NCSs has received much attention in recent years. The first part (Chapter 2 – Chapter 4) of the thesis is devoted to designing new controllers for NCSs by incorporating the network-induced delays. The thesis also conducts research on filtering of multirate systems and identification of Hammerstein systems in the second part (Chapter 5 – Chapter 6).

Network-induced delays exist in both sensor-to-controller (S-C) and controller-to-actuator (C-A) links. A novel two-mode-dependent control scheme is proposed, in which the to-be-designed controller depends on both S-C and C-A delays. The resulting closed-loop system is a special jump linear system. Then, the conditions for stochastic stability are obtained in terms of a set of linear matrix inequalities (LMIs) with nonconvex constraints, which can be efficiently solved by a sequential LMI optimization algorithm. Further, the control synthesis problem for the NCSs is considered. The definitions of H_2 and H_∞ norms for the special system are first proposed. Also, the plant uncertainties are considered in the design. Finally, the robust mixed H_2/H_∞ control problem is solved under the framework of LMIs.

To compensate for both S-C and C-A delays modeled by Markov chains, the generalized predictive control method is modified to choose certain predicted future control signal as the current control effort on the actuator node, whenever the control signal is delayed. Further, stability criteria in terms of LMIs are provided to check the system stability. The proposed method is also tested on an experimental hydraulic position control system.

Multirate systems exist in many practical applications where different sampling rates co-exist in the same system. The $l_2 - l_\infty$ filtering problem for multirate systems is considered in the thesis. By using the lifting technique, the system is first transformed to a linear time-invariant one, and then the filter design is formulated as an optimization problem which can be solved by using LMI techniques.

Hammerstein model consists of a static nonlinear block followed in series by a linear dynamic system, which can find many applications in different areas. New switching sequences to handle the two-segment nonlinearities are proposed in this thesis. This leads to less parameters to be estimated and thus reduces the computational cost. Further, a stochastic gradient algorithm based on the idea of replacing the unmeasurable terms with their estimates is developed to identify the Hammerstein model with two-segment nonlinearities.

Finally, several open problems are listed as the future research directions.

ACKNOWLEDGEMENTS

My research work has been supervised by Dr. Yang Shi. I gratefully acknowledge him to give me the opportunity to study in Canada. During the work, he has continuously provided me with his inspiration, encouragement, and unwavering confidence in my abilities. He always gives me opportunities to explore myself, run beyond the boundary, and visualize the bright side of the world. I always admire his enthusiasm, profound knowledge, and engineering vision. He is an outstanding teacher and researcher, and will continue to be a role model. I personally feel so proud and fortunate to have had him as my research advisor.

Several other professors have also enriched my education and research experience. I would like to thank the committee members, Professors Richard Burton and Daniel Chen. They have provided me many useful guidelines and constructive comments for the thesis. I would like to thank Professors Madan Gupta and Fang-Xiang Wu for their help. Also, my thanks go to Doug Bitner for his assistance and help in my lab instruction and doing hydraulic experiments.

I have been privileged to have friends who have helped me during the past two years in Saskatoon. I would like to thank Xiaohui Bao, Kyle Brownell, Jing Chen, Ran Chen, Ran Cheng, Harold & Dickie Crandall, Jan Cunningham, Fengzhan Li, Minggan Li, Juan Wang, Xianhao Yu, and Qingshu Zhang. Special thanks go to Huazhen Fang, Yang Lin, and Dr. Maode Yan. Since we joined the team, we have been learning, working, "suffering", and playing together. Last, I would like to thank my girlfriend Wenwen Yi for her love and support during my life road to achieve higher and better.

I gratefully acknowledge the financial support from the Department of Mechanical Engineering, University of Saskatchewan and the Natural Sciences and Engineering Research Council of Canada (NSERC).

Finally, but most importantly, I am greatly indebted to my family which has always been my source of inspiration, support, and encouragement. I would like to thank my parents and my brother Bing Yu.

To my parents and my brother.

CONTENTS

List of Tables

LIST OF FIGURES

LIST OF ABBREVIATIONS

C-A	Controller-to-Actuator
DMC	Dynamic Matrix Control
GPC	Generalized Predictive Control
HIL	Hardware-in-the-Loop
HPCS	Hydraulic Position Control System
LQG	Linear Quadratic Gaussian
LQR	Linear Quadratic Regulator
LTI	Linear Time-Invariant
M-GPC	Modified Generalized Predictive Control
MIMO	Multiple-Input Multiple-Output
MJLS	Markovian Jump Linear System
MPC	Model Predictive Control
NCS	Networked Control System
OE	Output-Error
PRA	Product Reduction Algorithm
S-C	Sensor-to-Controller
SISO	Single-Input Single-Output
SSR	Single Slow-Rate
TCP	Transmission Control Protocol
VFF	Varying Forgetting Factor

CHAPTER 1

INTRODUCTION

1.1 Networked Control Systems

Networked control systems (NCSs) are a kind of distributed control systems in which the data between the controller node and plant node are exchanged via communication networks as shown in Figure 1.1. Different from the traditional point-to-point control systems, the defining feature of NCSs is the integration of networks into closed-loop control systems.
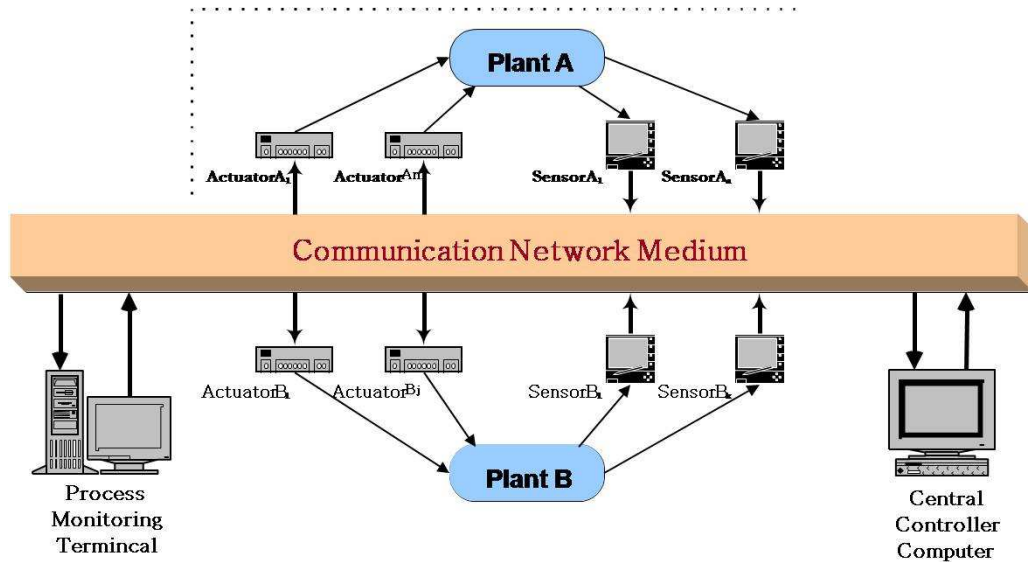
Figure 1.1: General NCS architecture.

The use of networks to connect the spatially distributed system components brings many advantages, such as reduced system wiring, low weight and space, ease of system diagnosis and maintenance, and increased system agility. Consequently, NCSs have found application in a wide range of areas, e.g., mobile sensor networks [68, 88], vehicle control [100], aircrafts [95, 113], distant learning [91], and telerehabilitation [11, 26, 96, 129], to name a few. Murray *et al.* identify "control in distributed, asynchronous, networked environments" as one of the key future directions for control [83].

However, the insertion of networks also introduces problems and presents new challenges. Tra-

ditional control theory is mainly based on the perfect data transmission, which means the system components are connected through "ideal links". However, according to the communication theory, the network is an "imperfect channel". The network characteristics make the NCSs distinct from the traditional control systems and also make the analysis, modeling, and control of NCSs more complex and challenging [54, 82]. These network characteristics include:

(1) **Time delay.** The network-induced delay [82] is the total time between the data being available at the source node (e.g., sampled from the environment or computed at the controller) and it being available at the destination node. The time delay is unavoidable under current technologies of shared digital networks and wireless connections. It depends on highly variable network conditions such as congestion and channel quality. The time delay in a network is generally time-varying. It is well-known from the control theory that the time delay can greatly degrade the performance of control systems and even cause instability. Hence, the time delay is one of the key elements determining the performance of an NCS [82].

(2) **Packet dropout.** Packet dropout is another source that degrades the control performance. Typically, packet dropouts arise from transmission errors in physical network links (which is far more common in wireless than in wired networks) or from buffer overflows due to congestion [54]. Long transmission delays sometimes result in packet re-ordering, which essentially amounts to a packet dropout if the receiver discards "outdated" arrivals. In some reliable transmission protocols, such as the transmission control protocol (TCP), when error in data transmission happens, data will be retransmitted until correct data are received. This guarantees the eventual delivery of packets. However, the re-transmission of old data is generally not very useful for NCSs. Therefore, packet dropout is an important issue that needs to be considered in NCS design.

(3) **Bandwidth limitation.** The bandwidth of an industrial network is given in terms of the number of bits that can be transmitted per second [82]. The effective bandwidth of a control network will depend not only on the physical bandwidth but also on the efficiency of encoding the data into packets (how much overhead is needed in terms of addressing and padding), how efficiently the network operates in terms of (long or short) interframe times, and whether network time is wasted due to message collisions. This imposes significant constraints on the operation of NCSs.

(4) **Sampling and quantization.** In order to transmit a continuous-time signal over a network, the signal must be sampled, encoded to a digital format, transmitted over the network, and finally the data must be decoded at the receiver side. In this process, the sampling and quantization are involved. Since the length of each data packet is finite, there must be errors between the real and quantization values. Note that, since a large portion of standard

industrial networks implement a large number of bits available to represent data, the error between the quantized value and the actual value is negligible. However, the inevitable quantization errors still have negative impact on the system performance. To study the effect of different quantization schemes on the performance of NCS can provide some guidelines on the NCS design.

The research on NCSs is interdisciplinary and lies primarily in the intersection of three research areas: Control systems, communication theories, and computer science [6]. The research of NCSs can greatly benefit from the advancement of communication theory and computer science. The main difficulty to merge the results of the three areas is the differences in emphasis in research so far. Let us take the "time delay" issue for example. In communication research, the time delay in the signal transmission is not a big issue because the accuracy is of the first importance. In contrast, for control systems, time delay is much more important than accuracy because time delay can greatly degrade the system performance and a feedback control system is robust to such inaccuracy to some extent. In computer science research, time delay is not the major issue since general computer systems are interacting with other computer systems or a human operator and not directly with the physical systems.

From the viewpoint of control systems, the time delay and packet dropout are sources that degrade the system performance. Meanwhile, the time delay in NCSs is different from the traditional constant time delay due to the hybrid, time-varying, and distributed property of NCSs. Hence, the analysis, modeling, and control of NCSs are much more complex than those of traditional control systems. Much work has been done in areas of NCSs so far. According to different aspects on the analysis and design of NCSs, the existing work can be generally divided into the following four categories: Stability analysis, state estimation, control synthesis, and control/communication co-design.

(1) **Stability analysis for NCSs.** Stability is of the principal importance in the system analysis and design. Many results have appeared in the literature to analyze the closed-loop stability in the presence of one or several NCS characteristics. In general, these approaches can be classified into two types: deterministic and stochastic [100]. Deterministic approaches assume that the network-induced delays are time-varying but bounded, and use the Lyapunov theory to determine the maximum delays [14,85,86,125–127,144], maximum rate of data loss [34,148], or minimum bit rate [70,116,118] that can be tolerated to guarantee the stability. Stochastic approaches explicitly consider the NCS characteristics in the system, and prove a version of stability such as mean square stability [80,133,136] or stochastic stability [130,147]. In [125–127], Walsh *et al.* propose the try-once-discard scheduling algorithm, then design the controller, and finally determine the maximum allowable transfer interval to maintain the exponential stability. In [148], the stability of NCSs with time delays is analyzed using

stability regions and a hybrid system technique; this method can determine whether the NCS is stable at a certain rate of data loss, and search for the highest rate of data loss for the NCS to preserve the stability. In [34], the author considers the packet dropout as a source of model uncertainty and the largest probability of packet dropout tolerable by the closed-loop system is obtained by solving the controller design problem via robust control synthesis approach. In [70, 116, 118], the authors consider the interaction between stability and bit rate constraints of the channels, and find the minimum bit rate for NCSs to be stable. In [80], the stability of model-based NCSs is considered where the time delays are varying either within a time interval or driven by a stochastic process with identically independent distribution and Markov chains; for stochastically modeled time delays, sufficient conditions for almost sure stability and mean square stability are presented. In [133], the time delays are modeled as Markov chains and further the closed-loop system is transformed to be a Markovian jump linear system (MJLS) [23, 62]; the well-established stability results for MJLSs are applied to solved the mean square stability problem for this system. In [147], the state feedback delay dependent controller is designed for NCSs with time delays governed by Markov chains and the sufficient and necessary condition to guarantee the stochastic stability is derived.

(2) **Estimation and filtering for NCSs.** In the networked environment, the data transmission suffers from time-varying delays and lossy measurements. This presents the challenges for estimation in NCSs. In [111], a jump linear estimator is designed to cope with the measurement loss process governed by Markov chains in NCSs; this method has less computational burden compared with the time-varying Kalman estimator. In [97], the authors consider the H_2 filtering problem for NCSs with packet dropouts; the generalized H_2 norm is defined considering both stochastic and deterministic inputs and the method shows better performance than classic H_2 filtering. In [115], a modified Kalman filter for NCSs is designed based on the send-on-delta method in which sensor data are transmitted only if their values change more than the specified δ value. In [89], the state estimation problem of a distributed NCS under lossy communication channels is considered. In [57], the stability of Kalman filter for NCSs with Markovian packet losses is studied; the authors give sufficient conditions for the stability of the peak covariance process in the general vector case and obtain a sufficient and necessary condition for the scalar case.

(3) **Control synthesis for NCSs.** Ample papers have been found to address the control synthesis of NCSs. So far the control synthesis results have employed linear quadratic Gaussian (LQG) method [52, 87], observer-based control to compensate for delays [87, 148], model predictive control (MPC) approach [73, 74, 117, 131], and robust H_2 and H_∞ control method [40, 41, 60, 100, 139, 143]. In [87], the time delays in NCSs are modeled as constant delays, random delays, and random delays modeled by Markov chains, respectively; the LQG

optimal controller design method is then proposed. In [52], the authors consider the optimal LQG control over packet-dropping links and by using the septation principle, the problem is decomposed into a standard linear quadratic regulator (LQR) state feedback controller design, together with an optimal encoder-decoder design for propagating and using the information across the unreliable links. In [73, 74], a novel observer-based predictive controller is provided. The system design is considered with only the controller-to-actuator (C-A) time delays in [74] and with both sensor-to-controller (S-C) and controller-to-actuator delays in [73]; the stability analysis is addressed in both papers via a switched system approach. In [117], the authors extend the generalized predictive control (GPC) to compensate for the delays, and propose an adaptive predictive control with variable prediction horizons; however, no stability is considered. In [60], the author proposes a periodic communication scheme, based on which, the H_∞ control problem is solved via a switched system approach for NCSs with limited communication and packet loss. In [100], Seiler *et al.* consider the Bernoulli packet dropout only in the S-C link and solved the H_∞ control problem for this specific NCSs based on the Bounded Real Lemma in [99]. In [139], the random delays are modeled as a linear function of the stochastic variable satisfying Bernoulli random binary distribution, and an observer-based controller is designed to guarantee the H_∞ performance. In [143], the authors consider the design of robust H_∞ controllers for uncertain NCSs with the effects of both the network-induced delay and data dropout. In [41], a new time delay model is proposed, which contains multiple successive delay components in the state; this results from the observation that sometimes in practical situations, signals transmitted from one point to another may experience several network segments; further, a sampled-data networked control system considering network induced delays, data packet dropouts, and measurement quantization is modeled as a nonlinear time delay system and the problem of network-based H_∞ control is solved accordingly. In [40], the sampled-data output tracking problem for NCSs is considered; the network-induced delays are assumed to have both an upper bound and a lower bound and the design method guarantees that the output of the closed-loop networked control system tracks the output of a given reference model well in the H_∞ sense.

(4) **Control/communication co-design.** The control and communication co-design is a new research area first appearing in [10]. In the co-design approach, network issues such as time delay, packet dropout, and bandwidth limitation will be considered simultaneously with control system issues such as stability and control performance. Generally, the network scheduling in NCSs is to assign a transmission schedule to each transmission entity (sensor, controller, actuator) based on a scheduling algorithm (a set of rules that, at any time, determine the order in which messages are transmitted). In the past, control system design and network scheduling design have normally been separated. This separation has allowed the control community to

focus on its own problem domain without worrying about how scheduling is being done; it has released the scheduling community from the need to understand what impact scheduling has on the stability and performance of the plant under control. How to seamlessly integrate the control and communications into the NCS design is promising yet challenging. Several papers have been devoted to the control/communication co-design [9, 16, 132, 145]. In [16], a control server model is proposed, which is especially suitable for co-design of real-time control systems; in this model, the task utilization factor links the scheduling design and the controller design. In [132], the authors give a survey on control/scheduling co-design from a perspective of integrating control and computing. In [145], the communication and control co-design for NCSs is considered; the authors propose a method for exponentially stabilizing an NCS by first identifying a pair of communication sequences that preserve reachability and observability, and then designing an observer-based feedback controller based on these sequences.

Although a wide variety of recent papers on NCSs have been reviewed, there are still some works which have not been included because of the multidisciplinary property and fast development of research in the area. Before wrapping up this NCS literature review section, the following table is provided to classify the reviewed papers into different categories.

Table 1.1: Classification of some important work on NCSs

	Stability	Estimation	Control Performance	Co-design
Time Delay	$[14, 80, 85, 86, 127]$ $[133, 144, 147, 148]$	$[98]$	$[73, 74, 87, 117]$	$[9, 10, 16,$ $132, 145]$
Packet Dropouts	$[34, 130, 148]$	$[57, 89, 97, 111]$	$[34, 52, 60, 100, 143]$	
Quantization	$[81]$	$[39]$	$[40]$	
Scheduling	$[85, 86, 127]$	$[115]$	$[151]$	

1.2   Filtering for Multirate Systems

When several sampling and updating rates co-exist in a system, the system is called a multirate system. Multirate systems are common in chemical [51, 77], mechanical [63, 140], aeronautic [37], and communication [108] applications. In [21], the authors state several reasons to use a multirate sampling scheme in traditional digital control systems, which are summarized as follows.

(1) In complex and multivariable control systems, it is unrealistic, or sometime impossible to sample all physical signals uniformly at one single rate. In this situation, multirate sampling is a must.

(2) In general, better performance can be achieved if one can sample and hold faster. But faster A/D and D/A conversions usually mean higher cost in implementation. Hence, better trade-off between performance and implementation cost can be obtained using A/D and D/A converters at different rates.

(3) Generally, multirate controllers are time-varying. Multirate control systems can achieve what single-rate systems cannot; for example, gain margin improvement, simultaneous stabilization, and decentralized control [21].

(4) Although multirate controllers are normally more complex than single-rate ones, they are periodic in a certain sense and hence can be implemented on microprocessor like the single-rate controllers.

In a networked environment, there are new motivations to employ the multirate sampling scheme.

(5) An NCS may have many sensors, plant, and controller distributed in different places. This increases the difficulty to use the single-rate sampling method.

(6) In NCSs, faster sampling means more data to be transmitted through the shared network. This may result in longer time delay and higher rate of packet dropout, and thus degrade the system performance. In this case, an alternative can be the multirate sampling scheme.

The study of multirate systems has attracted much attention since the late 1950's. In the literature, a majority of papers consider the control problems of multirate systems, e.g., the LQG design, robust H_2 and H_∞ control, adaptive control, model predictive control, sliding mode control, and sampled-data control $[7, 21, 35, 61, 79]$. On the other hand, the filtering of multirate system has received relatively less attention $[2, 18, 67, 101, 102]$.

The problem of filtering and estimation deals with recovering some desired state variables (or a linear combination of states) of a dynamic system from available measurements. For single-rate systems, the filtering problem has been extensively studied, see, e.g., $[42, 46, 50, 93, 135]$ and the references therein. One of the most famous filtering technique is the celebrated Kalman filter, which minimizes the error variance in the state estimation when the power spectral density of the process and the measurement noise is known [109]. The Kalman filtering techniques have found a wide variety of applications in aerospace guidance, navigation, and control problems [109]. However, in some applications, the power spectral density information is not precisely known. In this case, the Kalman filter is not applicable. Filters based on alternative performance criteria have been developed and attracted much attention in the past several decades. One of these is the H_2 filtering which minimizes the H_2 norm of the transfer function from the process noise to the estimation error $[43, 92]$. Another is the H_∞ filtering which minimizes the H_∞ norm of the transfer function from the process noise to the estimation error $[43, 50, 93, 138]$. The objective of $l_2 - l_\infty$

filtering is to design stable filters minimizing the peak value of the estimation error for all possible energy bounded disturbance, therefore it is also called energy-to-peak filtering. The $l_2 - l_\infty$ filtering design problems for single-rate systems have been studied in [42, 50, 154].

The extension of Kalman, H_2, and H_∞ filtering to multirate system has been studied [2, 18, 67, 101, 102]. In [2], the optimal and suboptimal multirate filtering algorithms using two decomposed Kalman filters are presented. In [18], the multirate Kalman synthesis filtering approach is presented for the optimal signal reconstruction problems. In [67], the authors consider the multirate optimal state estimation problems; two cases are investigated: faster output sampling and faster input sampling. Recently, Sheng *et al.* extend the H_2 and H_∞ design methods to multirate systems [101, 102]. In [102], the ratio of sampling rates between faster state and slower output is assumed to be an integer and the observer has the standard form. In [101], a more general case is considered where the ratio of sampling time of output and state is m/n with m and n being coprime integers. However, the $l_2 - l_\infty$ filtering for multirate systems has not been fully investigated in the literature, which is part of the research in this thesis.

1.3 Identification of Hammerstein Systems

The Hammerstein model consists of a static nonlinear block followed in series by a linear dynamic system shown in Figure 1.2, where $u(t)$ is the input, $\bar{u}(t)$ is the output of the nonlinear part, $x(t)$ is the noise-free output, $v(t)$ is the disturbance signal, and $y(t)$ is the output. The Hammer-
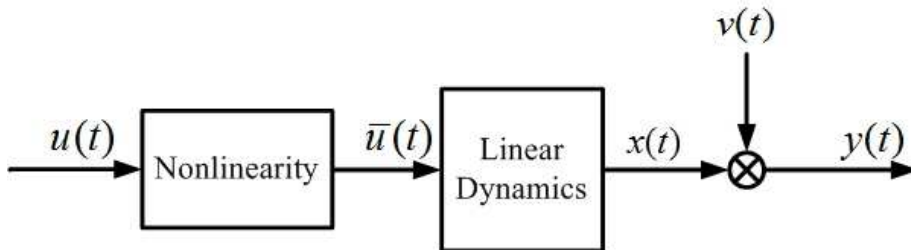
Figure 1.2: Hammerstein model.

stein system has many engineering applications, e.g., power systems [1], chemical processing [36], communication systems [38], biomedical engineering [114], and hydraulic systems [155], to name a few. Therefore, the identification of Hammerstein systems has been active in the area of system identification [4, 29, 33, 49, 58]. The difficulty for identification of Hammerstein system is that the output of nonlinearity $\bar{u}(t)$ and the noise-free output $x(t)$ are usually unknown. Recently, iterative and recursive identification algorithms for Hammerstein systems based on the idea of replacing unmeasurable noise terms in information vectors by their estimates have been presented and the convergence properties are also addressed [28, 29, 32]. In [106], the authors develop a stochastic gradient based identification algorithm by replacing the unknown variable with its estimate.

Many nonlinear characteristics can be approximated by polynomials over a restricted range in industrial applications. A large portion of existing literatures in Hammerstein modeling assume that the nonlinear function is analytic and can be represented by a single polynomial form. However, the single polynomial approximation may be inappropriate for the whole operating range of nonlinear systems. The two-segment nonlinearity, commonly existing in many physical systems, possesses significantly different characteristics for positive and negative inputs. Two-segment nonlinearity is more complex than the single polynomial nonlinearity. In the existing work, the method to handle the two-segment nonlinearity is to introduce the appropriate switching sequences to transform the two-segment nonlinearity into the single polynomial form. This approach has been used in parameter identification and adaptive control [66, 120]. However, this type of switching sequence may result in some redundance of parameters in the identification, especially when the degrees of the polynomials for positive and negative parts differ a lot. The method to handle the identification problem of Hammerstein systems with two-segment nonlinearities can be further improved, which is part of the research in this thesis.

1.4   Motivation and Objectives

The motivation and objectives of this thesis are listed in the following:

- In the literature, most controllers for NCSs are either one-mode-dependent (the controller only depends on S-C delays) or mode-independent (the controller does not depend on either S-C or C-A delays). Only few papers consider the two-mode-dependent controller design (the controller depends on both S-C and C-A delays) [56, 147]. However, in the general NCSs shown in Figure 1.3, the important fact that the C-A delay information cannot be immediately obtained at the controller node in practice is ignored in [56, 147]. Furthermore, once the full state information is not available, the state feedback controllers in [56, 147] are not applicable. Motivated by above observations, one objective of this thesis is to design an output feedback two-mode-dependent controller, which moves a further step towards applications. Both the stabilization and control synthesis problems are considered.

- How to compensate for the network-induced delay is a challenging issue for NCS design. A natural idea is to employ a predicted signal (if available) to replace the delayed one. MPC, a widely applied advanced control scheme in industry, does have the prediction feature. At each time step, the MPC not only creates the current control signal but also a sequence of future control signals. This sequence of future control actions can be used to compensate for the time delay in NCSs. To design a modified generalized predictive control method for NCSs with random time delays in both S-C and C-A links is another objective of this thesis.
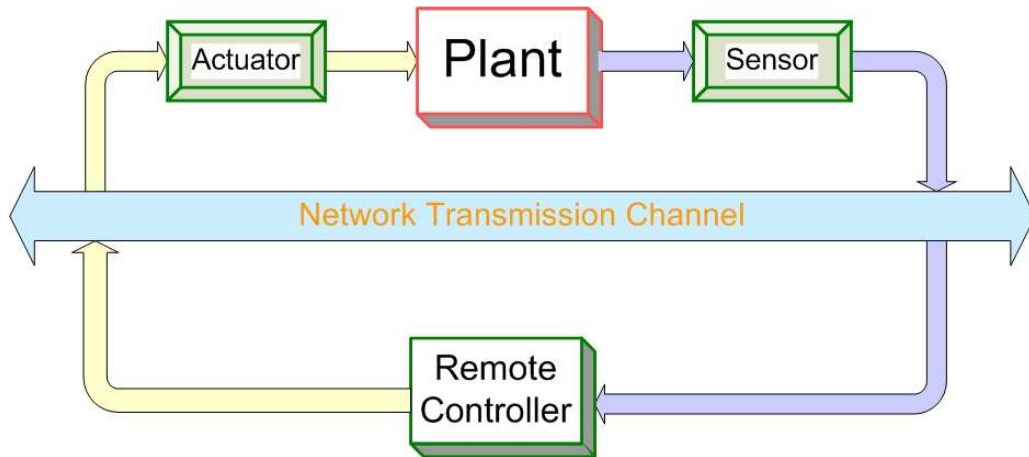
Figure 1.3: General diagram of a networked control system.

- The $l_2 - l_\infty$ filtering minimizes the energy to peak gain from the external input to the filtering error. The extension of $l_2 - l_\infty$ filtering to multirate systems is still open and need further investigation. This thesis aims to design the $l_2 - l_\infty$ filters for multirate systems.

- The existing switching sequences [120] to handle two-segment nonlinearities result in redundance in the identification of Hammerstein models. This thesis aims to propose a method to reduce the number of parameters to be estimated, and further to extend the identification method in [106] to identify the Hammerstein model with two-segment nonlinearity.

1.5   Organization of the Thesis

In Chapter 2, the the output feedback stabilization problem of NCSs is investigated. The S-C and C-A random network-induced delays are modeled as Markov chains. The focus is on the design of a two-mode-dependent controller that depends on not only the current S-C delay but also the most recent received C-A delay at the controller node. The resulting closed-loop system is transformed to a special discrete-time jump linear system. Further, the sufficient and necessary conditions for the stochastic stability are established, which can be solved by the iterative linear matrix inequality (LMI) approach.

In Chapter 3, the controller design problem in Chapter 2 is further studied to include the control performance in the design. Meanwhile, the uncertainties of the plant is assumed to be norm-bounded. The definitions of the H_2 and H_∞ norms for this special system are proposed. An optimization formulation for the robust mixed H_2/H_∞ control problem is developed, which can be solved using LMIs.

Chapter 4 is concerned with the design of the NCSs using the modified generalized predictive control (M-GPC) method. Both S-C and C-A network-induced time delays are modeled by two

Markov chains. The M-GPC uses the available output and previously predicted control information at the controller node to obtain the future control sequences. Different from the conventional generalized predictive control in which only the first element in control sequences is used, the M-GPC employs the whole control sequences to compensate for the S-C and C-A network-induced time delays. The closed-loop system is further formulated as a special jump linear system. The sufficient and necessary conditions to guarantee the stochastic stability are derived. Simulation studies and experimental tests for an experimental hydraulic position control system (HPCS) are given to verify the effectiveness of the proposed method.

In Chapter 5, the $l_2 - l_\infty$ filtering problem for multirate sampled-data systems where the output sampling rate is slower than the input updating rate is investigated based on the lifted model. The filtering problem is formulated to a set of LMIs with a nonconvex constraint, which is numerically solved by the product reduction algorithm. Compared with the slow single-rate filtering, the proposed method shows great improvement in performance.

In Chapter 6, a stochastic gradient identification algorithm for Hammerstein output-error systems with two-segment polynomial nonlinearities is provided. To reduce the number of parameters to be estimated, new switching sequences are proposed to handle the two-segment nonlinearities. Convergence analysis of the proposed algorithm is carried out under the stochastic framework. A varying forgetting factor scheme is further proposed to make a tradeoff between the convergence rate and estimation accuracy.

The last chapter summarizes the work in this thesis, and outlines some possible future research directions.

Chapter 2

Output Feedback Stabilization of Networked Control Systems with Random Delays Modeled by Markov Chains

2.1 Introduction

Networked control systems (NCSs) are a type of distributed control systems, where the information of control system components (reference input, plant output, control input, etc.) is exchanged via communication networks. Due to the introduction of networks, NCSs have many attractive advantages, such as reduced system wiring, low weight and space, ease of system diagnosis and maintenance, and increased system agility, which motivated the research in NCSs. On the other hand, the introduction of networks also presents some challenges such as time delays and packet dropouts due to the sharing and competition of the transmission medium which bring difficulties for analysis and design for NCSs. The study of NCSs has been an active research area in the past several years, see [55, 69, 78, 87, 119, 127, 128, 148], to name a few.

One of the challenges is the network-induced time delays, which can degrade the performance of systems or even cause instability. Various methodologies have been proposed for modeling, stability analysis, and controller design for NCSs in the presence of network-induced time delays and/or packet dropouts. Generally, existing results can be classified into two main categories: (1) To design a controller first, and then determine the network conditions such as the maximum allowable transfer interval to still guarantee the stability and maintain certain performance [14, 144, 148]; (2) to explicitly incorporate the network-induced delays using certain models, e.g., Markov process, into the controller design [56, 87, 100, 130, 133, 136, 139, 147]. The method developed in this chapter belongs to the latter.

The Markov chain is a discrete-time stochastic process with the Markov property, which can be effectively used to model the network-induced delays in NCSs. In [87], the time delays of NCSs are modeled as Markov chains, validated by experiments, and further an LQG optimal controller design method is proposed. Xiao *et al.* [133] propose two types of controller design methods for

NCSs modeled as finite-dimensional, discrete-time jump linear systems: One is the state feedback controller that only depends on the delays from sensor to controller (S-C delays), and is called the one-mode-dependent controller; the other is the static output feedback controller that does not depend on either the S-C delays or the C-A delays (delays from controller to actuator), and called the mode-independent one. In [100], H_∞ control for NCSs is investigated under the framework of Markovian jump linear systems (MJLSs) [23,62,103,104] based on the Bounded Real Lemma in [99]; but only the S-C delays, modeled as Markov chains, are considered. In [136], a mode-independent state feedback controller is designed for NCSs subject to Markovian packet loss process. In [130], the Markov chain is employed to model the packet loss and a one-mode-dependent state feedback controller is developed; the authors introduce buffers to the NCS, and avoid making the controller dependent on the C-A delays.

In all the aforementioned references, the developed controllers are either mode-independent or one-mode-dependent, and the design problem can thus be readily converted into the standard MJLS problem [23, 62, 103, 104]. To reduce the conservativeness of the stabilization conditions of an NCS, it is desirable to incorporate not only the S-C delay but also the C-A delay into the design. However, involving the C-A delay is complicated and challenging because the controller and actuator nodes are distributively located. Smart sensor technology [55], by adding a cost-effective embedded processor to the actuator node (Figure 2.1), can process and calculate the C-A delay in real-time at the actuator node, and send this information to the controller node via the S-C communication medium, also being subject to the S-C delay as measured signals transmitted from the sensor to the controller node. Zhang *et al.* [147] propose a promising two-mode-dependent state feedback control scheme to stabilize NCSs with the S-C and C-A delays modeled as two Markov chains. In [147], it is assumed that at each sampling time, the current S-C delay (τ_k) and previous C-A delay (d_{k-1}) are obtained by the time-stamping technique. However, practically the previous C-A delay (d_{k-1}) is not always available because the information about C-A delays needs to be transmitted through the S-C communication link before reaching the controller, as shown in a general setup of NCSs – see Figure 2.1. In addition, when the full state information is not available, the state feedback controller in [147] cannot be directly applied. To the best of author's knowledge, involving two network-induced delay modes to design the controller that simultaneously depends on both τ_k and $d_{k-\tau_k-1}$ has not been fully investigated, which is the focus of this chapter. It is worth noting that by incorporating both τ_k and $d_{k-\tau_k-1}$ into the controller design, the resulting closed-loop system cannot be transformed to a standard MJLS, and thus the well-developed results on MJLS [23, 62, 103, 104] cannot be directly applied in this chapter.

The rest of this chapter is organized in the following way. In Section 2.2, the available delay information at the controller node is analyzed and the formulation of the output feedback controller design problem is provided. In Section 2.3, the sufficient and necessary conditions to guarantee the

stochastic stability are presented first and the equivalent linear matrix inequality (LMI) conditions with constraints are derived which can be solved by the product reduction algorithm (PRA). A design example is given to illustrate the effectiveness of the proposed method in Section 2.4. The conclusion remarks are addressed in Section 2.5.

2.2 Problem Formulation

Consider the NCS setup in Figure 2.1. The discrete-time linear time-invariant plant model is

$$
\begin{align}
x(k+1) &= Ax(k) + Bu(k), \tag{2.1a}\\
y(k) &= Cx(k), \tag{2.1b}
\end{align}
$$

where $x(k) \in \mathbb{R}^n$, $u(k) \in \mathbb{R}^m$, $y(k) \in \mathbb{R}^p$, and A, B, and C are known real matrices with appropriate dimensions. Bounded random delays exist in the links from sensor to controller and controller to actuator as shown in Figure 2.1. Here, $\tau \geq \tau_k \geq 0$ represents the S-C delay and $d \geq d_k \geq 0$ stands for the C-A delay. The output feedback controller is to be designed.
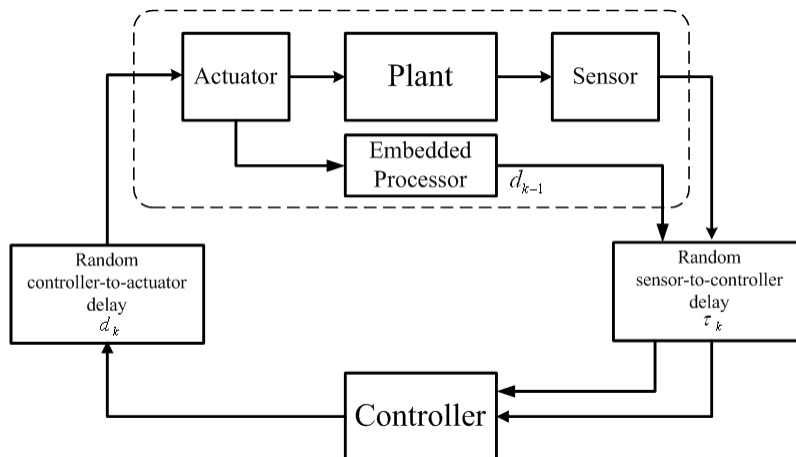
Figure 2.1: Diagram of a networked control system.

One way to model the delays τ_k and d_k is to use the finite state Markov chain as in [87,133,147]. The main advantages of the Markov model are: 1) The dependencies between delays are taken into account as in real networks the current time delays are usually related with the previous delays [87]; and 2) the packet dropout can be included naturally [133]. In this chapter, τ_k and d_k are modeled as two homogeneous Markov chains that take values in $\mathcal{M} = \{0, 1, ..., \tau\}$ and $\mathcal{N} = \{0, 1, ..., d\}$, and their transition probability matrices are $\Lambda = [\lambda_{ij}]$ and $\Pi = [\pi_{rs}]$, respectively. That means τ_k and d_k jump from mode i to j and from mode r to s, respectively, with probabilities λ_{ij} and π_{rs}, which are defined by

$$
\lambda_{ij} = \mathrm{Pr}(\tau_{k+1} = j | \tau_k = i), \quad \pi_{rs} = \mathrm{Pr}(d_{k+1} = s | d_k = r)
$$

14

with the constraints $\lambda_{ij}, \pi_{rs} \geq 0$ and

$$\sum_{j=0}^{\tau} \lambda_{ij} = 1, \quad \sum_{s=0}^{d} \pi_{rs} = 1$$

for all $i, j \in \mathcal{M}$ and $r, s \in \mathcal{N}$.

In NCSs, the delay information is important for controller design. It is noticed that at time instant k and at the controller node, τ_k can be obtained by comparing the current time and the time-stamp of the sensor information received. Similarly, at the actuator node, the embedded processor can compare the current time with the timestamp of the control signal received to calculate the C-A delay information d_{k-1} at current time k; however, this information cannot be received by the controller immediately, because it needs to be transmitted through the network from sensor to controller. So if the time delay τ_k exists, the value of $d_{k-\tau_k-1}$ at time instant k would be known at the controller node. Specially, if $\tau_k = 0$, d_{k-1} is available at the controller node. Consequently, it is desirable to design the output feedback controller that simultaneously depends on both τ_k and $d_{k-\tau_k-1}$. The dynamic output feedback control law is given by

$$
\begin{aligned}
z(k+1) &= F(\tau_k, d_{k-\tau_k-1})z(k) + G(\tau_k, d_{k-\tau_k-1})y(k-\tau_k), & \text{(2.2a)} \\
u(k) &= Hz(k) + Jy(k-\tau_k), & \text{(2.2b)}
\end{aligned}
$$

where $z(k) \in \mathbb{R}^n$ is the state vector of the output feedback controller; and $F(\tau_k, d_{k-\tau_k-1})$, $G(\tau_k, d_{k-\tau_k-1})$, H, and J are appropriately dimensioned matrices to be designed. It is worth noting that the controller (2.2) is two-mode-dependent.

Furthermore, the closed-loop system combining (2.1) and (2.2) can be expressed as

$$
\begin{aligned}
x(k+1) &= Ax(k) + BHz(k-d_k) + BJCx(k-\tau_k-d_k), & \text{(2.3a)} \\
z(k+1) &= F(\tau_k, d_{k-\tau_k-1})z(k) + G(\tau_k, d_{k-\tau_k-1})Cx(k-\tau_k). & \text{(2.3b)}
\end{aligned}
$$

At sampling time k, if augmenting the state variable as

$$
X(k) = \begin{bmatrix} x(k)^\mathrm{T} & x(k-1)^\mathrm{T} & \cdots & x(k-\tau-d)^\mathrm{T} & z(k)^\mathrm{T} & z(k-1)^\mathrm{T} & \cdots & z(k-d)^\mathrm{T} \end{bmatrix}^\mathrm{T},
$$

the closed-loop system can be rewritten in a concise form

$$
X(k+1) = \left[\tilde{A} + \tilde{I}_1 F(\tau_k, d_{k-\tau_k-1})\tilde{I}_1^\mathrm{T} + \tilde{B}H\tilde{E}_1(d_k) + \tilde{B}J\tilde{E}_2(\tau_k, d_k) + \tilde{I}_1 G(\tau_k, d_{k-\tau_k-1})\tilde{E}_3(\tau_k) \right] X(k),
$$
$$\text{(2.4)}$$

15

where

$$\tilde{A} = \begin{bmatrix} A & 0 & \cdots & 0 & 0 & 0 & \cdots & 0 \\ I & 0 & \cdots & 0 & 0 & 0 & \cdots & 0 \\ \vdots & \ddots & \cdots & 0 & 0 & 0 & \cdots & 0 \\ 0 & 0 & \cdots & I & 0 & 0 & \cdots & 0 \\ 0 & 0 & \cdots & 0 & 0 & 0 & \cdots & 0 \\ 0 & 0 & \cdots & 0 & 0 & I & \cdots & 0 \\ \vdots & 0 & \cdots & 0 & 0 & 0 & \ddots & 0 \\ 0 & 0 & \cdots & 0 & 0 & 0 & \cdots & 0 \end{bmatrix} \in \mathbb{R}^{(\tau+2d+2)n \times (\tau+2d+2)n}, \quad \tilde{B} = \begin{bmatrix} B \\ 0 \\ \vdots \\ 0 \\ 0 \\ 0 \\ \vdots \\ 0 \end{bmatrix} \in \mathbb{R}^{(\tau+2d+2)n \times m},$$

$$\tilde{I}_1 = \underbrace{\begin{bmatrix} 0 & \cdots & 0 & I & \cdots & 0 \end{bmatrix}}_{(1+\tau+d+1)th\ block\ being\ identity}^{\mathrm{T}} \in \mathbb{R}^{(\tau+2d+2)n \times n},$$

$$\tilde{E}_1(d_k) = \underbrace{\begin{bmatrix} 0 & \cdots & 0 & I & \cdots & 0 \end{bmatrix}}_{(1+\tau+d+1+d_k)th\ block\ being\ identity} \in \mathbb{R}^{n \times (\tau+2d+2)n},$$

$$\tilde{E}_2(\tau_k, d_k) = C E_2(\tau_k, d_k),$$

$$\tilde{E}_3(\tau_k) = C E_3(\tau_k),$$

$$E_2(\tau_k, d_k) = \underbrace{\begin{bmatrix} 0 & \cdots & 0 & I & \cdots & 0 \end{bmatrix}}_{(1+\tau_k+d_k)th\ block\ being\ identity} \in \mathbb{R}^{n \times (\tau+2d+2)n},$$

$$E_3(\tau_k) = \underbrace{\begin{bmatrix} 0 & \cdots & 0 & I & \cdots & 0 \end{bmatrix}}_{(1+\tau_k)th\ block\ being\ identity} \in \mathbb{R}^{n \times (\tau+2d+2)n}.$$

Remark 2.1. By applying the proposed two-mode-dependent controller (2.2), the resulting closed-loop system (2.4) cannot be transformed to a standard MJLS, because the closed-loop system depends on τ_k, d_k, and $d_{k-\tau_k-1}$, and $d_{k-\tau_k-1}$ is related with both τ_k and d_k. This makes the analysis and design more difficult and has not been investigated in literature.

The objective of this chapter is to design the output feedback controller to guarantee the stochastic stability of NCS in (2.4). For stochastic stability, the definition in [147] is adopted here. In the following, $\mathcal{E}(\cdot)$ stands for the mathematical expectation operator.

Definition 2.1. The system in (2.4) is stochastically stable if for every finite $X_0 = X(0)$, initial mode $\tau_0 = \tau(0) \in \mathcal{M}$, and $d_{-\tau_0-1} = d(-\tau_0 - 1) \in \mathcal{N}$, there exists a finite $W > 0$ such that the following holds:

$$\mathcal{E}\left\{ \sum_{k=0}^{\infty} \|X(k)\|^2 |_{X_0, \tau_0, d_{-\tau_0-1}} \right\} < X_0^{\mathrm{T}} W X_0. \tag{2.5}$$

2.3 Main Results

In this section, the sufficient and necessary conditions for output feedback stabilization of system (2.4) are first given, and then the equivalent conditions in terms of LMIs with nonconvex constraints are derived.

As $d_{k-\tau_k-1}$ is to be incorporated into the controller design, a natural question is: What is the transition probability matrix for the multi-step delay mode jump? This is of great importance for the derivation of sufficient and necessary conditions for output feedback controllers later. To answer this, Proposition 2.1 is given as follows.

Proposition 2.1. If the transition probability matrix from d_{k-1} to d_k is Π, then the transition probability matrix from $d_{k-\tau_{k+1}}$ to d_k is $\Pi^{\tau_{k+1}}$, which is still a transition probability matrix of Markov chain. Specially, when $\tau_{k+1} = 0$, the transition probability matrix is $\Pi^{\tau_{k+1}} = \Pi^0 = I$.

Proof. The transition probability matrix from $d_{k-\tau_{k+1}}$ to d_k is

$$
\Pi_{\tau_{k+1}} = \sum_{j_{\tau_{k+1}}=0}^{d} \cdots \sum_{j_3=0}^{d} \sum_{j_2=0}^{d}
\begin{bmatrix}
\pi_{0j_2}\pi_{j_2 j_3}\cdots\pi_{j_{\tau_{k+1}}0} & \pi_{0j_2}\pi_{j_2 j_3}\cdots\pi_{j_{\tau_{k+1}}1} & \cdots & \pi_{0j_2}\pi_{j_2 j_3}\cdots\pi_{j_{\tau_{k+1}}d} \\
\pi_{1j_2}\pi_{j_2 j_3}\cdots\pi_{j_{\tau_{k+1}}0} & \pi_{1j_2}\pi_{j_2 j_3}\cdots\pi_{j_{\tau_{k+1}}1} & \cdots & \pi_{1j_2}\pi_{j_2 j_3}\cdots\pi_{j_{\tau_{k+1}}d} \\
\vdots & \vdots & \ddots & \vdots \\
\pi_{dj_2}\pi_{j_2 j_3}\cdots\pi_{j_{\tau_{k+1}}0} & \pi_{dj_2}\pi_{j_2 j_3}\cdots\pi_{j_{\tau_{k+1}}1} & \cdots & \pi_{dj_2}\pi_{j_2 j_3}\cdots\pi_{j_{\tau_{k+1}}d}
\end{bmatrix}
$$

$$
= \Pi^{\tau_{k+1}}.
$$

A special case is that when $\tau_{k+1} = 0$, then $\Pi_{\tau_{k+1}} = \Pi^{\tau_{k+1}} = I$. This completes the proof. $\qquad\square$

The sufficient and necessary conditions to guarantee the stochastic stability of system in (2.4) can be derived with Definition 2.1, which are shown in Theorem 2.1. For the ease of presentation, when the system is in mode $i \in \mathcal{M}$ and $r \in \mathcal{N}$ (i.e., $\tau_k = i$, $d_{k-\tau_k-1} = r$), $F(\tau_k, d_{k-\tau_k-1})$ and $G(\tau_k, d_{k-\tau_k-1})$ are denoted as $F(i,r)$ and $G(i,r)$, respectively.

Theorem 2.1. Under the proposed output feedback control law (2.2), the resulting closed-loop system in (2.4) is stochastically stable if and only if there exists symmetric $P(i,r) > 0$ such that the following matrix inequality:

$$
L(i,r) = \sum_{j=0}^{\tau}\sum_{s_1=0}^{d}\sum_{s_2=0}^{d} \lambda_{ij}\Pi^{1+i-j}_{rs_2}\Pi^{j}_{s_2 s_1} \left[\tilde{A} + \tilde{I}_1 F(i,r)\tilde{I}_1^{\mathrm{T}} + \tilde{B}H\tilde{E}_1(s_1) + \tilde{B}J\tilde{E}_2(i,s_1) + \tilde{I}_1 G(i,r)\tilde{E}_3(i)\right]^{\mathrm{T}}
$$

$$
\times P(j,s_2)\left[\tilde{A} + \tilde{I}_1 F(i,r)\tilde{I}_1^{\mathrm{T}} + \tilde{B}H\tilde{E}_1(s_1) + \tilde{B}J\tilde{E}_2(i,s_1) + \tilde{I}_1 G(i,r)\tilde{E}_3(i)\right] - P(i,r) < 0. \quad (2.6)
$$

holds for all $i \in \mathcal{M}$ and $r \in \mathcal{N}$.

Proof. Sufficiency: For the closed-loop system (2.4), construct the Lyapunov function

$$
V(X(k), k) = X(k)^{\mathrm{T}} P(\tau_k, d_{k-\tau_k-1}) X(k).
$$

Then

$$\mathcal{E}\{\Delta(V(X(k),k)\}$$

$$= \mathcal{E}\{X(k+1)^{\mathrm{T}}P(\tau_{k+1},d_{k+1-\tau_{k+1}-1})X(k+1)|_{X_k,\tau_k=i,d_{k-\tau_k}-1=r}\} - X(k)^{\mathrm{T}}P(\tau_k,d_{k-\tau_k-1})X(k). \quad (2.7)$$

Define $\tau_{k+1} = j$, $d_k = s_1$, $d_{k-\tau_{k+1}} = s_2$. To evaluate the first term in (2.7), the probability transition matrices for $\tau_k \to \tau_{k+1}$, $d_{k-i-1} \to d_{k-j}$, and $d_{k-j} \to d_k$ are needed to apply, respectively. According to (2.4) and Proposition 2.1, these three probability transition matrices are

$$\tau_k \to \tau_{k+1} : \Lambda, \quad d_{k-i-1} \to d_{k-j} : \Pi^{1+i-j}, \quad d_{k-j} \to d_k : \Pi^j. \quad (2.8)$$

Then, (2.7) can be evaluated as

$$\mathcal{E}\{\Delta(V(X(k),k)\}$$

$$= X(k)^{\mathrm{T}}\left\{\sum_{j=0}^{\tau}\sum_{s_1=0}^{d}\sum_{s_2=0}^{d}\lambda_{ij}\Pi_{rs_2}^{1+i-j}\Pi_{s_2 s_1}^{j}\left[\tilde{A}+\tilde{I}_1 F(i,r)\tilde{I}_1^{\mathrm{T}}+\tilde{B}H\tilde{E}_1(s_1)+\tilde{B}J\tilde{E}_2(i,s_1)+\tilde{I}_1 G(i,r)\tilde{E}_3(i)\right]^{\mathrm{T}} \right.$$

$$\left. \times P(j,s_2)\left[\tilde{A}+\tilde{I}_1 F(i,r)\tilde{I}_1^{\mathrm{T}}+\tilde{B}H\tilde{E}_1(s_1)+\tilde{B}J\tilde{E}_2(i,s_1)+\tilde{I}_1 G(i,r)\tilde{E}_3(i)\right] - P(i,r)\right\}X(k).$$

Thus, if $L(i,r) < 0$, then

$$\mathcal{E}\{\Delta(V(X(k),k)\} = X(k)^{\mathrm{T}}L(i,r)X(k) \le -\lambda_{\min}(-L(i,r))X(k)^{\mathrm{T}}X(k) \le -\beta\|X(k)\|^2, \quad (2.9)$$

where $\beta = \inf\{\lambda_{\min}(-L(i,r))\} > 0$. From (2.9), it can be obtained that for any $T \ge 1$

$$\mathcal{E}\{V(X(T+1),T+1)\} - \mathcal{E}\{V(X_0,0)\} \le -\beta\mathcal{E}\left\{\sum_{t=0}^{T}\|X(t)\|^2\right\}.$$

Furthermore,

$$\mathcal{E}\left\{\sum_{t=0}^{T}\|X(t)\|^2\right\}$$

$$\le \frac{1}{\beta}\left(\mathcal{E}\{V(X_0,0)\} - \mathcal{E}\{V(X(T+1),T+1)\}\right) \le \frac{1}{\beta}\mathcal{E}\{V(X_0,0)\} = \frac{1}{\beta}X(0)^{\mathrm{T}}P(\tau_0,d_{-\tau_0-1})X(0).$$

From Definition 2.1, the closed-loop system (2.4) is stochastically stable.

Necessity: If the closed-loop system (2.4) is stochastically stable, or equivalently

$$\mathcal{E}\left\{\sum_{t=0}^{\infty}\|X(k)\|^2|_{X_0,\tau_0,d_{-\tau_0-1}}\right\} \le X_0^{\mathrm{T}}WX_0. \quad (2.10)$$

Define the following function:

$$X(t)^{\mathrm{T}}\tilde{P}(T-t,\tau_t,d_{t-\tau_t-1})X(t) \triangleq \mathcal{E}\left\{\sum_{k=t}^{T}X(k)^{\mathrm{T}}Q(\tau_k,d_{k-\tau_k-1})X(k)|_{X_t,\tau_t,d_{t-\tau_t-1}}\right\}$$

with $Q(\tau_k,d_{k-\tau_k-1}) > 0$. Assuming that $X(k) \ne 0$, since $Q(\tau_k,d_{k-\tau_k-1}) > 0$, as T increases, $X(t)^{\mathrm{T}}\tilde{P}(T-t,\tau_t,d_{t-\tau_t-1})X(t)$ is monotonically increasing. From (2.10), it can be obtained that

$X(t)^{\mathrm{T}}\tilde{P}(T-t,\tau_t,d_{t-\tau_t-1})X(t)$ is upper bounded; thus, the limit exists and can be expressed as

$$X(t)^{\mathrm{T}}P(i,r)X(t) \triangleq \lim_{T\to\infty} X(t)^{\mathrm{T}}\tilde{P}(T-t,\tau_t=i,d_{t-\tau_t-1}=r)X(t)$$

$$\triangleq \lim_{T\to\infty} \mathcal{E}\left\{\sum_{k=t}^{T} X(k)^{\mathrm{T}}Q(\tau_k,d_{k-\tau_k-1})X(k)|_{X_t,\tau_t=i,d_{t-\tau_t-1}=r}\right\}. \quad (2.11)$$

Since this is valid for any $X(t)$, then

$$P(i,r) = \lim_{T\to\infty} \tilde{P}(T-t,\tau_t=i,d_{t-\tau_t-1}=r). \quad (2.12)$$

From (2.11), $P(i,r) > 0$ is obtained since $Q(\tau_k,d_{k-\tau_k-1}) > 0$. Consider

$$\mathcal{E}\left\{X(t)^{\mathrm{T}}\tilde{P}(T-t,\tau_t,d_{t-\tau_t-1})X(t) - X(t+1)^{\mathrm{T}}\tilde{P}(T-t-1,\tau_{t+1},d_{t-\tau_{t+1}})X(t+1)|_{X_t,\tau_t=i,d_{t-\tau_t-1}=r}\right\}$$

$$= X(t)^{\mathrm{T}}Q(i,r)X(t). \quad (2.13)$$

By using Proposition 2.1, the second term in (2.13) can be evaluated as

$$\mathcal{E}\left\{X(t+1)^{\mathrm{T}}\tilde{P}(T-t-1,\tau_{t+1},d_{t-\tau_{t+1}})X(t+1)|_{X_t,\tau_t=i,d_{t-\tau_t-1}=r}\right\}$$

$$= X(t)^{\mathrm{T}}\left\{\sum_{s_1=0}^{d}\sum_{s_2=0}^{d}\sum_{j=0}^{\tau}\lambda_{ij}\Pi_{rs_2}^{1+i-j}\Pi_{s_2s_1}^{j}\left[\tilde{A}+\tilde{I}_1F(i,r)\tilde{I}_1^{\mathrm{T}}+\tilde{B}H\tilde{E}_1(s_1)+\tilde{B}J\tilde{E}_2(i,s_1)+\tilde{I}_1G(i,r)\tilde{E}_3(i)\right]^{\mathrm{T}}\right.$$

$$\left.\times\tilde{P}(T-t-1,j,s_2)\left[\tilde{A}+\tilde{I}_1F(i,r)\tilde{I}_1^{\mathrm{T}}+\tilde{B}H\tilde{E}_1(s_1)+\tilde{B}J\tilde{E}_2(i,s_1)+\tilde{I}_1G(i,r)\tilde{E}_3(i)\right]\right\}X(t). \quad (2.14)$$

Substituting (2.14) into (2.13) gives rise to

$$X(t)^{\mathrm{T}}\left\{\tilde{P}(T-t,\tau_t,d_{t-\tau_t-1})-\sum_{j=0}^{\tau}\sum_{s_1=0}^{d}\sum_{s_2=0}^{d}\lambda_{ij}\Pi_{rs_2}^{1+i-j}\Pi_{s_2s_1}^{j}\left[\tilde{A}+\tilde{I}_1F(i,r)\tilde{I}_1^{\mathrm{T}}+\tilde{B}H\tilde{E}_1(s_1)\right.\right.$$

$$\left.+\tilde{B}J\tilde{E}_2(i,s_1)+\tilde{I}_1G(i,r)\tilde{E}_3(i)\right]^{\mathrm{T}}\tilde{P}(T-t-1,j,s_2)\left[\tilde{A}+\tilde{I}_1F(i,r)\tilde{I}_1^{\mathrm{T}}+\tilde{B}H\tilde{E}_1(s_1)+\tilde{B}J\tilde{E}_2(i,s_1)\right.$$

$$\left.\left.+\tilde{I}_1G(i,r)\tilde{E}_3(i)\right]\right\}\times X(t) = X(t)^{\mathrm{T}}Q(i,r)X(t). \quad (2.15)$$

Letting $T\to\infty$ and noticing (2.12), (2.6) can be obtained. This completes the proof. $\square$

Theorem 2.1 gives sufficient and necessary conditions on the existence of the output feedback controller. However, the conditions in (2.6) are nonlinear in the controller matrices and hence not easily solved. To handle this, the equivalent LMI conditions to (2.6) with nonconvex constraints are given in the following theorem.

Theorem 2.2. There exists a controller (2.2) such that the closed-loop system (2.4) is stochastically stable if and only if there exist matrices $F(i,r)$, $G(i,r)$, H, J, and symmetric matrices $\bar{X}(j,s_2) > 0$, $P(i,r) > 0$, satisfying:

$$\begin{bmatrix} -P(i,r) & V(i,r)^{\mathrm{T}} \\ V(i,r) & -X(i,r) \end{bmatrix} < 0, \quad (2.16a)$$

$$\bar{X}(j,s_2)P(j,s_2) = I \quad (2.16b)$$

19

for all $i, j \in \mathcal{M}$ and $r, s_2 \in \mathcal{N}$, with

$$
\begin{aligned}
V(i,r) &= \begin{bmatrix} V_0(i,r); & V_1(i,r); & \cdots; & V_\tau(i,r) \end{bmatrix}, \\
V_j(i,r) &= \begin{bmatrix} V_{j,0}(i,r); & V_{j,1}(i,r); & \cdots; & V_{j,d}(i,r) \end{bmatrix}, \\
V_{j,s_2}(i,r) &= \Big[(\lambda_{ij} \Pi^{1+i-j}_{rs_2} \Pi^j_{s_2 0})^{\frac{1}{2}} [\tilde{A} + \tilde{I}_1 F(i,r) \tilde{I}_1^{\mathrm{T}} + \tilde{B} H \tilde{E}_1(0) + \tilde{B} J \tilde{E}_2(i,0) + \tilde{I}_1 G(i,r) \tilde{E}_3(i)]; \\
&\qquad (\lambda_{ij} \Pi^{1+i-j}_{rs_2} \Pi^j_{s_2 1})^{\frac{1}{2}} [\tilde{A} + \tilde{I}_1 F(i,r) \tilde{I}_1^{\mathrm{T}} + \tilde{B} H \tilde{E}_1(1) + \tilde{B} J \tilde{E}_2(i,1) + \tilde{I}_1 G(i,r) \tilde{E}_3(i)]; \\
&\qquad \vdots \\
&\qquad (\lambda_{ij} \Pi^{1+i-j}_{rs_2} \Pi^j_{s_2 d})^{\frac{1}{2}} [\tilde{A} + \tilde{I}_1 F(i,r) \tilde{I}_1^{\mathrm{T}} + \tilde{B} H \tilde{E}_1(d) + \tilde{B} J \tilde{E}_2(i,d) + \tilde{I}_1 G(i,r) \tilde{E}_3(i)] \Big], \\
X(i,r) &= \operatorname{diag}\Big\{ X_0(i,r) \quad X_1(i,r) \quad \cdots \quad X_\tau(i,r) \Big\}, \\
X_j(i,r) &= \operatorname{diag}\Big\{ X_{j,0}(i,r) \quad X_{j,1}(i,r) \quad \cdots \quad X_{j,d}(i,r) \Big\}, \\
X_{j,s_2}(i,r) &= \operatorname{diag}\Big\{ \underbrace{ \bar{X}(j,s_2) \quad \bar{X}(j,s_2) \quad \cdots \quad \bar{X}(j,s_2) }_{d+1} \Big\}.
\end{aligned}
$$

Proof. By applying the Schur complement [8] and letting $\bar{X}(j,s_2) = P(j,s_2)^{-1}$, the proof can be readily obtained. $\qquad \square$

The conditions in Theorem 2.2 are a set of LMIs with some nonconvex constraints. This can be solved by several existing iterative LMI algorithms. It is shown in [24] that PRA is the best and seldom fails to find a global optimum. Thus, PRA is employed and detailed procedures to solve the conditions (2.16) can be referred to [146].

Remark 2.2. The two-mode-dependent controller (2.2) makes full use of the delay information by involving both the S-C and C-A delays. Moreover, it includes the one-mode-dependent and mode-independent controllers as special cases. When $F(\tau_k, d_{k-\tau_k-1}) = F_1(\tau_k)$, $G(\tau_k, d_{k-\tau_k-1}) = G_1(\tau_k)$, $\forall \ d_{k-\tau_k-1} \in \mathcal{N}$, the controller (2.2) is reduced to be one-mode-dependent. When $F(\tau_k, d_{k-\tau_k-1}) = F_0$, $G(\tau_k, d_{k-\tau_k-1}) = G_0$, $\forall \ \tau_k \in \mathcal{M}$ and $d_{k-\tau_k-1} \in \mathcal{N}$, the controller (2.2) becomes a mode-independent one. Theorems 2.1 and 2.2 can also handle one-mode-dependent and mode-independent controller design problems as special cases.

2.4 Numerical Example

To illustrate the effectiveness of the results in Section 2.3, the proposed method is applied to a cart and inverted pendulum system [133, 147] shown in Figure 2.2, where x is the position of the cart, θ is the angular position of the pendulum, and u is the input force. The state variables are chosen as $x_d = \begin{bmatrix} x & \dot{x} & \theta & \dot{\theta} \end{bmatrix}^{\mathrm{T}}$. The output is $y = \begin{bmatrix} x & \theta \end{bmatrix}^{\mathrm{T}}$. It is assumed that no friction exists in surfaces and the parameters here are: $m_1 = 1 \ kg$, $m_2 = 0.5 \ kg$, $L = 1 \ m$. The output feedback
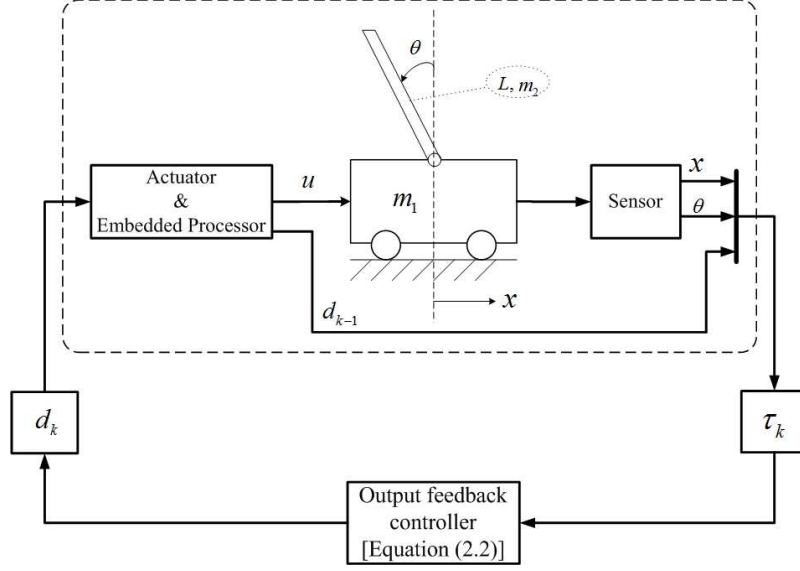
Figure 2.2: Cart and inverted pendulum system.

controller is designed for the following linearized discrete-time model with sampling time $T_s = 0.1s$:

$$\begin{aligned}
x_d(k+1) &= A_d x_d(k) + B_d u(k) \\
y(k) &= C_d x_d(k),
\end{aligned}$$

where

$$A_d = \begin{bmatrix} 1.0000 & 0.1000 & -0.0166 & -0.0005 \\ 0 & 1.0000 & -0.3374 & -0.0166 \\ 0 & 0 & 1.0996 & 0.1033 \\ 0 & 0 & 2.0247 & 1.0996 \end{bmatrix}, \quad B_d = \begin{bmatrix} 0.0045 \\ 0.0896 \\ -0.0068 \\ -0.1377 \end{bmatrix}, \quad C_d = \begin{bmatrix} 1 & 0 & 0 & 0 \\ 0 & 0 & 1 & 0 \end{bmatrix}.$$

The eigenvalues of A_d are $1, 1, 1.5569,$ and 0.6423. Hence, the discrete-time system is unstable.

The random delays involved in this NCS are assumed to be $\tau_k \in \{0, 1, 2\}$ and $d_k \in \{0, 1\}$, and their transition probability matrices are given by

$$\Lambda = \begin{bmatrix} 0.5 & 0.5 & 0 \\ 0.3 & 0.6 & 0.1 \\ 0.3 & 0.6 & 0.1 \end{bmatrix}, \quad \Pi = \begin{bmatrix} 0.2 & 0.8 \\ 0.5 & 0.5 \end{bmatrix}.$$

Figures 2.3 and 2.4 show part of the simulation run of the S-C delays τ_k and C-A delays d_k governed by their corresponding transition probability matrices, respectively.

Based on Proposition 2.1, the transition probability matrix for the delay mode jumping from d_{k-2} to d_k is Π^2. By using Theorem 2.2, the output feedback controller is designed with the

21
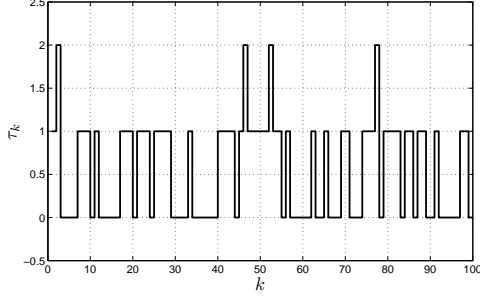
Figure 2.3: S-C random delays τ_k.
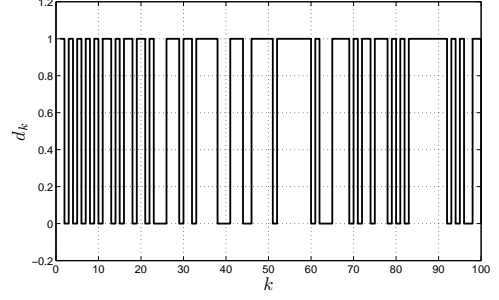
Figure 2.4: C-A random delays d_k.

following matrices – $F(\tau_k, d_{k-\tau_k-1})$, $G(\tau_k, d_{k-\tau_k-1})$, H, and J:

$$F(0,0) = \begin{bmatrix} 0.1550 & 0.0060 & -0.2786 & -0.1208 \\ -0.4991 & 0.7354 & -0.1394 & 0.1630 \\ 0.7808 & 0.5714 & -0.5284 & 0.7196 \\ 1.3487 & 0.8204 & -0.4543 & 0.7047 \end{bmatrix}, \quad G(0,0) = \begin{bmatrix} 0.1382 & -2.2709 \\ 0.0114 & -0.4115 \\ 0.0014 & 4.7681 \\ 0.0205 & 2.8083 \end{bmatrix},$$

$$F(0,1) = \begin{bmatrix} 0.2442 & 0.0667 & -0.4153 & -0.0819 \\ -0.3164 & 0.7816 & 0.0057 & 0.0097 \\ 0.7720 & 0.5720 & -0.6462 & 0.8203 \\ 0.9528 & 0.6863 & -0.6673 & 1.0157 \end{bmatrix}, \quad G(0,1) = \begin{bmatrix} 0.1419 & -1.8205 \\ 0.0064 & -0.4091 \\ -0.0039 & 5.0957 \\ 0.0223 & 2.6799 \end{bmatrix},$$

$$F(1,0) = \begin{bmatrix} 0.2196 & 0.2297 & -0.3241 & -0.2781 \\ -0.4005 & 0.8396 & 0.0009 & -0.0530 \\ 1.1818 & -0.0338 & 0.0570 & 1.0902 \\ 1.1678 & 0.3228 & -0.1786 & 1.0731 \end{bmatrix}, \quad G(1,0) = \begin{bmatrix} 0.1880 & -2.4980 \\ 0.0326 & -0.8274 \\ -0.2235 & 6.4868 \\ -0.0955 & 3.1831 \end{bmatrix},$$

$$F(1,1) = \begin{bmatrix} 0.1463 & 0.2323 & -0.0950 & -0.4695 \\ -0.3553 & 0.8349 & 0.0933 & -0.0928 \\ 0.9486 & -0.0424 & -0.8425 & 1.7401 \\ 1.0299 & 0.3265 & -0.9091 & 1.5751 \end{bmatrix}, \quad G(1,1) = \begin{bmatrix} 0.2052 & -3.3634 \\ 0.0251 & -0.8857 \\ -0.2175 & 8.1977 \\ -0.0915 & 4.6597 \end{bmatrix},$$

$$F(2,0) = \begin{bmatrix} 0.7736 & 0.3207 & -0.4226 & -0.1325 \\ -0.1310 & 0.8791 & 0.0370 & -0.0406 \\ -0.1927 & -0.2776 & 0.7051 & 0.3771 \\ 0.1745 & 0.2119 & 0.0517 & 0.6999 \end{bmatrix}, \quad G(2,0) = \begin{bmatrix} 0.1275 & -0.5579 \\ 0.0017 & -0.1489 \\ -0.0506 & 0.7241 \\ 0.0363 & -0.4882 \end{bmatrix},$$

$$F(2,1) = \begin{bmatrix} 0.5887 & 0.3064 & -0.6016 & 0.0070 \\ -0.1113 & 0.9407 & 0.1343 & -0.1566 \\ -0.1551 & -0.4189 & 0.5039 & 0.6367 \\ 0.4481 & 0.1047 & 0.1353 & 0.7477 \end{bmatrix}, \quad G(2,1) = \begin{bmatrix} 0.1411 & -0.5840 \\ 0.0152 & -0.5207 \\ -0.0909 & 1.7924 \\ -0.0197 & 0.4485 \end{bmatrix},$$

$$H = \begin{bmatrix} -1.0629 & -3.2705 & 3.8788 & 2.6564 \end{bmatrix}, \quad J = \begin{bmatrix} -0.8939 & 18.1636 \end{bmatrix}.$$

22
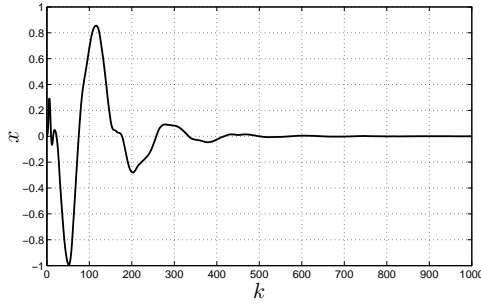
Figure 2.5: The response of x.
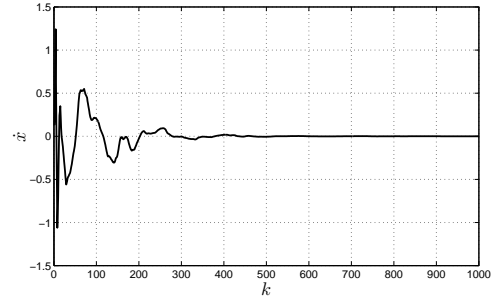
Figure 2.6: The response of $\dot{x}$.
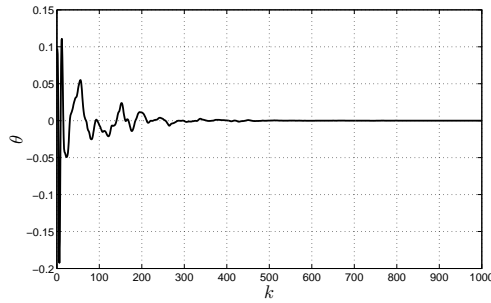
Figure 2.7: The response of θ.
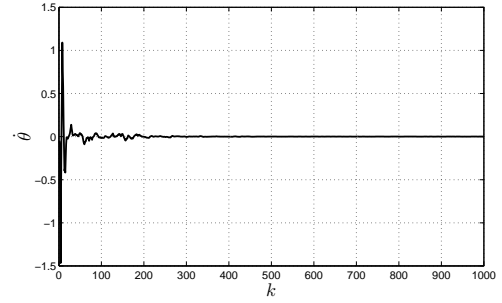
Figure 2.8: The response of $\dot{\theta}$.

The initial values of the discrete-time model and the output feedback controller are $x_d(-3) = x_d(-2) = x_d(-1) = [0\ 0\ 0\ 0]^{\mathrm{T}}$, $x_d(0) = [0\ 0\ 0.1\ 0]^{\mathrm{T}}$, and $z(-2) = z(-1) = z(0) = [0\ 0\ 0\ 0]^{\mathrm{T}}$. Figures 2.5–2.8 show the responses of four states, respectively. It is observed that the closed-loop system is stochastically stable.

2.5 Conclusion

In this chapter, an output feedback controller design method is proposed for NCSs with random network-induced delays. The S-C and C-A delays, modeled by two Markov chains, are simultaneously incorporated into the controller design in a general and practical way. Then the resulting closed-loop system is a special discrete-time jump linear system. The sufficient and necessary conditions of stochastic stability are derived in the form of a set of LMIs with some nonconvex constraints. The product reduction algorithm is employed to obtain the two-mode-dependent output feedback controller. Finally it is worth mentioning that the proposed two-mode-dependent controller could be extended to consider the control performance and system uncertainties, which will be solved in next chapter.

Chapter 3

Robust Mixed H_2/H_∞ Control of Networked Control Systems with Time Delays modeled by Markov Chains

3.1 Introduction

With the advancement of network techniques, the combination of network into control systems has attracted much attention recently. Networked control systems (NCSs) is a type of distributed systems, in which the information of system components is exchanged via the communication network. Compared with the traditional control system, the main advantages of NCSs include low cost, easy diagnosis, and high reliability. Hence, NCSs have been finding many industrial applications in automobiles, manufacturing plants, and aircrafts, see, e.g., [87, 100, 119] and the references therein. The insertion of communication network also brings some problems, such as time delays, packet dropouts, and quantization errors. It is well-known that the time delays and packet dropouts can degrade the system performance or even cause instability in control systems. Hence, how to handle the time delays and packet dropouts has attracted much attention. Also, the network-induced time delays are different from and more complex than the traditional constant time delays because of the time-varying property of network. Various methodologies have been proposed in the literature for the controller design considering the network characteristics. The controller design methods in the existing literature can be roughly classified into the three categories based on the ways they deal with time delay information.

In the first category, the controller design only deals with the sensor-to-controller (S-C) delays while another important type of delays, controller-to-actuator (C-A) delays, have not been considered. In [133], a mode-dependent state feedback controller is designed for NCSs with S-C delays; The authors first formulate the closed-loop system to be a discrete-time jump linear system and then solve the stabilization problem by using the stability result of Markovian jump linear systems (MJLSs). In [100], a sufficient and necessary condition for H_∞ control is proposed for NCSs where the controller co-locates with the plant under the framework of MJLSs based on the Bounded Real

Lemma in [99]; the design method is further applied to a vehicle following problem.

In the second category, both S-C and C-A time delays are considered in the controller design, but the controller is constant and does not depend on either S-C or C-A delays. Hence, the S-C and C-A delays can be lumped together and considered as one type of time delay. In [133], the time delays in S-C and C-A links are modeled by Markov chains and the mode-independent output feedback controller is designed to stabilize the NCSs. In [76], the suboptimal H_2 control of NCSs with both bounded S-C and C-A time delays is solved via the switched system approach. In [143], an H_∞ analysis method for NCSs is proposed by employing the lower bound of the network-induced delay and designing the mode-independent controller. In [136], the authors consider the arbitrary packet loss process and Markovian packet loss process with time delays in both S-C and C-A links; a mode-independent state feedback controller design method is developed to guarantee the asymptotical stability and mean square stability. In [149], the packet dropouts in both S-C and the C-A communication networks are considered and the network-induced delays are assumed to be shorter than one sampling period; the mode-independent output feedback controller is designed via a switched system approach and the relation between the packet dropout rate and the stability of the closed-loop NCS is explicitly established. The H_∞ output tracking in NCSs is considered in [40] where the S-C and C-A delays are assumed to have both an upper bound and a lower bound; a new model based on the updating instants of the holder is formulated and further state feedback controllers are designed to guarantee the H_∞ tracking performance using the LMI-based procedure.

In the third category, both S-C and C-A time delays are considered in the controller design and the controller depends on S-C and/or C-A delays. In [130], the Markov chain is used to model the packet loss and a mode-dependent state feedback controller design method is provided; the authors introduce a new classification with buffers to simplify the modeling of NCSs and avoid incorporating the C-A delay in the controller. A state feedback controller that simultaneously depends on S-C and C-A delays is designed for NCSs with delays modeled by Markov chains in [147]; the sufficient and necessary condition to guarantee the stochastic stability is derived. In [56], the Markov processes are used to model the random network-induced S-C and C-A delays, and a mode-dependent state feedback controller is proposed to stabilize this class of systems based on Lyapunov-Razumikhin method. In the aforementioned references, only the stabilization problem is investigated in the mode-dependent controller design and no control performance is considered. Hence, to solve the control synthesis for the mode-dependent controller design is the focus of this chapter.

In the presence of disturbances and uncertainties, robust control theory provides a powerful tool for controller analysis and synthesis. It is well-known that H_2 control and H_∞ control are two main streams of robust control theory [153]. The time domain interpretation of H_2 norm is the l_2 norm of the output driven by unit impulse and root-mean-square value of the output driven by unit intensity white noise. H_∞ norm is a measure of robust stability that represents the worst-

case energy attenuation for any energy-bounded disturbance. Thus, a combination of H_2 and H_∞ control, called mixed H_2/H_∞ control is to minimize the H_2 norm of the system subject to the H_∞ norm constraint. Hence, the mixed H_2/H_∞ provides the flexibility to tune the controller to achieve balanced performance between the H_2 cost (l_2 norm of impulse response) and H_∞ cost (robust stability with respect to disturbance and uncertainty).

The remainder of this chapter is organized as follows. Section 3.2 describes the systems and states the objectives of this work. In Section 3.3, some preliminaries are presented. Section 3.4 solves the mixed H_2/H_∞ control problem. Several illustrative design examples are given in Section 3.5. Finally, the concluding remarks are addressed in Section 3.6.

The notation in this chapter is fairly standard. The superscripts "T" and "-1" stand for matrix transposition and matrix inverse, respectively. $\mathbb{R}^n$ denotes the n-dimensional Euclidean space and the notation $P > 0 (\geq 0)$ means that P is real symmetric and positive definite (semidefinite). $\mathrm{diag}\{\cdots\}$ stands for a block-diagonal matrix and $\mathrm{tr}\{\cdot\}$ means the trace of a matrix. $\|\cdot\|_2$ refers to the Euclidean norm for vectors and induced 2-norm for matrices. $\mathcal{E}(\cdot)$ stands for the mathematical expectation operator.

3.2   Problem Formulation

Consider the NCS setup in Figure 2.1. The discrete-time linear time-invariant plant model is

$$
\begin{align}
x(k+1) &= (A + \Delta A)x(k) + (B + \Delta B)u(k) + J\omega(k), \tag{3.1a}\\
y(k) &= Cx(k), \tag{3.1b}
\end{align}
$$

where $x(k) \in \mathbb{R}^n$, $u(k) \in \mathbb{R}^m$, $y(k) \in \mathbb{R}^p$, $\omega(k) \in \mathbb{R}^l$ is the disturbance and A, B, C, J, ΔA, and ΔB are known real matrices with appropriate dimensions. Bounded random delays exist in the links from sensor to controller and controller to actuator as shown in Figure 2.1. Here, $\tau \geq \tau_k \geq 0$ represents the S-C delay and $d \geq d_k \geq 0$ stands for the C-A delay. The output feedback controller is to be designed.

In this chapter, τ_k and d_k are modeled as two homogeneous Markov chains [133, 147] that take values in $\mathcal{M} = \{0, 1, ..., \tau\}$ and $\mathcal{N} = \{0, 1, ..., d\}$, and their transition probability matrices are $\Lambda = [\lambda_{ij}]$ and $\Pi = [\pi_{rs}]$, respectively, meaning that τ_k and d_k jump from mode i to j and from mode r to s, respectively, with probabilities λ_{ij} and π_{rs}, which are defined by

$$
\begin{align}
\lambda_{ij} &= \Pr(\tau_{k+1} = j | \tau_k = i),\\
\pi_{rs} &= \Pr(d_{k+1} = s | d_k = r)
\end{align}
$$

with the constraints $\lambda_{ij}, \pi_{rs} \geq 0$ and

$$
\sum_{j=0}^{\tau} \lambda_{ij} = 1, \quad \sum_{s=0}^{d} \pi_{rs} = 1
$$

for all $i, j \in \mathcal{M}$ and $r, s \in \mathcal{N}$. The parameter uncertainties ΔA and ΔB are of the following form (norm-bounded uncertainty):

$$\begin{bmatrix} \Delta A & \Delta B \end{bmatrix} = G_1 \Delta_u \begin{bmatrix} U_1 & U_2 \end{bmatrix} \tag{3.2}$$

with $\Delta_u^{\mathrm{T}} \Delta_u \leq 1$.

It is noticed that when the controller is designed at current time k, the S-C delay τ_k can be obtained using the time-stamping technique [55] and the embedded processor can calculate the previous C-A time delay d_{k-1}. Furthermore, by considering the random delays in the S-C link, $d_{k-\tau_k-1}$ can be obtained at current time k for sure in the controller node.

The dynamic output controller is designed based on the available information $(\tau_k, d_{k-\tau_k-1})$ and thus has the following form:

$$\begin{align}
z(k+1) &= F(\tau_k, d_{k-\tau_k-1})z(k) + G(\tau_k, d_{k-\tau_k-1})y(k), \tag{3.3a} \\
u(k) &= Hz(k) + Ty(k), \tag{3.3b}
\end{align}$$

where $z(k) \in \mathbb{R}^n$ is the state vector of the output feedback controller; and $F(\tau_k, d_{k-\tau_k-1})$, $G(\tau_k, d_{k-\tau_k-1})$, H, and T are appropriately dimensioned matrices to be designed.

The closed-loop system combining (3.1) and (3.3) can be expressed as

$$\begin{align}
x(k+1) &= (A + \Delta A)x(k) + (B + \Delta B)Hz(k - d_k) + (B + \Delta B)TCx(k - \tau_k - d_k) + J\omega(k), \\
z(k+1) &= F(\tau_k, d_{k-\tau_k-1})z(k) + G(\tau_k, d_{k-\tau_k-1})Cx(k - \tau_k), \\
y(k) &= Cx(k).
\end{align}$$

At sampling time k, if augmenting the state variable as

$$X(k) = [x(k)^{\mathrm{T}} \ x(k-1)^{\mathrm{T}} \ \cdots \ x(k-\tau-d)^{\mathrm{T}} \ z(k)^{\mathrm{T}} \ z(k-1)^{\mathrm{T}} \ \cdots \ z(k-d)^{\mathrm{T}}]^{\mathrm{T}},$$

the closed-loop system can be rewritten in the following form

$$\begin{align}
X(k+1) &= \Big[\tilde{A} + \tilde{I}_1 F(\tau_k, d_{k-\tau_k-1})\tilde{I}_1^{\mathrm{T}} + \tilde{B}H\tilde{E}_1(d_k) + \tilde{B}T\tilde{E}_2(\tau_k, d_k) \\
&\qquad + \tilde{I}_1 G(\tau_k, d_{k-\tau_k-1})\tilde{E}_3(\tau_k)\Big] X(k) + \tilde{J}\omega(k), \tag{3.4a} \\
y(k) &= \tilde{C}X(k), \tag{3.4b}
\end{align}$$

where

$$
\tilde{A} = \begin{bmatrix}
A + \Delta A & 0 & \cdots & 0 & 0 & 0 & \cdots & 0 \\
I & 0 & \cdots & 0 & 0 & 0 & \cdots & 0 \\
\vdots & \ddots & \cdots & 0 & 0 & 0 & \cdots & 0 \\
0 & 0 & \cdots & 0 & 0 & 0 & \cdots & 0 \\
0 & 0 & \cdots & 0 & 0 & 0 & \cdots & 0 \\
0 & 0 & \cdots & 0 & 0 & I & \cdots & 0 \\
\vdots & 0 & \cdots & 0 & 0 & 0 & \ddots & 0 \\
0 & 0 & \cdots & 0 & 0 & 0 & \cdots & 0
\end{bmatrix} \in \mathbb{R}^{(\tau+2d+2)n \times (\tau+2d+2)n},
$$

$$
\tilde{B} = \begin{bmatrix}
B + \Delta B \\
0 \\
\vdots \\
0 \\
0 \\
0 \\
\vdots \\
0
\end{bmatrix} \in \mathbb{R}^{(\tau+2d+2)n \times m}, \quad
\tilde{J} = \begin{bmatrix}
J \\
0 \\
\vdots \\
0 \\
0 \\
0 \\
\vdots \\
0
\end{bmatrix} \in \mathbb{R}^{(\tau+2d+2)n \times l},
$$

$$
\tilde{C} = \begin{bmatrix} C & 0 & 0 & \cdots & 0 \end{bmatrix}^{\mathrm{T}} \in \mathbb{R}^{p \times (\tau+2d+2)n},
$$

$$
\tilde{I}_1 = \underbrace{\begin{bmatrix} 0 & \cdots & 0 & I & \cdots & 0 \end{bmatrix}}_{(2+\tau+d)th \ block \ being \ identity}^{\mathrm{T}} \in \mathbb{R}^{(\tau+2d+2)n \times n},
$$

$$
\tilde{E}_1(d_k) = \underbrace{\begin{bmatrix} 0 & \cdots & 0 & I & \cdots & 0 \end{bmatrix}}_{(2+\tau+d+d_k)th \ block \ being \ identity} \in \mathbb{R}^{n \times (\tau+2d+2)n},
$$

$$
\tilde{E}_2(\tau_k, d_k) = CE_2(\tau_k, d_k),
$$

$$
\tilde{E}_3(\tau_k) = CE_3(\tau_k),
$$

$$
E_2(\tau_k, d_k) = \underbrace{\begin{bmatrix} 0 & \cdots & 0 & I & \cdots & 0 \end{bmatrix}}_{(1+\tau_k+d_k)th \ block \ being \ identity} \in \mathbb{R}^{n \times (\tau+2d+2)n},
$$

$$
E_3(\tau_k) = \underbrace{\begin{bmatrix} 0 & \cdots & 0 & I & \cdots & 0 \end{bmatrix}}_{(1+\tau_k)th \ block \ being \ identity} \in \mathbb{R}^{n \times (\tau+2d+2)n}.
$$

Equation (3.4) is a discrete-time jump linear system. In the following, when the system is in mode $i \in \mathcal{M}$ and $r \in \mathcal{N}$ (i.e., $\tau_k = i$, $d_{k-\tau_k-1} = r$), $F(\tau_k, d_{k-\tau_k-1})$ and $G(\tau_k, d_{k-\tau_k-1})$ will be denoted as $F(i, r)$ and $G(i, r)$ respectively, for simplicity.

It is also worth noting that system (3.4) is with norm-bounded uncertainties shown as follows.

$$
\tilde{A} = \begin{bmatrix}
A + \Delta A & 0 & \cdots & 0 & 0 & 0 & \cdots & 0 \\
I & 0 & \cdots & 0 & 0 & 0 & \cdots & 0 \\
\vdots & \ddots & \cdots & 0 & 0 & 0 & \cdots & 0 \\
0 & 0 & \cdots & 0 & 0 & 0 & \cdots & 0 \\
0 & 0 & \cdots & 0 & 0 & 0 & \cdots & 0 \\
0 & 0 & \cdots & 0 & 0 & I & \cdots & 0 \\
\vdots & 0 & \cdots & 0 & 0 & 0 & \ddots & 0 \\
0 & 0 & \cdots & 0 & 0 & 0 & \cdots & 0
\end{bmatrix}
$$

$$
= \begin{bmatrix}
A & 0 & \cdots & 0 & 0 & 0 & \cdots & 0 \\
I & 0 & \cdots & 0 & 0 & 0 & \cdots & 0 \\
\vdots & \ddots & \cdots & 0 & 0 & 0 & \cdots & 0 \\
0 & 0 & \cdots & 0 & 0 & 0 & \cdots & 0 \\
0 & 0 & \cdots & 0 & 0 & 0 & \cdots & 0 \\
0 & 0 & \cdots & 0 & 0 & I & \cdots & 0 \\
\vdots & 0 & \cdots & 0 & 0 & 0 & \ddots & 0 \\
0 & 0 & \cdots & 0 & 0 & 0 & \cdots & 0
\end{bmatrix}
+
\begin{bmatrix}
I \\ 0 \\ \vdots \\ 0 \\ 0 \\ 0 \\ \vdots \\ 0
\end{bmatrix}
\Delta A \begin{bmatrix} I & 0 & \cdots & 0 & 0 & 0 & \cdots & 0 \end{bmatrix}, (3.5a)
$$

$$
\tilde{B} = \begin{bmatrix}
B + \Delta B \\ 0 \\ \vdots \\ 0 \\ 0 \\ 0 \\ \vdots \\ 0
\end{bmatrix}
=
\begin{bmatrix}
B \\ 0 \\ \vdots \\ 0 \\ 0 \\ 0 \\ \vdots \\ 0
\end{bmatrix}
+
\begin{bmatrix}
\Delta B \\ 0 \\ \vdots \\ 0 \\ 0 \\ 0 \\ \vdots \\ 0
\end{bmatrix}
=
\begin{bmatrix}
B \\ 0 \\ \vdots \\ 0 \\ 0 \\ 0 \\ \vdots \\ 0
\end{bmatrix}
+
\begin{bmatrix}
G_1 \\ 0 \\ \vdots \\ 0 \\ 0 \\ 0 \\ \vdots \\ 0
\end{bmatrix}
\Delta_u U_2. \tag{3.5b}
$$

Now define

$$
A_{Aug} = \begin{bmatrix}
A & 0 & \cdots & 0 & 0 & 0 & \cdots & 0 \\
I & 0 & \cdots & 0 & 0 & 0 & \cdots & 0 \\
\vdots & \ddots & \cdots & 0 & 0 & 0 & \cdots & 0 \\
0 & 0 & \cdots & 0 & 0 & 0 & \cdots & 0 \\
0 & 0 & \cdots & 0 & 0 & 0 & \cdots & 0 \\
0 & 0 & \cdots & 0 & 0 & I & \cdots & 0 \\
\vdots & 0 & \cdots & 0 & 0 & 0 & \ddots & 0 \\
0 & 0 & \cdots & 0 & 0 & 0 & \cdots & 0
\end{bmatrix},
\quad
I_2 = \begin{bmatrix}
I \\ 0 \\ \vdots \\ 0 \\ 0 \\ 0 \\ \vdots \\ 0
\end{bmatrix},
\quad
\text{then,} \quad \Delta A_{Aug} = I_2 G_1 \Delta_u U_1 I_2^{\mathrm{T}};
$$

$$
B_{Aug} = \begin{bmatrix} B \\ 0 \\ \vdots \\ 0 \\ 0 \\ 0 \\ \vdots \\ 0 \end{bmatrix}, \quad \tilde{G}_1 = \begin{bmatrix} G_1 \\ 0 \\ \vdots \\ 0 \\ 0 \\ 0 \\ \vdots \\ 0 \end{bmatrix}, \quad \text{then,} \quad \Delta B_{Aug} = \begin{bmatrix} \Delta B \\ 0 \\ \vdots \\ 0 \\ 0 \\ 0 \\ \vdots \\ 0 \end{bmatrix} = \tilde{G}_1 \Delta_u U_2.
$$

Then, (3.5) can be rewritten as

$$
\begin{align}
\tilde{A} &= A_{Aug} + \Delta A_{Aug} = A_{Aug} + \tilde{G}_1 \Delta_u U_1 I_2^{\mathrm{T}}; \tag{3.6a} \\
\tilde{B} &= B_{Aug} + \Delta B_{Aug} = B_{Aug} + \tilde{G}_1 \Delta_u U_2. \tag{3.6b}
\end{align}
$$

It is clear that the uncertainties in augmented system (3.4) is norm-bounded.

The objective (mixed H_2/H_∞ control) of this chapter is to design output feedback controller (3.3) to guarantee that

- The closed-loop system (3.4) is stochastically stable;

- The 2-norm of the system is minimized while the ∞-norm of the system is lower than the prescribed level.

3.3 Preliminaries

Definition 3.1 ([147]). System (3.4) with $\omega(k) = 0$ for all $k > 0$ is said to be stochastically stable if for every finite $X_0 = X(0)$, initial mode $\tau_0 = \tau(0) \in \mathcal{M}$, and $d_{-\tau_0-1} = d(-\tau_0 - 1) \in \mathcal{N}$, there exists a finite $W > 0$ such that the following holds:

$$
\mathcal{E} \left\{ \sum_{k=0}^{\infty} \|X(k)\|^2 | X_0, \tau_0, d_{-\tau_0-1} \right\} < X_0^{\mathrm{T}} W X_0. \tag{3.7}
$$

Definition 3.2 ([23]). System (3.4) is said to be mean square stable if

$$
\lim_{k \to \infty} \mathcal{E} \left[\|X(k)\|^2 \right] = 0 \tag{3.8}
$$

holds for any initial conditions.

Obviously, stochastic stability implies mean square stability.

The follow theorem provides the sufficient and necessary condition for stochastic stability of system (3.4).

Theorem 3.1. Under the proposed output feedback control law (3.3), the resulting closed-loop system in (3.4) is stochastically stable if and only if there exists symmetric $P(i,r) > 0$ such that the following matrix inequality:

$$\sum_{j=0}^{\tau}\sum_{s_1=0}^{d}\sum_{s_2=0}^{d}\lambda_{ij}\Pi_{rs_2}^{1+i-j}\Pi_{s_2s_1}^{j}\left[\tilde{A}+\tilde{I}_1F(i,r)\tilde{I}_1^{\mathrm{T}}+\tilde{B}H\tilde{E}_1(s_1)+\tilde{B}T\tilde{E}_2(i,s_1)+\tilde{I}_1G(i,r)\tilde{E}_3(i)\right]^{\mathrm{T}}$$
$$\times P(j,s_2)\left[\tilde{A}+\tilde{I}_1F(i,r)\tilde{I}_1^{\mathrm{T}}+\tilde{B}H\tilde{E}_1(s_1)+\tilde{B}T\tilde{E}_2(i,s_1)+\tilde{I}_1G(i,r)\tilde{E}_3(i)\right]-P(i,r)<0. \quad (3.9)$$

holds for all $i \in \mathcal{M}$ and $r \in \mathcal{N}$.

Proof. This theorem can be proved by following the similar way in the proof of Theorem 2.1 in Section 2.3. $\square$

Remark 3.1. An interesting property obtained from Theorem 3.1 is monotonically decreasing behavior of the following Lyapunov equation:

$$\Gamma(\mathcal{P})=\sum_{j=0}^{\tau}\sum_{s_1=0}^{d}\sum_{s_2=0}^{d}\lambda_{ij}\Pi_{rs_2}^{1+i-j}\Pi_{s_2s_1}^{j}\left[\tilde{A}+\tilde{I}_1F(i,r)\tilde{I}_1^{\mathrm{T}}+\tilde{B}H\tilde{E}_1(s_1)+\tilde{B}T\tilde{E}_2(i,s_1)+\tilde{I}_1G(i,r)\tilde{E}_3(i)\right]^{\mathrm{T}}$$
$$\times\mathcal{P}(j,s_2)\left[\tilde{A}+\tilde{I}_1F(i,r)\tilde{I}_1^{\mathrm{T}}+\tilde{B}H\tilde{E}_1(s_1)+\tilde{B}T\tilde{E}_2(i,s_1)+\tilde{I}_1G(i,r)\tilde{E}_3(i)\right]-\mathcal{P}(i,r), \quad (3.10)$$

where $\mathcal{P}$ contains $\mathcal{P}(i,r), \forall i \in \mathcal{M}, r \in \mathcal{N}$ and $\mathcal{P}(i,r)$ is the solution of Theorem 3.1. Suppose that both $\mathcal{P}_1(i,r)$ and $\mathcal{P}_2(i,r)$ satisfy (3.9), if $\mathcal{P}_1(i,r) > \mathcal{P}_2(i,r)$, then we have $\Gamma(\mathcal{P}_1) < \Gamma(\mathcal{P}_2)$. Also if we have $\Gamma(\mathcal{P}_1) < \Gamma(\mathcal{P}_2)$, we can obtain that $\mathcal{P}_1(i,r) > \mathcal{P}_2(i,r)$.

3.4   Robust Mixed H_2/H_∞ Control

The control performance is very important in the controller design. In this section, the definitions of H_2 and H_∞ norms for the special systems are first introduced. Then, the robust mixed H_2/H_∞ control problem is solved under the framework of LMI. Before presenting the main results of this section, a lemma will be introduced, which plays an important role in the following derivation.

Lemma 3.1 ([134]). Let $\mathcal{Z}$, $\mathcal{F}$, Δ, $\mathcal{G}$ be matrices with appropriate dimensions. Suppose $\mathcal{Z}$ is symmetric and $\Delta^{\mathrm{T}}\Delta \leq I$, then

$$\mathcal{Z} + \mathcal{F}\Delta\mathcal{G} + \mathcal{G}^{\mathrm{T}}\Delta^{\mathrm{T}}\mathcal{F}^{\mathrm{T}} < 0, \quad (3.11)$$

if and only if there exists scalar $\varepsilon > 0$ satisfying

$$\mathcal{Z} + \varepsilon\mathcal{F}\mathcal{F}^{\mathrm{T}} + \frac{1}{\varepsilon}\mathcal{G}^{\mathrm{T}}\mathcal{G} < 0. \quad (3.12)$$

Lemma 3.1 will be used to handle norm-bounded uncertainties. Moreover, Proposition 2.1 in Section 2.3 will be utilized to deal with the multi-step jumps of delay modes.

Consider system (3.4) with initial conditions shown as follows:

$$X(k+1) = \hat{A}(\tau_k, d_{k-\tau_k-1}, d_k)X(k) + \tilde{J}\omega(k), \tag{3.13a}$$

$$y(k) = \tilde{C}X(k), \tag{3.13b}$$

$$X(0) = 0, \quad \tau(0) = \tau_0, \quad d(-\tau_0 - 1) = d_{-\tau_0 - 1}, \tag{3.13c}$$

where

$$\hat{A}(\tau_k, d_{k-\tau_k-1}, d_k) = \tilde{A} + \tilde{I}_1 F(\tau_k, d_{k-\tau_k-1})\tilde{I}_1^{\mathrm{T}} + \tilde{B}H\tilde{E}_1(d_k) + \tilde{B}T\tilde{E}_2(\tau_k, d_k) + \tilde{I}_1 G(\tau_k, d_{k-\tau_k-1})\tilde{E}_3(\tau_k).$$
$$\tag{3.14}$$

The initial distribution for $(\tau_0, d_{-\tau_0-1})$ is given by $\alpha = (\alpha_{(i,r)})$, where $i \in \mathcal{M}$, $r \in \mathcal{N}$ and $\sum_{i \in \mathcal{M},\ r \in \mathcal{N}} \alpha_{(i,r)} = 1$.

3.4.1 Definitions of H_2 and H_∞ norms

For a stable discrete-time LTI system, the classical H_2 norm has the following interpretation: The l_2 norm of the output equals the H_2 norm of the system if the input is the unit impulse [20]. A definition of H_2 norm for MJLSs is given in [22]. As the closed-loop system under consideration is formulated as a special discrete-time jump linear system, the definitions of the classical norm and MJLS norm are not suitable and need to be modified to reflect the special dynamics. Following the general definition of the H_2 norms of the LTI system and MJLS, the following H_2 norm for the special system (3.13) is defined, which can be used as a performance index.

Definition 3.3. The H_2 norm of system (3.13) is defined as

$$\|H_{y\omega}\|_2^2 = \sum_{s=1}^{l} \sum_{i=0}^{\tau} \sum_{r=0}^{d} \alpha_{(i,r)} \|\mathcal{E}(y_{s,i,r})\|_2^2, \tag{3.15}$$

where $y_{s,i,r}$ is the output sequence of system (3.13) when

(1) the input sequence is given by $\omega = (\omega(0), \omega(1), \cdots)$, $\omega(0) = e_s$, $\omega(k) = 0$, $k > 0$, $e_s \in \mathbb{R}^l$ the unitary vector formed by one at the sth position and zero elsewhere;

(2) $\tau(0) = i$;

(3) $d(-\tau_0 - 1) = r$.

Remark 3.2. When $\tau = 0$, $d = 0$, the above definition of H_2 norm is reduced to the classical H_2 norm. Hence, the definition can be view as a generalization of the H_2 norm from LTI systems to the special jump linear system. Moreover, when $d = 0$, the Definition 3.3 is reduced to the H_2 norm for MJLSs [22].

The definition of classical H_∞ norm for LTI systems can be interpreted as a measure of robust stability that represents the worst-case energy attenuation for any energy-bounded disturbance. Following this, the H_∞ norm for the special system is defined as follows.

Definition 3.4. Let $X(0) = 0$ and define the H_∞ norm as

$$\|H_{y\omega}\|_\infty = \sup_{\tau(0)\in\mathcal{M}} \sup_{d(-\tau_0-1)\in\mathcal{N}} \sup_{\omega\in l_2(0,\infty)} \frac{\|y\|_2}{\|\omega\|_2}. \tag{3.16}$$

The following theorem establishes the relation between the H_2 norm and the state-space model of the jump linear system.

Theorem 3.2.

$$\|H_{y\omega}\|_2^2 = \sum_{i=0}^{\tau}\sum_{r=0}^{d}\sum_{j=0}^{\tau}\sum_{s_1=0}^{d} \alpha_{(i,r)}\lambda_{ij}\Pi_{rs_1}^{1+i-j}\mathrm{tr}\left\{\tilde{J}^\mathrm{T}S(j,s_1)\tilde{J}\right\}, \tag{3.17}$$

where $S(i,r) > 0$ is the observability gramian obtained from the following discrete-time Lyapunov equation

$$S(i,r) = \sum_{j=0}^{\tau}\sum_{s_1=0}^{d}\sum_{s_2=0}^{d} \lambda_{ij}\Pi_{rs_2}^{1+i-j}\Pi_{s_2s_1}^{j}\left[\hat{A}(i,r,s_1)\right]^\mathrm{T} \times S(j,s_2)\left[\hat{A}(i,r,s_1)\right] + \tilde{C}^\mathrm{T}\tilde{C}. \tag{3.18}$$

Proof. Suppose that $y(k)$ is an impulse response of system (3.13). Then, for $k \geq 1$ and considering (3.18), the following equation can be obtained.

$$\mathcal{E}\left[y(k)^\mathrm{T}y(k)\right] \tag{3.19}$$

$$= \mathcal{E}\left[X(k)^\mathrm{T}\tilde{C}^\mathrm{T}\tilde{C}X(k)\right]$$

$$= \mathcal{E}\left\{X(k)^\mathrm{T}\left[S(i,r) - \sum_{j=0}^{\tau}\sum_{s_1=0}^{d}\sum_{s_2=0}^{d} \lambda_{ij}\Pi_{rs_2}^{1+i-j}\Pi_{s_2s_1}^{j}\hat{A}(i,r,s_1)^\mathrm{T}S(j,s_2)\hat{A}(i,r,s_1)\right]X(k)\right\}$$

$$= \mathcal{E}\left\{X(k)^\mathrm{T}S(i,r)X(k)\right\}$$

$$- \mathcal{E}\left\{\sum_{j=0}^{\tau}\sum_{s_1=0}^{d}\sum_{s_2=0}^{d} \lambda_{ij}\Pi_{rs_2}^{1+i-j}\Pi_{s_2s_1}^{j}X(k)^\mathrm{T}\hat{A}(i,r,s_1)^\mathrm{T}S(j,s_2)\hat{A}(i,r,s_1)X(k)\right\}. \tag{3.20}$$

Here, $i = \tau_k$, $r = d_{k-\tau_k-1}$. Note that the second term in (3.20) is the mathematical expectation of $X(k+1)^\mathrm{T}S(\tau_{k+1}, d_{k-\tau_{k+1}})X(k+1)$ based on the information of previous step: $X(k)$, τ_k, and $d_{k-\tau_k-1}$. Define $\tau_{k+1} = j, d_k = s_1, d_{k-\tau_{k+1}} = s_2$. The probability transition matrices for $\tau_k \to \tau_{k+1}$, $d_{k-i-1} \to d_{k-j}$, and $d_{k-j} \to d_k$ are needed to evaluate the second term in (3.20). According to (3.13) and Lemma 2.1, these three probability transition matrices are

$$\tau_k \to \tau_{k+1} : \Lambda, \quad d_{k-i-1} \to d_{k-j} : \Pi^{1+i-j}, \quad d_{k-j} \to d_k : \Pi^j. \tag{3.21}$$

Then,

$$\mathcal{E}\left[X(k+1)^\mathrm{T}S(\tau_{k+1}, d_{k-\tau_{k+1}})X(k+1)\right]$$

$$= \sum_{j=0}^{\tau}\sum_{s_1=0}^{d}\sum_{s_2=0}^{d} \lambda_{ij}\Pi_{rs_2}^{1+i-j}\Pi_{s_2s_1}^{j}X(k)^\mathrm{T}\hat{A}(i,r,s_1)^\mathrm{T}S(j,s_2)\hat{A}(i,r,s_1)X(k).$$

Further, (3.19) can be rewritten as

$$\mathcal{E}\left[y(k)^\mathrm{T}y(k)\right] = \mathcal{E}\left[X(k)^\mathrm{T}S(\tau_k, d_{k-\tau_k-1})X(k)\right] - \mathcal{E}\left[X(k+1)^\mathrm{T}S(\tau_{k+1}, d_{k-\tau_{k+1}})X(k+1)\right]. \tag{3.22}$$

Notice that $S(i,r)$ in (3.18) satisfies the inequalities (3.9). Hence, the system (3.13) is stochastically stable. Further, it is mean square stable. Recalling that $\mathcal{E}(\|X(k)\|)^2 \to 0$ as $k \to \infty$, and taking the sum of (3.22) from 1 to ∞ , the following can be obtained:

$$
\begin{aligned}
\|\mathcal{E}(y_{s,i,j})\|_2^2 &= \sum_{k=1}^{\infty} \|\mathcal{E}\left[y_{s,i,j}(k)\right]\|^2 \big|_{\tau_0,d-\tau_0-1} \\
&= \mathcal{E}\left\{X(1)^{\mathrm{T}} S(\tau_1, d_{-\tau_1}) X(1)|_{\tau_0,d-\tau_0-1}\right\} \\
&= \mathcal{E}\left\{e_s^{\mathrm{T}} \tilde{J}^{\mathrm{T}} S(\tau_1, d_{-\tau_1}) \tilde{J} e_s\right\} \\
&= \sum_{j=0}^{\tau} \sum_{s_1=0}^{d} \lambda_{ij} \Pi_{rs_1}^{1+i-j} \left\{e_s^{\mathrm{T}} \tilde{J}^{\mathrm{T}} S(j, s_2) \tilde{J} e_s\right\}.
\end{aligned}
$$

Thus,

$$
\|H_{y\omega}\|_2^2 = \sum_{s=1}^{l} \sum_{i=0}^{\tau} \sum_{r=0}^{d} \alpha_{(i,r)} \|\mathcal{E}(y_{s,i,j})\|_2^2 = \sum_{i=0}^{\tau} \sum_{r=0}^{d} \sum_{j=0}^{\tau} \sum_{s_1=0}^{d} \alpha_{(i,r)} \lambda_{ij} \Pi_{rs_1}^{1+i-j} \mathrm{tr}\left\{\tilde{J}^{\mathrm{T}} S(j, s_2) \tilde{J}\right\}.
$$

This completes the proof. □

3.4.2 Mixed H_2/H_∞ control

In this section, the robust mixed H_2/H_∞ control problem for system (3.13) is solved in term of LMIs with nonconvex constraints. The following theorem provides the sufficient condition for mixed H_2/H_∞ control.

Theorem 3.3 (Mixed H_2/H_∞ Control). If

$$
\sum_{j=0}^{\tau} \sum_{s_1=0}^{d} \sum_{s_2=0}^{d} \lambda_{ij} \Pi_{rs_2}^{1+i-j} \Pi_{s_2 s_1}^{j} \hat{A}(i,r,s_1)^{\mathrm{T}} P(j,s_2) \hat{A}(i,r,s_1) + \tilde{C}^{\mathrm{T}} \tilde{C} + \frac{1}{\gamma^2} P(i,r) \tilde{J} \tilde{J}^{\mathrm{T}} P(i,r) < P(i,r),
$$
(3.23)

then system (3.13) is stochastically stable, $\|H_{y\omega}\|_\infty < \gamma$,
and $\|H_{y\omega}\|_2^2 \leq \sum_{i=0}^{\tau} \sum_{r=0}^{d} \sum_{j=0}^{\tau} \sum_{s_1=0}^{d} \alpha_{(i,r)} \lambda_{ij} \Pi_{rs_1}^{1+i-j} \mathrm{tr}\left\{\tilde{J}^{\mathrm{T}} P(j,s_1) \tilde{J}\right\}$.

Proof. It is easy to obtain that inequality (3.23) implies the inequality (3.9). Hence, system (3.13) is stochastically stable.

$$
\begin{aligned}
&\mathcal{E}\left\{X(k+1)^{\mathrm{T}} P(\tau_{k+1}, d_{k-\tau_{k+1}}) X(k+1)\right\} \\
=\ &\mathcal{E}\left\{X(k)^{\mathrm{T}} \hat{A}(\tau_k, d_{k-\tau_k-1}, d_k)^{\mathrm{T}} P(\tau_{k+1}, d_{k-\tau_{k+1}}) \hat{A}(\tau_k, d_{k-\tau_k-1}, d_k) X(k)\right\} \\
&+\mathcal{E}\left\{\omega(k)^{\mathrm{T}} \tilde{J}^{\mathrm{T}} P(\tau_{k+1}, d_{k-\tau_{k+1}}) \hat{A}(\tau_k, d_{k-\tau_k-1}, d_k) X(k)\right\} \\
&+\mathcal{E}\left\{X(k)^{\mathrm{T}} \hat{A}(\tau_k, d_{k-\tau_k-1}, d_k)^{\mathrm{T}} P(\tau_{k+1}, d_{k-\tau_{k+1}}) \tilde{J} \omega(k)\right\} \\
&+\mathcal{E}\left\{\omega(k)^{\mathrm{T}} \tilde{J}^{\mathrm{T}} P(\tau_{k+1}, d_{k-\tau_{k+1}}) \tilde{J} \omega(k)\right\} \\
<\ &\mathcal{E}\left\{X(k)^{\mathrm{T}} \left[P(\tau_k, d_{k-\tau_k-1}) - \tilde{C}^{\mathrm{T}} \tilde{C} - \frac{1}{\gamma^2} P(i,r) \tilde{J} \tilde{J}^{\mathrm{T}} P(i,r)\right] X(k)\right\}
\end{aligned}
$$

$$+\mathcal{E}\left\{\omega(k)^{\mathrm{T}}\tilde{J}^{\mathrm{T}}P(\tau_{k+1},d_{k-\tau_{k+1}})\hat{A}(\tau_k,d_{k-\tau_k-1},d_k)X(k)\right\}$$

$$+\mathcal{E}\left\{X(k)^{\mathrm{T}}\hat{A}(\tau_k,d_{k-\tau_k-1},d_k)^{\mathrm{T}}P(\tau_{k+1},d_{k-\tau_{k+1}})\tilde{J}\omega(k)\right\}$$

$$+\mathcal{E}\left\{\omega(k)^{\mathrm{T}}\tilde{J}^{\mathrm{T}}P(\tau_{k+1},d_{k-\tau_{k+1}})\tilde{J}\omega(k)\right\}. \tag{3.24}$$

So that

$$\|P(\tau_{k+1},d_{k-\tau_{k+1}})^{\frac{1}{2}}x(k+1)\|_2^2-\|P(\tau_k,d_{k-\tau_k-1})^{\frac{1}{2}}x(k)\|_2^2+\|y(k)\|_2^2$$

$$<\quad -\frac{1}{\gamma^2}\|\tilde{J}^{\mathrm{T}}P(\tau_k,d_{k-\tau_k-1})x(k)\|_2^2$$

$$+\mathcal{E}\left\{\omega(k)^{\mathrm{T}}\tilde{J}^{\mathrm{T}}P(\tau_{k+1},d_{k-\tau_{k+1}})\hat{A}(\tau_k,d_{k-\tau_k-1},d_k)X(k)\right\}$$

$$+\mathcal{E}\left\{X(k)^{\mathrm{T}}\hat{A}(\tau_k,d_{k-\tau_k-1},d_k)^{\mathrm{T}}P(\tau_{k+1},d_{k-\tau_{k+1}})\tilde{J}\omega(k)\right\}$$

$$+\mathcal{E}\left\{\omega(k)^{\mathrm{T}}\tilde{J}^{\mathrm{T}}P(\tau_{k+1},d_{k-\tau_{k+1}})\tilde{J}\omega(k)\right\}$$

$$=\quad -\frac{1}{\gamma^2}\|\tilde{J}^{\mathrm{T}}P(\tau_k,d_{k-\tau_k-1})x(k)\|_2^2+\frac{1}{\gamma^2}\|\tilde{J}^{\mathrm{T}}P(\tau_{k+1},d_{k-\tau_{k+1}})x(k+1)\|_2^2$$

$$-\frac{1}{\gamma^2}\|\tilde{J}^{\mathrm{T}}P(\tau_{k+1},d_{k-\tau_{k+1}})x(k+1)\|_2^2$$

$$+2\mathcal{E}\left\{\omega(k)^{\mathrm{T}}\tilde{J}^{\mathrm{T}}P(\tau_{k+1},d_{k-\tau_{k+1}})\left\{\hat{A}(\tau_k,d_{k-\tau_k-1},d_k)X(k)+\tilde{J}\omega(k)\right\}\right\} \tag{3.25}$$

$$-\mathcal{E}\left\{\omega(k)^{\mathrm{T}}\tilde{J}^{\mathrm{T}}P(\tau_{k+1},d_{k-\tau_{k+1}})\tilde{J}\omega(k)\right\}.$$

Thus,

$$\|P(\tau_{k+1},d_{k-\tau_{k+1}})^{\frac{1}{2}}x(k+1)\|_2^2-\|P(\tau_k,d_{k-\tau_k-1})^{\frac{1}{2}}x(k)\|_2^2+\|y(k)\|_2^2$$

$$-\frac{1}{\gamma^2}\|\tilde{J}^{\mathrm{T}}P(\tau_{k+1},d_{k-\tau_{k+1}})x(k+1)\|_2^2+\frac{1}{\gamma^2}\|\tilde{J}^{\mathrm{T}}P(\tau_k,d_{k-\tau_k-1})x(k)\|_2^2$$

$$<\quad -\frac{1}{\gamma^2}\|\tilde{J}^{\mathrm{T}}P(\tau_{k+1},d_{k-\tau_{k+1}})x(k+1)\|_2^2+2\mathcal{E}\left\{\omega(k)^{\mathrm{T}}\tilde{J}^{\mathrm{T}}P(\tau_{k+1},d_{k-\tau_{k+1}})x(k+1)\right\}-\gamma^2\|\omega(k)\|_2^2$$

$$+\mathcal{E}\left\{\omega(k)^{\mathrm{T}}\left[\gamma^2I-\tilde{J}^{\mathrm{T}}P(\tau_{k+1},d_{k-\tau_{k+1}})\tilde{J}\right]\omega(k)\right\}$$

$$=\quad -\left\|\frac{1}{\gamma}\tilde{J}P(\tau_{k+1},d_{k-\tau_{k+1}})x(k+1)-\gamma\omega(k)\right\|_2^2+\mathcal{E}\left\{\omega(k)^{\mathrm{T}}\left[\gamma^2I-\tilde{J}^{\mathrm{T}}P(\tau_{k+1},d_{k-\tau_{k+1}})\tilde{J}\right]\omega(k)\right\}$$

$$\leq\quad \mathcal{E}\left\{\omega(k)^{\mathrm{T}}\left[\gamma^2I-\tilde{J}^{\mathrm{T}}P(\tau_{k+1},d_{k-\tau_{k+1}})\tilde{J}\right]\omega(k)\right\}$$

Taking the sum from $k=0$ to ∞, and recalling that $X(0)=0$, $\|X(k)\|_2\to0$ as $k\to\infty$, the following can be obtained:

$$\|y\|_2^2\quad\leq\quad\sum_{k=0}^{\infty}\mathcal{E}\left\{\omega(k)^{\mathrm{T}}\left[\gamma^2I-\tilde{J}^{\mathrm{T}}P(\tau_{k+1},d_{k-\tau_{k+1}})\tilde{J}\right]\omega(k)\right\}=\gamma^2(1-v)\|\omega\|_2^2\leq\gamma^2\|\omega\|_2^2,$$

where $v\in\left(0,\frac{1}{\gamma^2}\sum_{i=0}^{\tau}\sum_{j=0}^{d}\mathrm{tr}(\tilde{J}^{\mathrm{T}}P(i,r)\tilde{J})\right)$. Thus, $\frac{\|y\|_2}{\|\omega\|_2}<\gamma$.

Moreover, considering the Theorem 3.2 and the monotonically decreasing property of (3.10), and comparing (3.18) and (3.23), $P(i,r)>S(i,r)$ can be obtained. Then, it is straightforward that

$$\|H_{y\omega}\|_2^2\quad=\quad\sum_{i=0}^{\tau}\sum_{r=0}^{d}\sum_{j=0}^{\tau}\sum_{s_1=0}^{d}\alpha_{(i,r)}\lambda_{ij}\Pi_{rs_1}^{1+i-j}\mathrm{tr}\left\{\tilde{J}^{\mathrm{T}}S(j,s_1)\tilde{J}\right\}$$

35

$$\leq \sum_{i=0}^{\tau}\sum_{r=0}^{d}\sum_{j=0}^{\tau}\sum_{s_1=0}^{d}\alpha_{(i,r)}\lambda_{ij}\Pi_{rs_1}^{1+i-j}\mathrm{tr}\left\{\tilde{J}^{\mathrm{T}}P(j,s_1)\tilde{J}\right\}.$$

This completes the proof. □

The condition (3.23) is difficult to check because it is nonlinear. So, it is further transformed to an equivalent condition of a set of LMIs with nonconvex constraints shown in the following theorem.

Theorem 3.4. Under the proposed output feedback control law (3.3), the system (3.13) is stochastically stable, $\|H_{y\omega}\|_\infty < \gamma$, $\|H_{y\omega}\|_2^2 \leq \sum_{i=0}^{\tau}\sum_{r=0}^{d}\sum_{j=0}^{\tau}\sum_{s_1=0}^{d}\alpha_{(i,r)}\lambda_{ij}\Pi_{rs_1}^{1+i-j}\mathrm{tr}\left\{\tilde{J}^{\mathrm{T}}P(j,s_1)\tilde{J}\right\}$ if there exist matrices $F(i,r)$, $G(i,r)$, H, T, and symmetric matrices $\bar{X}(j,s_2) > 0$, $P(i,r) > 0$, satisfying:

$$\begin{bmatrix} -P(i,r)+\tilde{C}^{\mathrm{T}}\tilde{C} & V(i,r)^{\mathrm{T}} & \frac{1}{\gamma}P(i,r)\tilde{J} \\ V(i,r) & -X(i,r) & 0 \\ \frac{1}{\gamma}\tilde{J}^{\mathrm{T}}P(i,r) & 0 & -I \end{bmatrix} < 0, \qquad (3.26\text{a})$$

$$\bar{X}(j,s_2)P(j,s_2) = I, \qquad (3.26\text{b})$$

for all $i,j \in \mathcal{M}$ and $r, s_2 \in \mathcal{N}$, with

$$V(i,r) = \begin{bmatrix} V_0(i,r); & V_1(i,r); & \cdots & V_\tau(i,r); \end{bmatrix},$$

$$V_j(i,r) = \begin{bmatrix} V_{j,0}(i,r); & V_{j,1}(i,r); & \cdots & V_{j,d}(i,r); \end{bmatrix},$$

$$V_{j,s_2}(i,r) = \left[(\lambda_{ij}\Pi_{rs_2}^{1+i-j}\Pi_{s_20}^{j})^{\frac{1}{2}}[\tilde{A}+\tilde{I}_1 F(i,r)\tilde{I}_1{}^{\mathrm{T}}+\tilde{B}H\tilde{E}_1(0)+\tilde{B}T\tilde{E}_2(i,0)+\tilde{I}_1 G(i,r)\tilde{E}_3(i)];\right.$$

$$(\lambda_{ij}\Pi_{rs_2}^{1+i-j}\Pi_{s_21}^{j})^{\frac{1}{2}}[\tilde{A}+\tilde{I}_1 F(i,r)\tilde{I}_1{}^{\mathrm{T}}+\tilde{B}H\tilde{E}_1(1)+\tilde{B}T\tilde{E}_2(i,1)+\tilde{I}_1 G(i,r)\tilde{E}_3(i)];$$

$$\vdots$$

$$\left.(\lambda_{ij}\Pi_{rs_2}^{1+i-j}\Pi_{s_2d}^{j})^{\frac{1}{2}}[\tilde{A}+\tilde{I}_1 F(i,r)\tilde{I}_1{}^{\mathrm{T}}+\tilde{B}H\tilde{E}_1(d)+\tilde{B}T\tilde{E}_2(i,d)+\tilde{I}_1 G(i,r)\tilde{E}_3(i)]\right],$$

$$X(i,r) = \mathrm{diag}\{X_0(i,r) \quad X_1(i,r) \quad \cdots \quad X_\tau(i,r)\},$$

$$X_j(i,r) = \mathrm{diag}\{X_{j,0}(i,r) \quad X_{j,1}(i,r) \quad \cdots \quad X_{j,d}(i,r)\},$$

$$X_{j,s_2}(i,r) = \mathrm{diag}\left\{\underbrace{\bar{X}(j,s_2) \quad \bar{X}(j,s_2) \quad \cdots \quad \bar{X}(j,s_2)}_{d+1}\right\}. \qquad (3.27)$$

Proof. The theorem can be proved by using the Schur complement [8] and letting $\bar{X}(j,s_2) = P(j,s_2)^{-1}$. □

Theorem 3.4 provides the condition with LMIs and nonconvex constraints for the mixed H_2/H_∞ control problem. This can be efficiently used for the nominal systems without uncertainties. However, the condition in Theorem 3.4 is not easily solved for the systems with norm-bounded uncertainties. To deal with the uncertainties, it is converted to be an equivalent condition with the help of Lemma 3.1 shown in the following theorem.

Theorem 3.5. Under the proposed output feedback control law (3.3), the system (3.13) is stochastically stable and $\|H_{y\omega}\|_\infty < \gamma$, $\|H_{y\omega}\|_2^2 \leq \sum_{i=0}^{\tau} \sum_{r=0}^{d} \sum_{j=0}^{\tau} \sum_{s_1=0}^{d} \alpha_{(i,r)} \lambda_{ij} \Pi_{rs_1}^{1+i-j} \mathrm{tr}\left\{\tilde{J}^{\mathrm{T}} P(j, s_1)\tilde{J}\right\}$ if there exist matrices $F(i,r)$, $G(i,r)$, H, T and symmetric matrices $\bar{X}(j, s_2) > 0$, $P(i,r) > 0$ and a series of scalars $\varepsilon_1(i,r) > 0$, $\varepsilon_2(i,r) > 0$, $\cdots$, $\varepsilon_{(\tau+1)(d+1)(d+1)}(i,r) > 0$ satisfying:

$$
\begin{bmatrix}
-P(i,r) + \tilde{C}^{\mathrm{T}}\tilde{C} & Vc(i,r)^{\mathrm{T}} & \frac{1}{\gamma}P(i,r)\tilde{J} & \Delta V(i,r)^{\mathrm{T}} \\
Vc(i,r) & -X(i,r) + \hat{G}(i,r) & 0 & \\
\frac{1}{\gamma}\tilde{J}^{\mathrm{T}}P(i,r) & 0 & -I & 0 \\
\Delta V(i,r) & 0 & 0 & -\hat{\varepsilon}(i,r)I
\end{bmatrix} < 0, \qquad (3.28a)
$$

$$
\bar{X}(j, s_2)P(j, s_2) = I, \qquad (3.28b)
$$

with the matrices defined in (3.27) and

$$
\begin{aligned}
\hat{G}(i,r) &= \mathrm{diag}\{\varepsilon_1(i,r)\tilde{G}_1\tilde{G}_1^{\mathrm{T}} \quad \varepsilon_2(i,r)\tilde{G}_1\tilde{G}_1^{\mathrm{T}} \quad \cdots \quad \varepsilon_{(\tau+1)(d+1)(d+1)}(i,r)\tilde{G}_1\tilde{G}_1^{\mathrm{T}}\}, \\
\hat{\varepsilon}(i,r) &= \mathrm{diag}\{\varepsilon_1(i,r) \quad \varepsilon_2(i,r) \quad \cdots \quad \varepsilon_{(\tau+1)(d+1)(d+1)}(i,r)\}, \\
Vc_{(i,r)} &= \begin{bmatrix} Vc_0(i,r); & Vc_1(i,r); & \cdots; & Vc_\tau(i,r); \end{bmatrix}, \\
Vc_j(i,r) &= \begin{bmatrix} Vc_{j,0}(i,r); & Vc_{j,1}(i,r); & \cdots; & Vc_{j,d}(i,r;) \end{bmatrix}, \\
Vc_{j,s_2}(i,r) &= \Big[(\lambda_{ij}\Pi_{rs_2}^{1+i-j}\Pi_{s_20}^{j})^{\frac{1}{2}}[A_{Aug} + \tilde{I}_1 F(i,r)\tilde{I}_1^{\mathrm{T}} + B_{Aug}H\tilde{E}_1(0) + B_{Aug}T\tilde{E}_2(i,0) + \tilde{I}_1 G(i,r)\tilde{E}_3(i)]; \\
&\qquad (\lambda_{ij}\Pi_{rs_2}^{1+i-j}\Pi_{s_21}^{j})^{\frac{1}{2}}[A_{Aug} + \tilde{I}_1 F(i,r)\tilde{I}_1^{\mathrm{T}} + B_{Aug}H\tilde{E}_1(1) + B_{Aug}T\tilde{E}_2(i,1) + \tilde{I}_1 G(i,r)\tilde{E}_3(i)]; \\
&\qquad \vdots \\
&\qquad (\lambda_{ij}\Pi_{rs_2}^{1+i-j}\Pi_{s_2d}^{j})^{\frac{1}{2}}[A_{Aug} + \tilde{I}_1 F(i,r)\tilde{I}_1^{\mathrm{T}} + B_{Aug}H\tilde{E}_1(d) + B_{Aug}T\tilde{E}_2(i,d) + \tilde{I}_1 G(i,r)\tilde{E}_3(i)]\Big], \\
\Delta V(i,r) &= \begin{bmatrix} \Delta V_0(i,r); & \Delta V_1(i,r); & \cdots; & \Delta V_\tau(i,r); \end{bmatrix}, \\
\Delta V_j(i,r) &= \begin{bmatrix} \Delta V_{j,0}(i,r); & \Delta V_{j,1}(i,r); & \cdots; & \Delta V_{j,d}(i,r); \end{bmatrix}, \\
\Delta V_{j,s_2}(i,r) &= \Big[(\lambda_{ij}\Pi_{rs_2}^{1+i-j}\Pi_{s_20}^{j})^{\frac{1}{2}}[\tilde{G}_1\Delta_u U_1 I_2^{\mathrm{T}} + \tilde{G}_1\Delta_u U_2 H\tilde{E}_1(0) + \tilde{G}_1\Delta_u U_2 T\tilde{E}_2(i,0)]; \\
&\qquad (\lambda_{ij}\Pi_{rs_2}^{1+i-j}\Pi_{s_21}^{j})^{\frac{1}{2}}[\tilde{G}_1\Delta_u U_1 I_2^{\mathrm{T}} + \tilde{G}_1\Delta_u U_2 H\tilde{E}_1(1) + \tilde{G}_1\Delta_u U_2 T\tilde{E}_2(i,1)]; \\
&\qquad \vdots; \\
&\qquad (\lambda_{ij}\Pi_{rs_2}^{1+i-j}\Pi_{s_2d}^{j})^{\frac{1}{2}}[\tilde{G}_1\Delta_u U_1 I_2^{\mathrm{T}} + \tilde{G}_1\Delta_u U_2 H\tilde{E}_1(d) + \tilde{G}_1\Delta_u U_2 T\tilde{E}_2(i,d)]\Big], \\
\Delta Vu_{(i,r)} &= \begin{bmatrix} \Delta Vu_0(i,r); & \Delta Vu_1(i,r); & \cdots; & \Delta Vu_\tau(i,r); \end{bmatrix}, \\
\Delta Vu_j(i,r) &= \begin{bmatrix} \Delta Vu_{j,0}(i,r); & \Delta Vu_{j,1}(i,r); & \cdots; & \Delta Vu_{j,d}(i,r); \end{bmatrix}, \\
\Delta Vu_{j,s_2}(i,r) &= \Big[(\lambda_{ij}\Pi_{rs_2}^{1+i-j}\Pi_{s_20}^{j})^{\frac{1}{2}}[U_1 I_2^{\mathrm{T}} + U_2 H\tilde{E}_1(0) + U_2 T\tilde{E}_2(i,0)]; \\
&\qquad (\lambda_{ij}\Pi_{rs_2}^{1+i-j}\Pi_{s_21}^{j})^{\frac{1}{2}}[U_1 I_2^{\mathrm{T}} + U_2 H\tilde{E}_1(1) + U_2 T\tilde{E}_2(i,1)]; \\
&\qquad \vdots \\
&\qquad (\lambda_{ij}\Pi_{rs_2}^{1+i-j}\Pi_{s_2d}^{j})^{\frac{1}{2}}[U_1 I_2^{\mathrm{T}} + U_2 H\tilde{E}_1(d) + U_2 T\tilde{E}_2(i,d)]\Big].
\end{aligned}
$$

Proof. By applying Lemma 3.1 and Schur complement to inequality (3.26), inequalities (3.28) can be readily obtained. □

The conditions (3.28) contain a set of LMIs (3.28a) and nonconvex constraints (3.28b). This

can be efficiently solved by the PRA algorithm [24]. Detailed procedure about how to apply PRA to this problem can be referred to [146].

Now, the robust mixed H_2/H_∞ control method is presented: Let γ be a certain given value, minimize $\sum_{i=0}^{\tau} \sum_{r=0}^{d} \sum_{j=0}^{\tau} \sum_{s_1=0}^{d} \alpha_{(i,r)} \lambda_{ij} \Pi_{rs_1}^{1+i-j} \text{tr} \left\{ \tilde{J}^\mathsf{T} P(j, s_1) \tilde{J} \right\}$, subject to (3.28). If the focus is on the H_∞ norm, the problem is robust H_∞ control: Let γ be a variable, minimize γ subject to (3.28).

3.5   Numerical Examples

Consider an inverted pendulum system shown in Figure 3.1, where θ is the angular position of the pendulum, and u is the input torque. The state variables are chosen as $[\ \theta^\mathsf{T} \quad \dot{\theta}^\mathsf{T}\ ]^\mathsf{T}$. The output is $y = [\ \theta\ ]$. The parameters here are: $m = 0.1\ kg$, $L = 1\ m$. The output feedback controller is designed using the discrete-time model. Hence, the linearized nominal discrete-time system (sampling time $T_s = 0.05s$) is

$$
\begin{aligned}
x(k+1) &= A_d x(k) + B_d u(k) + J_d \omega(k), & \text{(3.29a)} \\
y(k) &= C_d x(k), & \text{(3.29b)}
\end{aligned}
$$

where

$$
A_d = \begin{bmatrix} 1.0123 & 0.0502 \\ 0.4920 & 1.0123 \end{bmatrix}, \quad B_d = \begin{bmatrix} 0.0125 \\ 0.5020 \end{bmatrix}, \quad J_d = \begin{bmatrix} 0.100 \\ 0.100 \end{bmatrix}, \quad C_d = \begin{bmatrix} 1 & 0 \end{bmatrix}. \quad \text{(3.30)}
$$

The eigenvalues of A_d are 0.7312 and 1.3676. Hence, the discrete-time system is unstable. The norm-bounded uncertainty matrices are

$$
G_1 = \begin{bmatrix} 0.01 \\ 0.5 \end{bmatrix}, \quad U_1 = \begin{bmatrix} 0.2 & 0.1 \end{bmatrix}, \quad U_2 = 0.1. \quad \text{(3.31)}
$$

The random delays involved in this NCS are assumed to be $\tau_k \in \{0, 1, 2\}$ and $d_k \in \{0, 1\}$, and their transition probability matrices are given by

$$
\Lambda = \begin{bmatrix} 0.5 & 0.5 & 0 \\ 0.3 & 0.6 & 0.1 \\ 0.3 & 0.6 & 0.1 \end{bmatrix}, \quad \Pi = \begin{bmatrix} 0.2 & 0.8 \\ 0.5 & 0.5 \end{bmatrix}.
$$

According to Proposition 2.1 in Section 2.3, the transition probability matrix for the delay mode jumping from d_{k-2} to d_k is Π^2.

The initial distribution for $(\tau_0, d_{-\tau_0-1})$ is equal for every $(\alpha_{(i,r)})$, where $i \in \mathcal{M}$, $r \in \mathcal{N}$, which means $\alpha_{(i,r)} = \frac{1}{6}$ in the following examples. To illustrate the performance of the design methods,
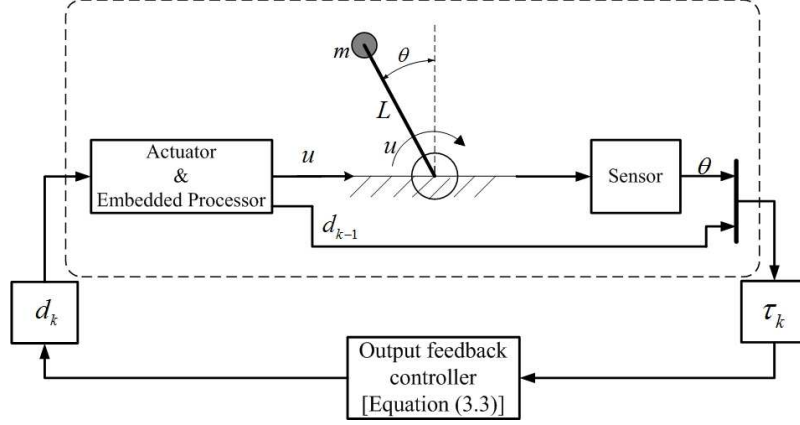
Figure 3.1: An inverted pendulum system.

let us select a set of input signals as follows:

$$
\omega(k) = \begin{cases}
1, & \text{for } 1 \le k \le 10, & \text{(3.32a)} \\
-1, & \text{for } 21 \le k \le 30, & \text{(3.32b)} \\
0, & \text{otherwise.} & \text{(3.32c)}
\end{cases}
$$

3.5.1 Mixed H_2/H_∞ control

Example 1: In this example, the mixed H_2/H_∞ control for the nominal system without uncertainties is considered. The system matrices are shown in (3.30). γ is set to be 2. By using Theorem 3.4, the minimum value of $\|H_{y\omega}\|_2$ can be obtained as $\|H_{y\omega}\|_2 = 0.31$ and the corresponding controller is

$$
\begin{aligned}
F(0,0) &= \begin{bmatrix} 0.6381 & -0.2795 \\ 1.5862 & 0.1193 \end{bmatrix}, \quad G(0,0) = \begin{bmatrix} -0.2839 \\ -0.2885 \end{bmatrix}, \\[1em]
F(0,1) &= \begin{bmatrix} 0.4230 & -0.1787 \\ 0.9434 & 0.4008 \end{bmatrix}, \quad G(0,1) = \begin{bmatrix} -0.2702 \\ -0.2701 \end{bmatrix}, \\[1em]
F(1,0) &= \begin{bmatrix} 0.4791 & -0.3242 \\ 0.8619 & 0.4258 \end{bmatrix}, \quad G(1,0) = \begin{bmatrix} -0.3429 \\ -0.2565 \end{bmatrix}, \\[1em]
F(1,1) &= \begin{bmatrix} 0.5538 & -0.3507 \\ 1.0446 & 0.3477 \end{bmatrix}, \quad G(1,1) = \begin{bmatrix} -0.3406 \\ -0.2605 \end{bmatrix}, \\[1em]
F(2,0) &= \begin{bmatrix} 1.0795 & -0.3557 \\ 0.6227 & 0.3569 \end{bmatrix}, \quad G(2,0) = \begin{bmatrix} -0.1968 \\ -0.3263 \end{bmatrix}, \\[1em]
F(2,1) &= \begin{bmatrix} 0.9886 & -0.3332 \\ 0.6021 & 0.4222 \end{bmatrix}, \quad G(2,1) = \begin{bmatrix} -0.2016 \\ -0.2880 \end{bmatrix}, \\[1em]
H &= \begin{bmatrix} 11.1873 & -9.7076 \end{bmatrix}, \quad T = \begin{bmatrix} -6.4574 \end{bmatrix}.
\end{aligned}
$$

The responses of θ and $\dot{\theta}$ are shown in Figures 3.2 and 3.3, respectively. By calculation, the
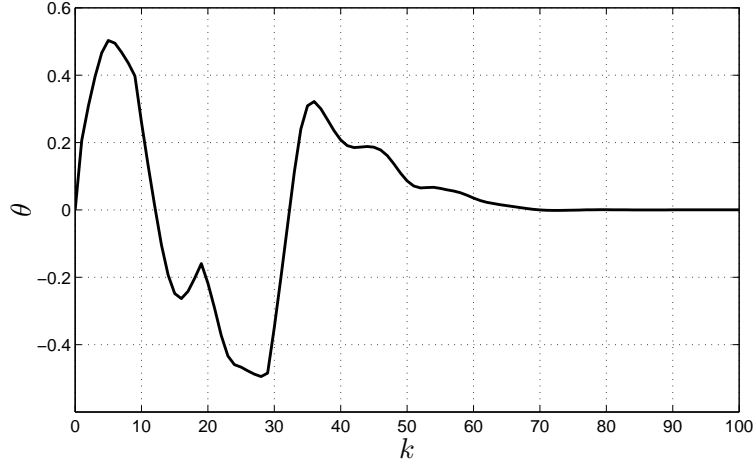
Figure 3.2: Mixed H_2/H_∞ control: The response of θ.
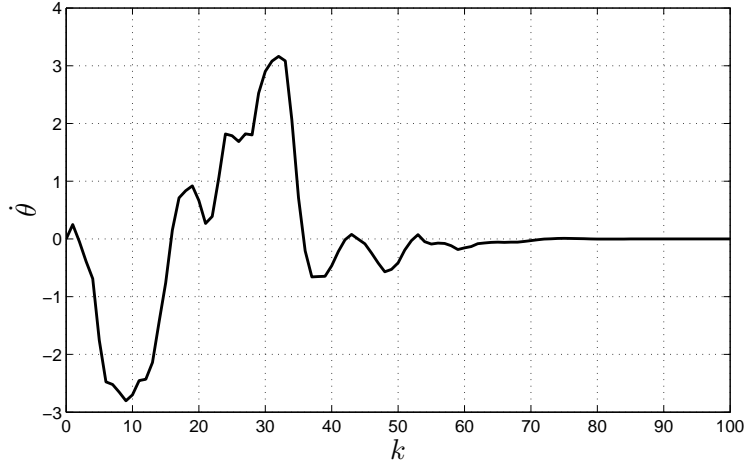
Figure 3.3: Mixed H_2/H_∞ control: The response of $\dot{\theta}$.

following can be obtained: $\|\omega\|_2 = 4.4721$, $\|y\|_2 = 2.1914$, which yields

$$\frac{\|y\|_2}{\|\omega\|_2} = 0.4900 < \gamma = 2.$$

The impulse response can also be calculated according to Definition 3.3 and the result is

$$\sqrt{\sum_{s=1}^{l}\sum_{i=0}^{\tau}\sum_{r=0}^{d}\alpha_{(i,r)}\|y_{s,i,r}\|_2^2} = 0.2402 < 0.31.$$

The above simulation results show the effectiveness of the mixed H_2/H_∞ control.

Example 2: In this example, the robust mixed H_2/H_∞ control for the inverted pendulum system will be considered. The system matrices are shown in (3.30) and the norm-bounded uncertainty is shown in (3.31). γ is set to be 2. By using Theorem 3.5, the minimum value of $\|H_{y\omega}\|_2$

can be obtained as $\|H_{y\omega}\|_2 = 0.43$ and the corresponding controller is

$$F(0,0) = \begin{bmatrix} 0.5054 & -0.2679 \\ 1.3869 & 0.1546 \end{bmatrix}, \quad G(0,0) = \begin{bmatrix} -0.3254 \\ -0.2921 \end{bmatrix},$$

$$F(0,1) = \begin{bmatrix} 0.4119 & -0.2106 \\ 0.9760 & 0.3572 \end{bmatrix}, \quad G(0,1) = \begin{bmatrix} -0.3099 \\ -0.2635 \end{bmatrix},$$

$$F(1,0) = \begin{bmatrix} 0.5402 & -0.4101 \\ 0.8231 & 0.3720 \end{bmatrix}, \quad G(1,0) = \begin{bmatrix} -0.4086 \\ -0.2843 \end{bmatrix},$$

$$F(1,1) = \begin{bmatrix} 0.5504 & -0.4296 \\ 0.9382 & 0.3121 \end{bmatrix}, \quad G(1,1) = \begin{bmatrix} -0.4195 \\ -0.2945 \end{bmatrix},$$

$$F(2,0) = \begin{bmatrix} 1.0342 & -0.3214 \\ 0.6951 & 0.3028 \end{bmatrix}, \quad G(2,0) = \begin{bmatrix} -0.1968 \\ -0.3476 \end{bmatrix},$$

$$F(2,1) = \begin{bmatrix} 0.9891 & -0.3273 \\ 0.6734 & 0.3640 \end{bmatrix}, \quad G(2,1) = \begin{bmatrix} -0.2149 \\ -0.3093 \end{bmatrix},$$

$$H = \begin{bmatrix} 10.6207 & -9.6592 \end{bmatrix}, T = \begin{bmatrix} -6.5343 \end{bmatrix}.$$
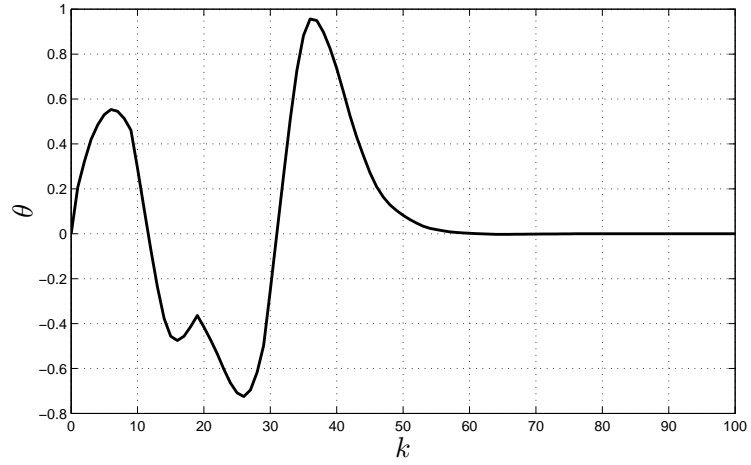
Figure 3.4: Robust mixed H_2/H_∞ control: The response of θ.

In the simulation, it is assumed $\Delta_u = \sin(t)$, and it can be seen that $\Delta_u^{\mathrm{T}}\Delta_u \leq 1$. The responses of θ and $\dot{\theta}$ are shown in Figures 3.4 and 3.5. By calculation, the following can be obtained: $\|\omega\|_2 = 4.4721$, $\|y\|_2 = 3.6761$, which yields

$$\frac{\|y\|_2}{\|\omega\|_2} = 0.8220 < \gamma = 2.$$
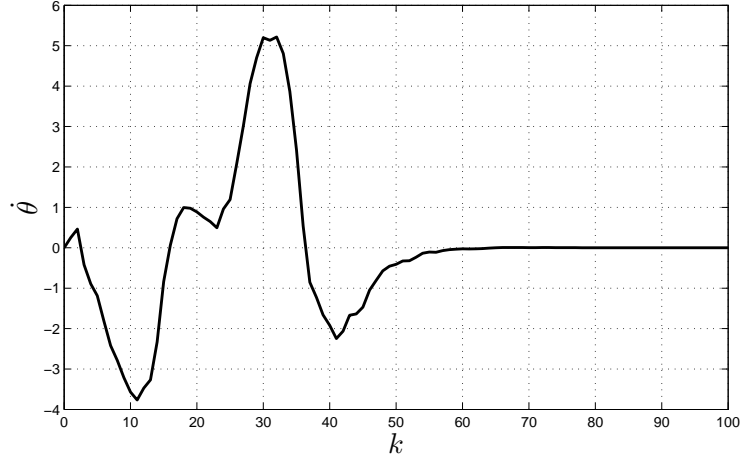
Figure 3.5: Robust mixed H_2/H_∞ control: The response of $\dot\theta$.

The impulse response can also be calculated according to Definition 3.3 and the result is

$$\sqrt{\sum_{s=1}^{l}\sum_{i=0}^{\tau}\sum_{r=0}^{d}\alpha_{(i,r)}\|y_{s,i,r}\|_2^2} = 0.2613 < 0.43.$$

From the above simulation results, it is observed that the system is stabilized and control performance is satisfied in the presence of parameter uncertainties.

3.5.2 H_∞ control

Example 3: In this example, the H_∞ control for the nominal system without uncertainties is considered. The system matrices are shown in (3.30). The minimal value of γ obtained is 0.85. The corresponding controller matrices are

$$F(0,0) = \begin{bmatrix} 0.4972 & -0.3050 \\ 1.2544 & 0.1776 \end{bmatrix}, \quad G(0,0) = \begin{bmatrix} -0.3675 \\ -0.3192 \end{bmatrix},$$

$$F(0,1) = \begin{bmatrix} 0.4405 & -0.2485 \\ 0.9726 & 0.3875 \end{bmatrix}, \quad G(0,1) = \begin{bmatrix} -0.3468 \\ -0.2649 \end{bmatrix},$$

$$F(1,0) = \begin{bmatrix} 0.5433 & -0.5043 \\ 0.8023 & 0.3694 \end{bmatrix}, \quad G(1,0) = \begin{bmatrix} -0.4987 \\ -0.3174 \end{bmatrix},$$

$$F(1,1) = \begin{bmatrix} 0.5514 & -0.5177 \\ 0.8758 & 0.3074 \end{bmatrix}, \quad G(1,1) = \begin{bmatrix} -0.5052 \\ -0.3364 \end{bmatrix},$$

$$F(2,0) = \begin{bmatrix} 1.1625 & -0.3722 \\ 0.7598 & 0.2785 \end{bmatrix}, \quad G(2,0) = \begin{bmatrix} -0.2011 \\ -0.3740 \end{bmatrix},$$

$$F(2,1) = \begin{bmatrix} 1.1377 & -0.3831 \\ 0.7387 & 0.3313 \end{bmatrix}, \quad G(2,1) = \begin{bmatrix} -0.2197 \\ -0.3408 \end{bmatrix},$$

$$H \;\; = \;\; \left[\begin{array}{cc} 10.5759 & -9.5935 \end{array}\right], \;\; T = \left[\begin{array}{c} -6.5916 \end{array}\right].$$

Figures 3.6 and 3.7 depict the responses of θ and $\dot{\theta}$, respectively. By calculation, $\|\omega\|_2 = 4.4721$ and $\|y\|_2 = 1.9040$ can be obtained, which yield

$$\frac{\|y\|_2}{\|\omega\|_2} = 0.4257 < 0.85,$$

showing the effectiveness of the H_∞ control.
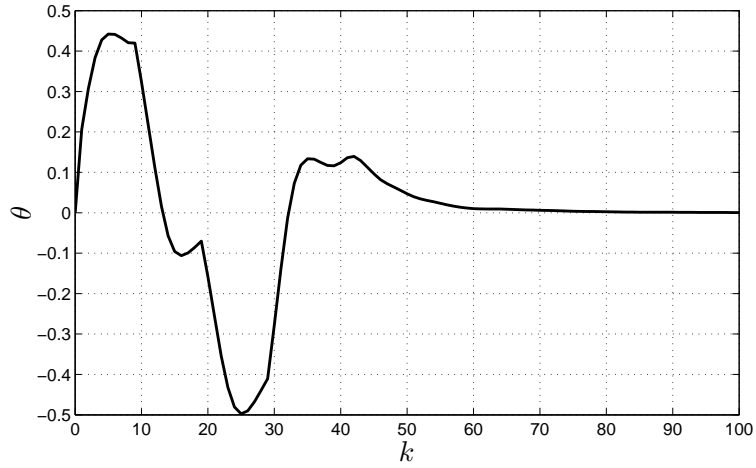
Figure 3.6: H_∞ control: The response of θ.
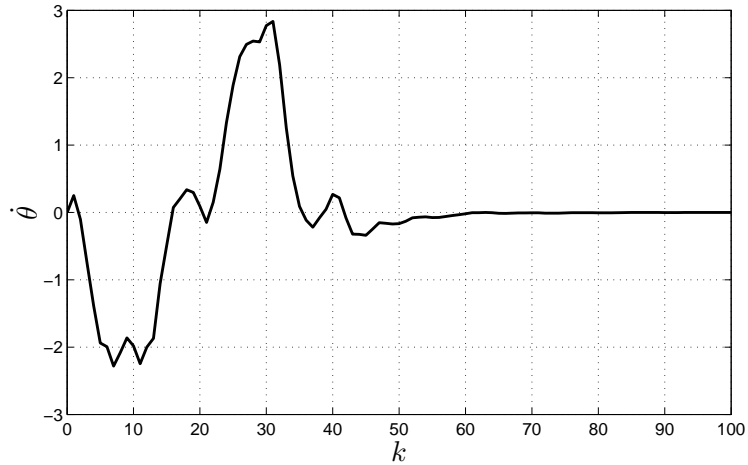
Figure 3.7: H_∞ control: The response of $\dot{\theta}$.

Example 4: In this example, the robust H_∞ control for the inverted pendulum system is considered. The system matrices are shown in (3.30) and the norm-bounded uncertainty is shown in (3.31). The minimal value of γ obtained is 1.16. The corresponding controller matrices are

$$F(0,0) \;\; = \;\; \left[\begin{array}{cc} 0.4675 & -0.2801 \\ 1.4334 & 0.1386 \end{array}\right], \;\; G(0,0) = \left[\begin{array}{c} -0.3539 \\ -0.3408 \end{array}\right],$$

43

$$
F(0,1) = \begin{bmatrix} 0.4170 & -0.2416 \\ 1.1179 & 0.2991 \end{bmatrix}, \quad G(0,1) = \begin{bmatrix} -0.3391 \\ -0.3104 \end{bmatrix},
$$

$$
F(1,0) = \begin{bmatrix} 0.5662 & -0.5119 \\ 0.8448 & 0.2272 \end{bmatrix}, \quad G(1,0) = \begin{bmatrix} -0.5055 \\ -0.4361 \end{bmatrix},
$$

$$
F(1,1) = \begin{bmatrix} 0.5731 & -0.5225 \\ 0.9123 & 0.1806 \end{bmatrix}, \quad G(1,1) = \begin{bmatrix} -0.5115 \\ -0.4518 \end{bmatrix},
$$

$$
F(2,0) = \begin{bmatrix} 1.1922 & -0.4205 \\ 0.9357 & 0.1575 \end{bmatrix}, \quad G(2,0) = \begin{bmatrix} -0.2640 \\ -0.4489 \end{bmatrix},
$$

$$
F(2,1) = \begin{bmatrix} 1.1872 & -0.4391 \\ 0.9108 & 0.2002 \end{bmatrix}, \quad G(2,1) = \begin{bmatrix} -0.2818 \\ -0.4225 \end{bmatrix},
$$

$$
H = \begin{bmatrix} 11.4773 & -10.7035 \end{bmatrix}, \quad T = \begin{bmatrix} -7.7051 \end{bmatrix}.
$$

Figures 3.8 and 3.9 depict the responses of θ and $\dot{\theta}$, respectively. By calculation, $\|\omega\|_2 = 4.4721$ and $\|y\|_2 = 2.2181$ can be obtained, which yield

$$
\frac{\|y\|_2}{\|\omega\|_2} = 0.4960 < 1.16.
$$

From the simulation results, it can be observed that the proposed robust H_∞ control method can achieve the control performance in the presence of norm-bounded uncertainties in the plant.
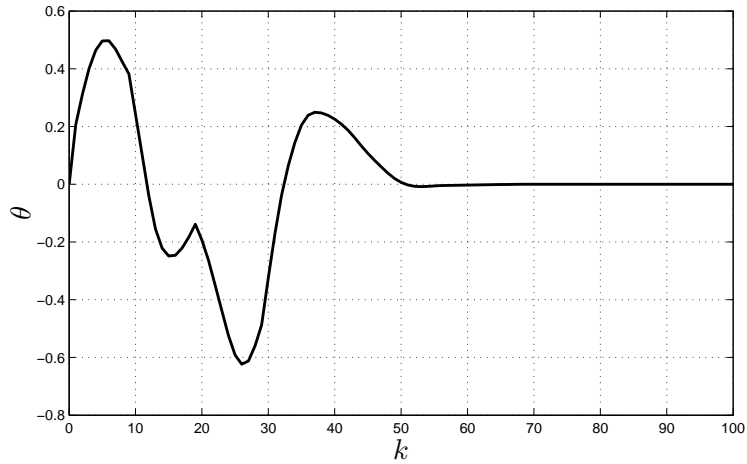
Figure 3.8: Robust H_∞ control: The response of θ.

3.6 Conclusion

In this chapter, the controller design problem in Chapter 2 is further studied. The H_2 and H_∞ norms for this special system are defined. The robust mixed H_2/H_∞ control problem is solved
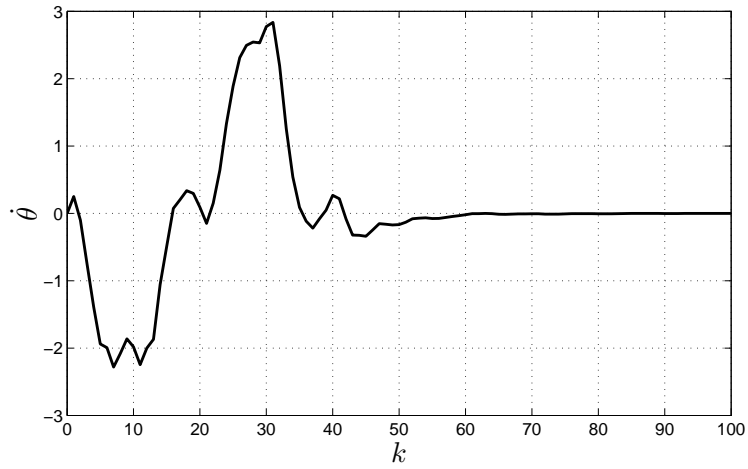
Figure 3.9: Robust H_∞ control: The response of $\dot{\theta}$.

under the framework of LMIs. The condition is a set of LMIs with nonconvex constraints, which are efficiently solved by PRA. Design examples are given to illustrate the effectiveness of proposed methods.

CHAPTER 4

MODIFIED GENERALIZED PREDICTIVE CONTROL FOR
NETWORKED SYSTEMS WITH APPLICATION TO A HY-
DRAULIC POSITION CONTROL SYSTEM

4.1 Introduction

The study of control systems in which the data between the controller side and plant side are exchanged via a communication network has recently received much attention. This type of system falls into the class of networked control system (NCS) [52, 119, 127, 148]. The use of networks has several attractive advantages such as reduced equipment wiring, low installation cost, ease of maintenance, easy installation, and flexible reconfiguration. There are, nevertheless, several problems such as network-induced time delays, packet dropouts, and quantization errors, which can greatly degrade the closed-loop system performance or even deteriorate the stability. These network-induced problems present new challenges to the control design. Among all the challenges, study on the network-induce delay has attracted much attention [87, 133, 147].

In an NCS illustrated in Figure 4.1, there are two types of time delays: Sensor-to-controller (S-C) and controller-to-actuator (C-A) delays. The S-C delays exist in the S-C link and can be obtained by using the time-stamping technique [55]. Hence, the S-C delay information is available at the controller node. The other type of time delay is the C-A delay existing in the C-A links. Different from the S-C delay, the current C-A delay cannot be known at the controller node when the control actions are generated by the controller. In fact, the control signal that has been sent out and transmitted to the actuator node has to suffer from the unknown C-A delays. Therefore, it is more challenging yet demanding to compensate for the C-A delays to improve the control system performance. Generally, to handle the network-induced delay problem for NCS design, two questions are to be addressed: (1) How to model the network-induced delays? (2) How to incorporate the delay information into the controller design? In the literature, the network-induced delays in NCSs have been modeled as constant delays [87], random but bounded delays [40], and random delays governed by a Markov process [87, 130, 133, 147]. The advantages of modeling

network-induced delays as Markov chains lie in that it takes the dependency of the delays into account and the packet dropouts can be included naturally [133]. In [87], the LQG control is applied to the NCS by modeling the time delays as Markov chains. But the time delay is assumed to be less than one sampling period. In [133], the authors design both delay-independent and delay-dependent controllers for NCSs with S-C and C-A delays modeled by Markov chains under the framework of jump linear systems. In [100], the H_∞ control problem of NCSs with time delays modeled by Markov chains is solved using the bounded real lemma, but only the S-C time delays are considered. In [56, 142, 147], the delay-dependent state feedback controller design problems are considered; the controllers depend on both C-A and S-C time delays modeled by Markov processes.

How to compensate for the C-A network-induced delay is a challenging issue. A natural idea is to employ a predicted signal (if available) to replace the delayed one whenever the C-A delay exists. Model predictive control (MPC) does have the prediction feature: At each time step, it not only generates the current control signal, but also a sequence of future control signals, under certain optimal settings. MPC has been one of the most popular advanced control methods in industry [13]. Recently, MPC strategies have been used in the NCS design [47, 72–74, 90, 131, 141, 152]. In [141], the authors employ the dynamic matrix control (DMC) method with a variable sampling time to compensate for the time delays; however, no stability analysis is provided. In [131], a state feedback controller is designed using the MPC approach; both S-C and C-A delays are modeled as Markov chains and the stochastic delay-dependent stability conditions are presented. In [72], Liu *et al.* propose a modified generalized predictive control (GPC) method to compensate for the time delays and data packet dropouts. In [117], the authors extend the GPC to compensate for the delays and propose an adaptive predictive control method with variable prediction horizons; but, the stability is not addressed. In [65], model-based estimation algorithms are developed to compensate for time delays and packet losses, but no stability analysis is given. Novel observer-based predictive controllers are proposed by incorporating only the C-A delays in [74], and both S-C and C-A delays in [73], respectively; the stability analysis is addressed via a switched system approach [73, 74]. Further, a recursive predictive control scheme is proposed and the sufficient condition to guarantee the stability is analyzed via a switched system approach in [17].

Hydraulic systems are very important for the industrial application of NCSs, e.g., remote robot position control, aircraft flight control, and so on. Many control synthesis methods have been applied to hydraulic systems such as sliding mode control [53], neural network control [12], adaptive control [155], and H_2 control [71]. However, very few papers have addressed the networked control design for hydraulic systems. In [64], the authors present an approach for analyzing the performance of dropout compensation strategies in the H_2 and H_∞ senses for NCSs with data losses under the framework of Markovian jump linear systems (MJLSs), which is tested on an experimental hydraulic servo system.

To the best of the author's knowledge, the modified GPC (M-GPC) approach for NCSs has not been fully investigated, especially for NCSs with S-C and C-A delays modeled as Markov chains, which is the focus of this chapter. On the other hand, application oriented research for NCSs has received relatively less attention in the literature, which is another important motivation for this work.

The contributions of this chapter are as follows.

1) Unlike [17,72–74] in which the S-C and C-A delays are assumed to be constant or random, both S-C and C-A delays are modeled as Markov chains, and further the modified GPC is employed to compensate for both types of network-induced delays.

2) The closed-loop system is further formulated to be a special jump linear system, and the sufficient and necessary conditions to guarantee the stochastic stability are provided in terms of easily checked linear matrix inequalities (LMIs).

3) To move a step further towards practical applications, the developed NCS design scheme is applied to an experimental hydraulic position control system (HPCS).

The remainder of this chapter is organized as follows. Section 4.2 describes the networked system and the M-GPC algorithm; the compensated schemes for both S-C and C-A delays are also given in detail. In Section 4.3, the sufficient and necessary conditions to guarantee the stochastic stability are presented. Section 4.4 details the controller design, experiments, and results analysis for an experimental HPCS. Finally, the concluding remarks are addressed in Section 4.5.

4.2   Modified Generalized Predictive Control for NCSs

Consider a single-input single-output discrete-time plant described as follows:

$$A(z^{-1})y(k) = z^{-d}B(z^{-1})u(k-1), \qquad (4.1)$$

where $d \geq 0$ is the dead time of the system and

$$
\begin{aligned}
A(z^{-1}) &= 1 + a_1 z^{-1} + \cdots + a_{n_a} z^{-n_a}, \\
B(z^{-1}) &= b_0 + b_1 z^{-1} + \cdots + b_{n_b} z^{-n_b}.
\end{aligned}
$$

Bounded random delays exist in the links from sensor to controller and controller to actuator as shown in Figure 4.1. Here, $\bar{\tau} \geq \tau_k \geq 0$ represents the S-C delay and $\bar{d} \geq d_k \geq 0$ stands for the C-A delay. In this chapter, τ_k and d_k are modeled as two homogeneous Markov chains that take values in $\mathcal{M} = \{0, 1, ..., \bar{\tau}\}$ and $\mathcal{N} = \{0, 1, ..., \bar{d}\}$, and their transition probability matrices are $\Lambda = [\lambda_{ij}]$ and $\Pi = [\pi_{rs}]$, respectively, meaning that τ_k and d_k jump from mode i to j and from mode r to s,
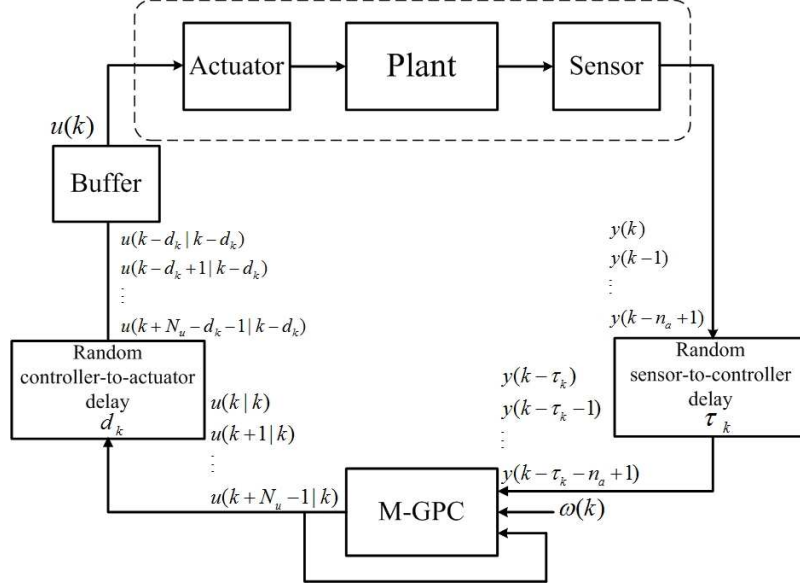
Figure 4.1: Diagram of the networked control system

respectively, with probabilities λ_{ij} and π_{rs}, which are defined by

$$\lambda_{ij} = \Pr(\tau_{k+1} = j | \tau_k = i)$$

$$\pi_{rs} = \Pr(d_{k+1} = s | d_k = r)$$

with the constraints $\lambda_{ij}, \pi_{rs} \geq 0$ and

$$\sum_{j=0}^{\tau} \lambda_{ij} = 1, \quad \sum_{s=0}^{d} \pi_{rs} = 1,$$

for all $i, j \in \mathcal{M}$ and $r, s \in \mathcal{N}$.

Remark 4.1. Modeling the network-induced delays as Markov chains is reasonable and widely used [87, 130, 133, 147]. This type of model takes the dependency of the delays into account, and thus appropriately characterizes the real scenario of that the current time delays are usually related with the previous delays in a network environment. In addition, another advantage of this type of model is that the packet dropouts can be included naturally [133].

The conventional GPC algorithm consists of applying a control sequence that minimizes the following objective function [13]:

$$J(N_1, N_2, N_u) = \sum_{j=N_1}^{N_2} \delta(j) \left[\hat{y}(k+j|k) - \omega(k+j) \right]^2 + \sum_{j=1}^{N_u} \rho(j) \left[\Delta u(k+j-1) \right]^2, \qquad (4.2)$$

where $\hat{y}(k+j|k)$ is j step ahead prediction of the system output based on data up to k; N_1 and N_2 are the minimum and maximum prediction horizons, respectively; N_u is the control horizon; $\delta(j)$ and $\rho(j)$ are weighting sequences and $\omega(k+j)$ is the future reference trajectory; $\Delta = 1 - z^{-1}$. The

control constraint here is

$$\Delta u(k+j-1) = 0, \qquad j > N_u. \tag{4.3}$$

The future control predictions can be obtained based on the past output $y(k)$ up to time k and the past control signal $u(k)$ up to time $k-1$. For more details of calculating the prediction control signals using the conventional GPC, the readers are refereed to [13].

In an NCS shown in Figure 4.1, due to the network-induced delays, the output signal $y(k)$ and control signal $u(k)$ at the plant node may not be received by the controller node immediately. Meanwhile, the current control signal might not reach the plant node in time. Hence, the conventional GPC cannot be directly applied to NCSs, which will be shown soon in the design examples. To compensate for the network-induced delays in a network environment, the GPC scheme needs to be modified. During the network transmission, a sequence of signals can be packed up and transmitted together. To start with, some assumptions on the data transmission are made in the following:

A 1: A sequence of output signals with length of n_a: $\begin{bmatrix} y(k)^{\mathrm{T}} & y(k-1)^{\mathrm{T}} & \cdots & y(k-n_a+1)^{\mathrm{T}} \end{bmatrix}^{\mathrm{T}}$ are packed and sent to the controller node together.

A 2: A sequence of prediction control signals with length of N_u: $\begin{bmatrix} u(k|k)^{\mathrm{T}} & u(k+1|k)^{\mathrm{T}} & \cdots & u(k+N_u-1|k)^{\mathrm{T}} \end{bmatrix}^{\mathrm{T}}$ are packed and sent to the plant node together.

In the following, the compensation schemes for the S-C and C-A network-induced delays will be presented in detail.

4.2.1 Compensation for S-C delays

Considering the time delays in the S-C link, at current time k, the measurement information received by the controller is delayed by τ_k. Hence, the received output signal is $\begin{bmatrix} y(k-\tau_k)^{\mathrm{T}} & y(k-\tau_k-1)^{\mathrm{T}} & \cdots & y(k-\tau_k-n_a+1)^{\mathrm{T}} \end{bmatrix}^{\mathrm{T}}$. Meanwhile, the control signal at the plant node up to time instance $k-1$ may not be available. To handle this, the previous prediction control signal at the controller node $\begin{bmatrix} u(k-1|k-1)^{\mathrm{T}} & u(k-2|k-2)^{\mathrm{T}} & \cdots \end{bmatrix}^{\mathrm{T}}$ can be employed instead. These two information vectors will be used to obtain the prediction of $y(t+j)$.

In order to minimize the cost function (4.2) and take the S-C delays τ_k into account, the prediction of $y(k+j)$ will be obtained by considering the following delay-dependent Diophantine equation:

$$1 = E_j(z^{-1})\tilde{A}(z^{-1}) + z^{-j-\tau_k}F_j(z^{-1}) \quad \text{with} \quad \tilde{A}(z^{-1}) = \Delta A(z^{-1}). \tag{4.4}$$

The polynomials E_j and F_j are uniquely defined with degrees $j+\tau_k-1$ and n_a, respectively. Then, the future prediction of $y(k+j)$ is

$$\hat{y}(k+j) = G_j(z^{-1})\Delta u(k+j-d-1) + F_j(z^{-1})y(k-\tau_k), \tag{4.5}$$

50

for $d + 1 \leq j \leq N_2$, where

$$G_j(z^{-1}) = E_j(z^{-1})B(z^{-1}) = g_0 + g_1 z^{-1} + \cdots + g_{j+\tau_k-1+n_b} z^{1-j-\tau_k-n_b}.$$

Equation (4.5) can be rewritten as

$$\hat{y}(k + j) = \bar{G}_j(z^{-1})\Delta u(k + j - d - 1|k) + z^{j-d-1}\left[G_j(z^{-1}) - \bar{G}_j(z^{-1})\right]\Delta u(k|k) + F_j(z^{-1})y(k - \tau_k),$$

(4.6)

where

$$\bar{G}_j(z^{-1}) = g_0 + g_1 z^{-1} + \cdots + g_{j-d-1} z^{d+1-j}.$$

Note that the last two terms in (4.6) only depend on the past data and the first term is related with future control actions. Further, the following equation is obtained:

$$\mathbf{y}(k) = \Gamma \mathbf{u}(k) + G(z^{-1})\Delta u(k - 1|k - 1) + F(z^{-1})y(k - \tau_k),$$

(4.7)

where

$$\mathbf{y}(k) = \begin{bmatrix} \hat{y}(k + d + 1|k) \\ \hat{y}(k + d + 2|k) \\ \vdots \\ \hat{y}(k + N_2|k) \end{bmatrix}, \quad \mathbf{u}(k) = \begin{bmatrix} \Delta u(k|k) \\ \Delta u(k + 1|k) \\ \vdots \\ \Delta u(k + N_u - 1|k) \end{bmatrix},$$

$$\Gamma = \begin{bmatrix} g_0 & 0 & \cdots & 0 \\ g_1 & g_0 & \cdots & 0 \\ \vdots & \vdots & \ddots & \vdots \\ g_{N_u-1} & \cdots & \cdots & g_0 \\ \vdots & \vdots & \cdots & \vdots \\ g_{N_2-1} & g_{N_2-2} & \cdots & g_{N_2-N_u} \end{bmatrix},$$

$$G(z^{-1}) = \begin{bmatrix} \left(G_{d+1}(z^{-1}) - \bar{G}_{d+1}(z^{-1})\right)z \\ \left(G_{d+2}(z^{-1}) - \bar{G}_{d+2}(z^{-1})\right)z^2 \\ \vdots \\ \left(G_{N_2}(z^{-1}) - \bar{G}_{N_2}(z^{-1})\right)z^{N_2-d} \end{bmatrix}, \quad F(z^{-1}) = \begin{bmatrix} F_{d+1}(z^{-1}) \\ F_{d+2}(z^{-1}) \\ \vdots \\ F_{N_2}(z^{-1}) \end{bmatrix}.$$

The objective function (4.2) can be rewritten as

$$\begin{aligned} J(N_1&, N_2, N_u) \\ = & \sum_{j=N_1}^{N_2} \delta(j)\left[\hat{y}(k + j|k) - \omega(k + j)\right]^2 + \sum_{j=1}^{N_u} \rho(j)\left[\Delta u(k + j - 1|k)\right]^2, \\ = & \left[\Gamma \mathbf{u}(k) + G(z^{-1})\Delta u(k - 1|k - 1) + F(z^{-1})y(k - \tau_k) - \omega(k)\right]^{\mathrm{T}} Q \\ & \times \left[\Gamma \mathbf{u}(k) + G(z^{-1})\Delta u(k - 1|k - 1) + F(z^{-1})y(k - \tau_k) - \omega(k)\right] + \mathbf{u}(k)^{\mathrm{T}} R\mathbf{u}(k), \quad (4.8) \end{aligned}$$

where

$$Q = \text{diag}\left\{ \begin{array}{cccc} \delta(N_1) & \delta(N_1+1) & \cdots & \delta(N_2) \end{array} \right\};$$

$$R = \text{diag}\left\{ \begin{array}{cccc} \rho(1) & \rho(2) & \cdots & \rho(N_u) \end{array} \right\};$$

$$\omega(k) = \left[\begin{array}{cccc} \omega(k+N_1)^{\mathrm{T}} & \omega(k+N_1+1)^{\mathrm{T}} & \cdots & \omega(k+N_2)^{\mathrm{T}} \end{array} \right]^{\mathrm{T}}.$$

Here, $N_1 = d+1$ and $N_u \geq \bar{d}+1$.

By making the gradient of J to be zero, the optimal control increment signal can be obtained as

$$\mathbf{u}(k) = (\Gamma^{\mathrm{T}}Q\Gamma + R)^{-1}\Gamma^{\mathrm{T}}Q\left[\omega(k) - G(z^{-1})\Delta u(k-1|k-1) - F(z^{-1})y(k-\tau_k)\right]. \tag{4.9}$$

Further, the control signal can be determined by

$$\begin{bmatrix} u(k|k) \\ u(k+1|k) \\ \vdots \\ u(k+N_u-1|k) \end{bmatrix} = \begin{bmatrix} 1 \\ 1 \\ \vdots \\ 1 \end{bmatrix} u(k-1|k-1) + \begin{bmatrix} H_1 \\ H_2 \\ \vdots \\ H_{N_u} \end{bmatrix} \left[\omega(k) - G(z^{-1})\Delta u(k-1|k-1) - F(z^{-1})y(k-\tau_k)\right],$$

$$\tag{4.10}$$

where

$$H = \begin{bmatrix} H_1 \\ H_2 \\ \vdots \\ H_{N_u} \end{bmatrix} = \begin{bmatrix} 1 & 0 & \cdots & 0 \\ 1 & 1 & \cdots & 0 \\ \vdots & \vdots & \ddots & \vdots \\ 1 & 1 & \cdots & 1 \end{bmatrix} \times \left[(\Gamma^{\mathrm{T}}Q\Gamma + R)^{-1}\Gamma^{\mathrm{T}}Q\right]. \tag{4.11}$$

Remark 4.2. The S-C time delays τ_k can be obtained by using the time-stamping technique [55]. The effect of S-C time delays τ_k has been considered in (4.4) in the compensation scheme. It is worth noting that the matrices and vectors $G(z^{-1})$ and $F(z^{-1})$ are functions of τ_k, which will be used in the stability analysis. Also, $G(z^{-1})$, $F(z^{-1})$, and Γ can be calculated offline.

4.2.2 Compensation for C-A delays

The C-A time delays are even harder to handle because the C-A time delays d_k cannot be known when the control action is made. Due to the inherent predictive feature of GPC, the future control sequences can be made full use of to compensate for the effect of d_k.

Different from the conventional GPC in which only the current control signal $u(k|k)$ is used, the M-GPC uses the whole control signal sequences, which are packed and sent to the actuator/plant node together. Considering the time delay d_k from controller to actuator, the control signal received

at the actuator/plant node at current time k is

$$\begin{bmatrix} u(k - d_k|k - d_k) \\ u(k - d_k + 1|k - d_k) \\ \vdots \\ u(k|k - d_k) \\ \vdots \\ u(k - d_k + N_u - 1|k - d_k) \end{bmatrix}. \tag{4.12}$$

$N_u \geq \bar{d} + 1$ has been pre-set. Therefore, even though the control signal $u(k|k)$ may not be received at time k at the actuator/plant node, the previous prediction control signal for time k, $u(k|k - d_k)$ in the control package (4.12), is always already available at the actuator/plant node. Then, $u(k|k - d_k)$ will be chosen to be implemented on the plant.

Remark 4.3. A similar modified GPC method for NCSs was reported in [72], but the S-C time delay is assumed to be fixed. In this chapter, the S-C delays are random and governed by Markov chains, which are more general in NCSs and also can include the fixed delays as special cases. However, the random S-C delays make the algorithm and the following stability analysis much more complex and challenging.

4.3   Stability Analysis

Stability analysis is of great importance for the designed control system. In this section, the closed-loop system is first formulated as a special jump linear system. Then, the sufficient and necessary conditions for stochastic stability are derived, which can be efficiently checked using the LMI toolbox.

4.3.1   Closed-loop system

Without losing the generality, the reference input $\omega(k)$ is assumed to be zero. Let G_0 and F_0 be the coefficient matrices of polynomial vectors $G(z^{-1})\Delta$ and $F(z^{-1})$ in (4.10), respectively; n_g and n_f be the highest order of polynomials in vectors $G(z^{-1})\Delta$ and $F(z^{-1})$. Note that G_0 and F_0 vary with τ_k. Hence, they are denoted as $G_0(\tau_k)$ and $F_0(\tau_k)$, respectively.

Then, (4.10) can be rewritten in the following form

$$\bar{U}(k) = G_1(\tau_k)\tilde{U}(k - 1) + F_1(\tau_k)\tilde{Y}(k - \tau_k), \tag{4.13}$$

where

$$\bar{U}(k) \quad = \quad \begin{bmatrix} u(k|k)^{\mathrm{T}} & u(k + 1|k)^{\mathrm{T}} & \cdots & u(k + N_u - 1|k)^{\mathrm{T}} \end{bmatrix}^{\mathrm{T}},$$

$$\tilde{U}(k-1) \;=\; \left[\begin{array}{cccc} u(k-1|k-1)^{\mathrm{T}} & u(k-2|k-2)^{\mathrm{T}} & \cdots & u(k-n_g-1|k-n_g-1)^{\mathrm{T}} \end{array}\right]^{\mathrm{T}},$$

$$\tilde{Y}(k-\tau_k) \;=\; \left[\begin{array}{cccc} y(k-\tau_k)^{\mathrm{T}} & y(k-\tau_k-1)^{\mathrm{T}} & \cdots & y(k-\tau_k-n_f)^{\mathrm{T}} \end{array}\right]^{\mathrm{T}},$$

$$G_1(\tau_k) \;=\; \left[\left[\begin{array}{cccc} 1 & 1 & \cdots & 1 \end{array}\right]^{\mathrm{T}} \; 0_{N_u \times n_g}\right] - HG_0(\tau_k),$$

$$F_1(\tau_k) \;=\; -HF_0(\tau_k).$$

Then, the control prediction sequence received at the actuator/plant node is

$$
\begin{aligned}
\bar{U}(k-d_k) \;=\;& G_1(\tau_{k-d_k})\tilde{U}(k-d_k-1) + F_1(\tau_{k-d_k})\tilde{Y}(k-d_k-\tau_{k-d_k}) \\
\;=\;& \left[\begin{array}{ccc} 0_{N_u \times d_k} & G_1(\tau_{k-d_k}) & 0_{N_u \times (\bar{d}-d_k)} \end{array}\right] \hat{U}(k-1) \\
& + \left[\begin{array}{ccc} 0_{N_u \times (\tau_{k-d_k}+d_k)} & F_1(\tau_{k-d_k}) & 0_{N_u \times (\bar{d}+\bar{\tau}-d_k-\tau_{k-d_k})} \end{array}\right] Y(k), \qquad (4.14)
\end{aligned}
$$

where

$$\hat{U}(k) \;=\; \left[\begin{array}{cccc} u(k|k)^{\mathrm{T}} & u(k-1|k-1)^{\mathrm{T}} & \cdots & u(k-n_g-\bar{d}|k-n_g-\bar{d})^{\mathrm{T}} \end{array}\right]^{\mathrm{T}},$$

$$Y(k) \;=\; \left[\begin{array}{cccc} y(k)^{\mathrm{T}} & y(k-1)^{\mathrm{T}} & \cdots & y(k-\bar{\tau}-\bar{d}-n_f)^{\mathrm{T}} \end{array}\right]^{\mathrm{T}}.$$

Further, the control input of the plant is the $(1+d_k)$th element in vector $\bar{U}(k-d_k)$, which is

$$
\begin{aligned}
u(k) \;=\;& u(k|k-d_k) \\
\;=\;& \left[\begin{array}{ccc} 0_{1 \times d_k} & 1 & 0_{1 \times (N_u-d_k-1)} \end{array}\right] \bar{U}(k-d_k) \\
\;=\;& \left[\begin{array}{ccc} 0_{1 \times d_k} & 1 & 0_{1 \times (N_u-d_k-1)} \end{array}\right] \Big\{ \left[\begin{array}{ccc} 0_{N_u \times d_k} & G_1(\tau_{k-d_k}) & 0_{N_u \times (\bar{d}-d_k)} \end{array}\right] \hat{U}(k-1) \\
& + \left[\begin{array}{ccc} 0_{N_u \times (\tau_{k-d_k}+d_k)} & F_1(\tau_{k-d_k}) & 0_{N_u \times (\bar{d}+\bar{\tau}-d_k-\tau_{k-d_k})} \end{array}\right] Y(k) \Big\}, \\
\;=\;& c(\tau_k, d_k, \tau_{k-d_k})\hat{U}(k-1) + d(\tau_k, d_k, \tau_{k-d_k})Y(k), \qquad (4.15)
\end{aligned}
$$

where

$$c(\tau_k, d_k, \tau_{k-d_k}) \;=\; \left[\begin{array}{ccc} 0_{1 \times d_k} & 1 & 0_{1 \times (N_u-d_k-1)} \end{array}\right]\left[\begin{array}{ccc} 0_{N_u \times d_k} & G_1(\tau_{k-d_k}) & 0_{N_u \times (\bar{d}-d_k)} \end{array}\right],$$

$$d(\tau_k, d_k, \tau_{k-d_k}) \;=\; \left[\begin{array}{ccc} 0_{1 \times d_k} & 1 & 0_{1 \times (N_u-d_k-1)} \end{array}\right]\left[\begin{array}{ccc} 0_{N_u \times (\tau_{k-d_k}+d_k)} & F_1(\tau_{k-d_k}) & 0_{N_u \times (\bar{d}+\bar{\tau}-d_k-\tau_{k-d_k})} \end{array}\right].$$

Thus, based on (4.15), the control vector on the plant side can be expressed by

$$U(k) = EU(k-1) + C(\tau_k, d_k, \tau_{k-d_k})\hat{U}(k-1) + D(\tau_k, d_k, \tau_{k-d_k})Y(k), \qquad (4.16)$$

where

$$U(k) \;=\; \left[\begin{array}{cccc} u(k)^{\mathrm{T}} & u(k-1)^{\mathrm{T}} & \cdots & u(k-n_b-d)^{\mathrm{T}} \end{array}\right]^{\mathrm{T}},$$

$$C(\tau_k, d_k, \tau_{k-d_k}) \;=\; \left[\begin{array}{c} c(\tau_k, d_k, \tau_{k-d_k}) \\ 0_{(n_b+d) \times (n_g+\bar{d}+1)} \end{array}\right],$$

$$D(\tau_k, d_k, \tau_{k-d_k}) \;=\; \left[\begin{array}{c} d(\tau_k, d_k, \tau_{k-d_k}) \\ 0_{(n_b+d) \times (\bar{\tau}+\bar{d}+n_f+1)} \end{array}\right],$$

$$E \;=\; \left[\begin{array}{cc} 0_{1 \times (n_b+d)} & 0_{1 \times 1} \\ I_{(n_b+d) \times (n_b+d)} & 0_{(n_b+d) \times 1} \end{array}\right].$$

It is clear from (4.1) that the output vector of the plant can be described by

$$Y(k) = A_1 Y(k-1) + B_1 U(k-1), \qquad (4.17)$$

where

$$A_1 = \begin{bmatrix} \begin{bmatrix} -a_1 & -a_2 & \cdots & -a_{n_a} \end{bmatrix} & 0_{1\times(\bar{\tau}+\bar{d}+n_f+1-n_a)} \\ I_{(\bar{\tau}+\bar{d}+n_f)\times(\bar{\tau}+\bar{d}+n_f)} & 0_{(\bar{\tau}+\bar{d}+n_f)\times 1} \end{bmatrix},$$

$$B_1 = \begin{bmatrix} \begin{bmatrix} 0_{1\times d} & b_0 & b_1 & \cdots & b_{n_b} \end{bmatrix} \\ 0_{(\bar{\tau}+\bar{d}+n_f)\times(n_b+d+1)} \end{bmatrix}.$$

In addition, since $u(k|k)$ is the first row of $\bar{U}(k)$ in (4.13), it can be calculated by

$$u(k|k) = \begin{bmatrix} 1 & 0 & \cdots & 0 \end{bmatrix}_{N_u\times 1} G_1(\tau_k)\tilde{U}(k-1) + \begin{bmatrix} 1 & 0 & \cdots & 0 \end{bmatrix}_{N_u\times 1} F_1(\tau_k)\tilde{Y}(k-\tau_k). \quad (4.18)$$

Let

$$\begin{bmatrix} \bar{g}_0(\tau_k) & \bar{g}_1(\tau_k) & \cdots & \bar{g}_{n_g}(\tau_k) \end{bmatrix} = \begin{bmatrix} 1 & 0 & \cdots & 0 \end{bmatrix}_{N_u\times 1} G_1(\tau_k), \qquad (4.19)$$

$$\begin{bmatrix} \bar{f}_0(\tau_k) & \bar{f}_1(\tau_k) & \cdots & \bar{f}_{n_f}(\tau_k) \end{bmatrix} = \begin{bmatrix} 1 & 0 & \cdots & 0 \end{bmatrix}_{N_u\times 1} F_1(\tau_k). \qquad (4.20)$$

Using (4.18), the vector $\hat{U}(k)$ can be constructed by

$$\hat{U}(k) = G_2(\tau_k)\hat{U}(k-1) + F_2(\tau_k)Y(k), \qquad (4.21)$$

where

$$G_2(\tau_k) = \begin{bmatrix} \begin{bmatrix} \bar{g}_0(\tau_k) & \bar{g}_1(\tau_k) & \cdots & \bar{g}_{n_g}(\tau_k) & 0_{1\times\bar{d}} \end{bmatrix} \\ \begin{bmatrix} I_{(n_g+\bar{d})\times(n_g+\bar{d})} & 0_{(n_g+\bar{d})\times 1} \end{bmatrix} \end{bmatrix},$$

$$F_2(\tau_k) = \begin{bmatrix} \begin{bmatrix} 0_{1\times\tau_k} & \bar{f}_0(\tau_k) & \bar{f}_1(\tau_k) & \cdots & \bar{f}_{n_f}(\tau_k) & 0_{1\times(\bar{d}+\bar{\tau}-\tau_k)} \end{bmatrix} \\ \begin{bmatrix} 0_{(n_g+\bar{d})\times(\bar{\tau}+\bar{d}+n_f+1)} \end{bmatrix} \end{bmatrix}.$$

Further, combining (4.16), (4.17), and (4.21) yields the following closed-loop system

$$X(k) = A_c(\tau_k, d_k, \tau_{k-d_k})X(k-1), \qquad (4.22)$$

where

$$X(k) = \begin{bmatrix} Y(k) \\ U(k) \\ \hat{U}(k) \end{bmatrix},$$

$$A_c(\tau_k, d_k, \tau_{k-d_k}) = \begin{bmatrix} A_1 & B_1 & 0 \\ D(\tau_k, d_k, \tau_{k-d_k})A_1 & E + D(\tau_k, d_k, \tau_{k-d_k})B_1 & C(\tau_k, d_k, \tau_{k-d_k}) \\ F_2(\tau_k)A_1 & F_2(\tau_k)B_1 & G_2(\tau_k) \end{bmatrix}.$$

Remark 4.4. The closed-loop system (4.22) is a special jump linear system. Due to the random time delay in S-C link, the state matrix A_c varies with $\tau_k, d_k, \tau_{k-d_k}$, which is different from and more complex than the closed-loop system in [72]. Meanwhile, the closed-loop system (4.22) is not the standard Markovian jump linear system (MJLS) [23, 62, 104], because it depends not only on τ_k, d_k, but also τ_{k-d_k}. Hence, the existing results of stability analysis on MJLSs cannot be directly applied to this system.

4.3.2 Stochastic stability

For stochastic stability, the definition in [142, 147] is adopted here.

Definition 4.1. ([142, 147]) The system in (4.22) is stochastically stable if for every finite $X_{-1} = X(-1)$, initial mode $\tau_{-d_0} = \tau(-d_0) \in \mathcal{M}$, and $d_0 = d(0) \in \mathcal{N}$, there exists a finite $W > 0$ such that the following holds:

$$\mathcal{E}\left\{\sum_{k=0}^{\infty}\|X_k\|^2|_{X_{-1},\ \tau_{-d_0},\ d_0}\right\} < X_{-1}{}^{\mathrm{T}}WX_{-1}. \tag{4.23}$$

Before presenting the main theorem about stochastic stability, the following proposition is given, which results from the existence of τ_{k-d_k} in the closed-loop system (4.22) and is of great importance for the derivation of the sufficient and necessary conditions for the stochastic stability.

Proposition 4.1. If the transition probability matrix from τ_{k-1} to τ_k is Λ, then the transition probability matrix from τ_{k-n} to τ_k is Λ^n, which is also a transition probability matrix of Markov chain. Specially, when $n = 0$, the transition probability matrix is $\Lambda^0 = I$.

Proof. This proposition can be proved by following the same way in the proof of Proposition 2.1 in Section 2.3. □

The sufficient and necessary conditions to guarantee the stochastic stability of system (4.22) are shown in Theorem 4.1. In the following, when the system is in mode $i \in \mathcal{M}$ and $r \in \mathcal{N}$ (i.e., $\tau_{k-d_k} = i,\ d_k = r$), $P(\tau_{k-d_k}, d_k)$ will be denoted as $P(i, r)$ for simplicity.

Theorem 4.1. The closed-loop system (4.22) is stochastically stable if and only if there exists symmetric $P(i, r) > 0$ such that the following linear matrix inequality:

$$\begin{aligned}
L(i,r) &= \left(\sum_{j=1}^{\bar{d}}\sum_{s_1=0}^{\bar{\tau}}\sum_{s_2=0}^{\bar{\tau}}\pi_{rj}\Lambda_{is_2}^{1+r-j}\Lambda_{s_2s_1}^{j-1} + \sum_{s_1=0}^{\bar{\tau}}\sum_{s_2=0}^{\bar{\tau}}\pi_{r0}\Lambda_{is_1}^r\Lambda_{s_1s_2}\right)A_c(s_1,r,i)^{\mathrm{T}}P(s_2,j)A_c(s_1,r,i) \\
&\quad -P(i,r) \\
&< 0 \tag{4.24}
\end{aligned}$$

holds for all $i \in \mathcal{M}$ and $r \in \mathcal{N}$.

Proof. Sufficiency: For the closed-loop system (4.22), construct the Lyapunov function candidate

$$V(X(k-1),k) = X(k-1)^{\mathrm{T}} P(\tau_{k-d_k}, d_k) X(k-1). \tag{4.25}$$

Then

$$\mathcal{E}\{\Delta(V(X(k-1),k)\}$$
$$= \mathcal{E}\{X(k)^{\mathrm{T}} P(\tau_{k+1-d_{k+1}}, d_{k+1}) X(k)|_{X_{k-1}, \tau_{k-d_k}=i, d_k=r}\} - X(k-1)^{\mathrm{T}} P(\tau_{k-d_k}, d_k) X(k-1). \tag{4.26}$$

For simplicity of expression, define $d_{k+1} = j$, $\tau_k = s_1$, $\tau_{k+1-d_{k+1}} = s_2$. To evaluate the first term in (4.26), the mathematic expectation of $X(k)^{\mathrm{T}} P(\tau_{k+1-d_{k+1}}, d_{k+1}) X(k)$ are needed to be calculated based on the available previous step information $X_{k-1}, \tau_{k-d_k} = i, d_k = r$. To achieve this, the following state jumps of the Markov chains are involved:

$$\begin{array}{ll} & d_k \to d_{k+1}, \quad \tau_{k-d_k} \to \tau_{k+1-d_{k+1}}, \quad \tau_{k+1-d_{k+1}} \to \tau_k, \quad \text{if } d_{k+1} = j \geq 1. \\ \text{or} & \\ & d_k \to d_{k+1}, \quad \tau_{k-d_k} \to \tau_k, \quad \tau_k \to \tau_{k+1-d_{k+1}}, \quad \text{if } d_{k+1} = j < 1. \end{array} \tag{4.27}$$

According to (4.22) and Proposition 4.1, the following three probability transition matrices are

$$\begin{array}{ll} & d_k \to d_{k+1} : \Pi, \quad \tau_{k-d_k} \to \tau_{k+1-d_{k+1}} : \Lambda^{1+r-j}, \quad \tau_{k+1-d_{k+1}} \to \tau_k : \Lambda^{j-1}. \\ \text{or} & \\ & d_k \to d_{k+1} : \Pi, \quad \tau_{k-d_k} \to \tau_k : \Lambda^r, \quad \tau_k \to \tau_{k+1-d_{k+1}} : \Lambda^{1-j}. \end{array} \tag{4.28}$$

Then, (4.26) can be evaluated as

$$\mathcal{E}\{\Delta(V(X(k-1),k)\}$$
$$= X(k-1)^{\mathrm{T}} \left\{ \sum_{j=1}^{\bar{d}} \sum_{s_1=0}^{\bar{\tau}} \sum_{s_2=0}^{\bar{\tau}} \pi_{rj} \Lambda_{is_2}^{1+r-j} \Lambda_{s_2 s_1}^{j-1} [A_c(s_1, r, i)]^{\mathrm{T}} P(s_2, j) [A_c(s_1, r, i)] + \right.$$
$$\left. \sum_{s_1=0}^{\bar{\tau}} \sum_{s_2=0}^{\bar{\tau}} \pi_{r0} \Lambda_{is_1}^{r} \Lambda_{s_1 s_2} [A_c(s_1, r, i)]^{\mathrm{T}} P(s_2, j) [A_c(s_1, r, i)] - P(i, r) \right\} X(k-1).$$

Thus, if $L(i, r) < 0$, then

$$\mathcal{E}\{\Delta(V(X(k-1),k)\} = X(k-1)^{\mathrm{T}} L(i,r) X(k-1)$$
$$\leq -\lambda_{\min}(-L(i,r)) X(k-1)^{\mathrm{T}} X(k-1) \leq -\beta \|X(k-1)\|^2, \tag{4.29}$$

where $\beta = \inf\{\lambda_{\min}(-L(i,r))\} > 0$. From (4.29), it can be obtained that for any $T \geq 1$

$$\mathcal{E}\{V(X(T), T+1)\} - \mathcal{E}\{V(X_{-1}, 0)\} \leq -\beta \mathcal{E}\left\{ \sum_{t=0}^{T} \|X(t)\|^2 \right\}.$$

Furthermore,

$$\mathcal{E}\left\{ \sum_{t=0}^{T} \|X(t)\|^2 \right\} \leq \frac{1}{\beta} \left(\mathcal{E}\{V(X_{-1}, 0)\} - \mathcal{E}\{V(X(T), T+1)\} \right)$$
$$\leq \frac{1}{\beta} \mathcal{E}\{V(X_{-1}, 0)\} = \frac{1}{\beta} X(-1)^{\mathrm{T}} P(\tau_{-d_0}, d_0) X(-1).$$

From Definition 4.1 and taking $T \to \infty$, the closed-loop system (4.22) is stochastically stable.

Necessity: If the closed-loop system (4.22) is stochastically stable, or equivalently

$$\mathcal{E}\left\{\sum_{t=0}^{\infty}\|X_t\|^2|_{X_0,\tau_{-d_0},d_0}\right\} \leq X_{-1}^{\mathrm{T}}WX_{-1}. \tag{4.30}$$

Define the following function:

$$X(t-1)^{\mathrm{T}}\tilde{P}(T-t,\tau_{t-d_t},d_t)X(t-1) \triangleq \mathcal{E}\left\{\sum_{k=t}^{T}X(k-1)^{\mathrm{T}}Q(\tau_{k-d_k},d_k)X(k-1)|_{X_{t-1},\tau_{t-d_t},d_t}\right\} \tag{4.31}$$

with $Q(\tau_{k-d_k}, d_k) > 0$. Assuming that $X(k) \neq 0$, since $Q(\tau_{k-d_k}, d_k) > 0$, as T increases, $X(t-1)^{\mathrm{T}}\tilde{P}(T-t,\tau_{t-d_t},d_t)X(t-1)$ is monotonically increasing. From (4.30), it can be obtained that $X(t-1)^{\mathrm{T}}\tilde{P}(T-t,\tau_{t-d_t},d_t)X(t-1)$ is upper bounded; thus, the limit exists and can be expressed as

$$\begin{aligned} X(t-1)^{\mathrm{T}}P(i,r)X(t-1) &\triangleq \lim_{T\to\infty}X(t-1)^{\mathrm{T}}\tilde{P}(T-t,\tau_{t-d_t}=i,d_t=r)X(t-1) \\ &\triangleq \lim_{T\to\infty}\mathcal{E}\left\{\sum_{k=t}^{T}X(k-1)^{\mathrm{T}}Q(\tau_{k-d_k},d_k)X(k-1)|_{X_{t-1},\tau_{t-d_t}=i,d_t=r}\right\} \end{aligned} \tag{4.32}$$

Since this is valid for any $X(t)$, then

$$P(i,r) = \lim_{T\to\infty}\tilde{P}(T-t,\tau_{t-d_t}=i,d_t=r). \tag{4.33}$$

From (4.32), it can be seen that $P(i,r) > 0$ since $Q(\tau_{k-d_k}, d_k) > 0$. Consider

$$\mathcal{E}\left\{X(t-1)^{\mathrm{T}}\tilde{P}(T-t,\tau_{t-d_t},d_t)X(t-1) - X(t)^{\mathrm{T}}\tilde{P}(T-t-1,\tau_{t+1-d_{t+1}},d_{t+1})X(t)|_{X_{t-1},\tau_{t-d_t}=i,d_t=r}\right\}$$
$$= X(t-1)^{\mathrm{T}}Q(i,r)X(t-1). \tag{4.34}$$

Notice that

$$\begin{aligned} &\mathcal{E}\left\{X(t)^{\mathrm{T}}\tilde{P}(T-t-1,\tau_{t+1-d_{t+1}},d_{t+1})X(t)|_{X_{t-1},\tau_{t-d_t}=i,d_t=r}\right\} \\ &= X(t-1)^{\mathrm{T}}\left\{\left(\sum_{j=1}^{\bar{d}}\sum_{s_1=0}^{\bar{\tau}}\sum_{s_2=0}^{\bar{\tau}}\pi_{rj}\Lambda_{is_2}^{1+r-j}\Lambda_{s_2s_1}^{j-1} + \sum_{s_1=0}^{\bar{\tau}}\sum_{s_2=0}^{\bar{\tau}}\pi_{r0}\Lambda_{is_1}^{r}\Lambda_{s_1s_2}\right)A_c(s_1,r,i)^{\mathrm{T}} \right. \\ &\quad \left. \times \tilde{P}(T-t-1,s_2,j)A_c(s_1,r,i)\right\}X(t-1). \end{aligned}$$

This, together with (4.34), implies that for any $X(t)$

$$\begin{aligned} X(t-1)^{\mathrm{T}}&\left\{\tilde{P}(T-t,\tau_{t-d_t},d_t) - \left(\sum_{j=1}^{\bar{d}}\sum_{s_1=0}^{\bar{\tau}}\sum_{s_2=0}^{\bar{\tau}}\pi_{rj}\Lambda_{is_2}^{1+r-j}\Lambda_{s_2s_1}^{j-1} + \sum_{s_1=0}^{\bar{\tau}}\sum_{s_2=0}^{\bar{\tau}}\pi_{r0}\Lambda_{is_1}^{r}\Lambda_{s_1s_2}\right)A_c(s_1,r,i)^{\mathrm{T}}\right. \\ &\quad \left. \times \tilde{P}(T-t-1,s_2,j)A_c(s_1,r,i)\right\} \times X(t-1) = X(t-1)^{\mathrm{T}}Q(i,r)X(t-1). \end{aligned}$$

Letting $T \to \infty$ and noticing (4.33), (4.24) can be obtained. This completes the proof. $\square$

The condition in (4.24) is sufficient and necessary, which is comprised of a set of LMIs. This can be efficiently verified using the LMI toolbox in Matlab.

Remark 4.5. When there is no delays in the system, e.g., $\bar{\tau} = 0$ and $\bar{d} = 0$, the M-GPC reduces to the conventional GPC. Moreover, the constant time delays can be considered as special cases of time delays governed by Markov chains. Hence, the proposed algorithm and stability analysis can include the conventional GPC and M-GPC with constant time delays as special cases.

4.4 Experimental Test on A Networked Hydraulic Position Control System

In this section, the M-GPC algorithm is tested in an experimental HPCS shown in Figure 4.2. In a network environment, the control computer and the HPCS are connected via network medium, as illustrated in Figure 4.3. The design objective is to design a controller that can remotely control the HPCS over network to achieve the step tracking.
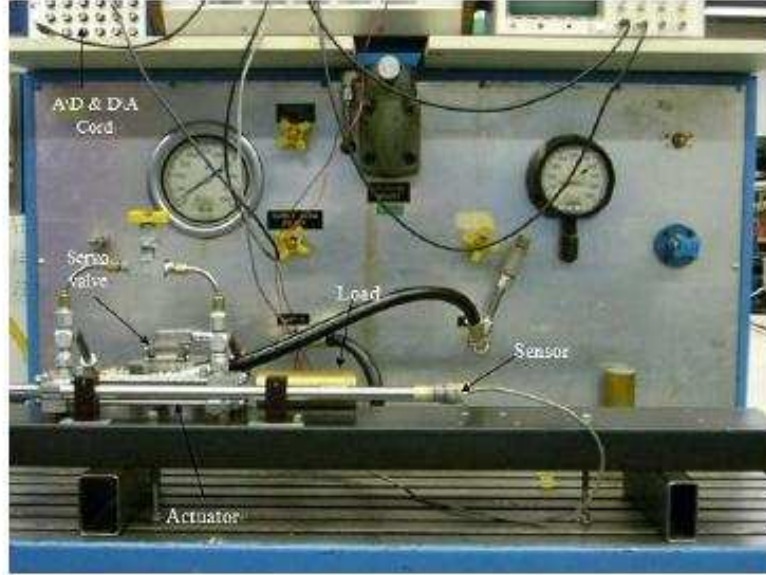
Figure 4.2: Hydraulic position control system.

4.4.1 Controller design and simulation studies

The identified continuous-time transfer function for the HPCS is [71]

$$G(s) = \frac{Y(s)}{U(s)} = \frac{422000}{s^3 + 141s^2 + 12100s}. \tag{4.35}$$

The output y is the cylinder position and the input u is the voltage.

Its discrete-time model with the sampling time $t_s = 0.03$s can be obtained as

$$G(z^{-1}) = \frac{0.5946z^{-1} + 0.6178z^{-2} + 0.05628z^{-3}}{1 - 0.802z^{-1} - 0.1834z^{-2} - 0.01455z^{-3}}. \tag{4.36}$$
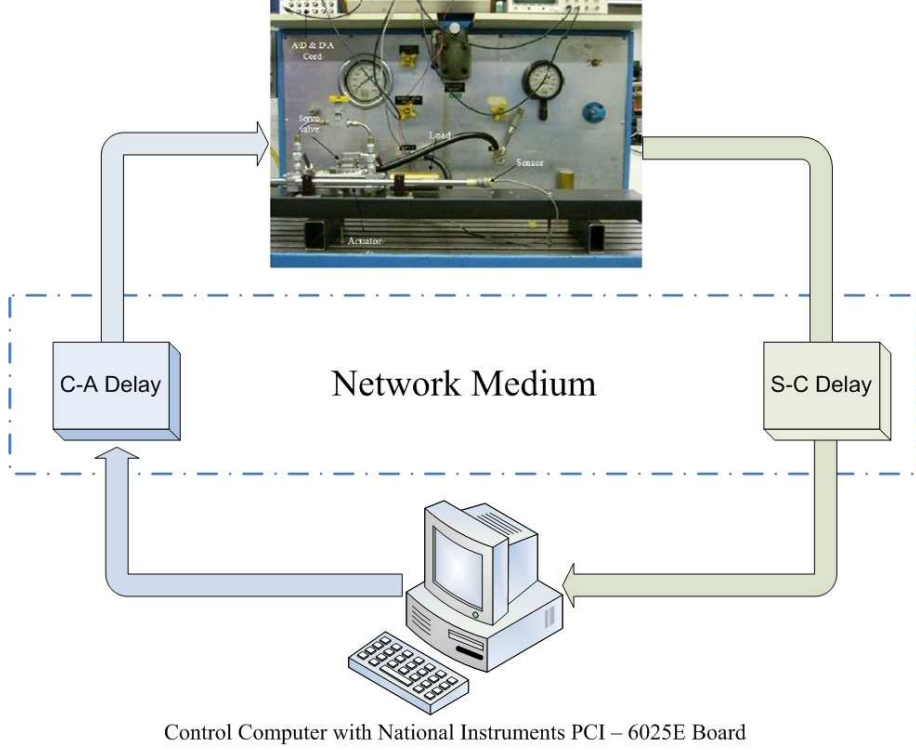
Figure 4.3: Networked hydraulic position control system.

From the discrete-time transfer function, $d = 0$ can be obtained.

Simulation 1: Conventional GPC for local tracking control of HPCS. First, the local tracking control performance of GPC is examined in the simulation. Apply the conventional GPC to the HPCS. The input $\omega(k)$ is $5u(t)$, where $u(t)$ is the step signal. The parameters of GPC are chosen as $N_1 = 1$, $N_2 = 12$, $N_u = 10$, $Q = I_{12 \times 12}$, and $R = 50 \times I_{10 \times 10}$. The simulation result is shown in Figure 4.4.

Simulation 2: Conventional GPC for networked HPCS tracking control. Next, the networked HPCS shown in Figure 4.3 is considered. In a network environment, both S-C and C-A delays exist. The random delays involved are assumed to be $\tau_k \in \{0, 1, 2, 3\}$ and $d_k \in \{0, 1, 2, 3\}$, and their transition probability matrices are given by

$$\Lambda = \begin{bmatrix} 0.2 & 0.8 & 0 & 0 \\ 0.1 & 0.4 & 0.5 & 0 \\ 0.1 & 0.2 & 0.5 & 0.2 \\ 0.1 & 0.2 & 0.5 & 0.2 \end{bmatrix}, \quad \Pi = \begin{bmatrix} 0.2 & 0.8 & 0 & 0 \\ 0.1 & 0.4 & 0.5 & 0 \\ 0.1 & 0.2 & 0.5 & 0.2 \\ 0.1 & 0.2 & 0.5 & 0.2 \end{bmatrix}. \quad (4.37)$$

The time delays τ_k and d_k are shown in Figures 4.5 and 4.6, respectively. Directly applying the designed conventional GPC (as used in the first example) to the networked HPCS, the tracking performance is shown in Figure 4.7. It is observed that the system becomes unstable due to the networked-induced delays. Obviously, the stability cannot be guaranteed, let alone the tracking per-

60
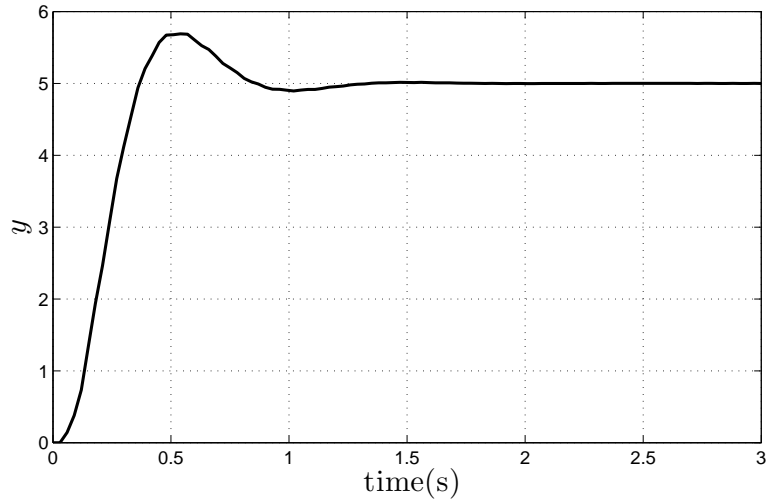
Figure 4.4: Simulation 1: Tracking performance of conventional GPC applied to the local HPCS.

formance. Therefore, the conventional GPC cannot be directly applied in a network environment.
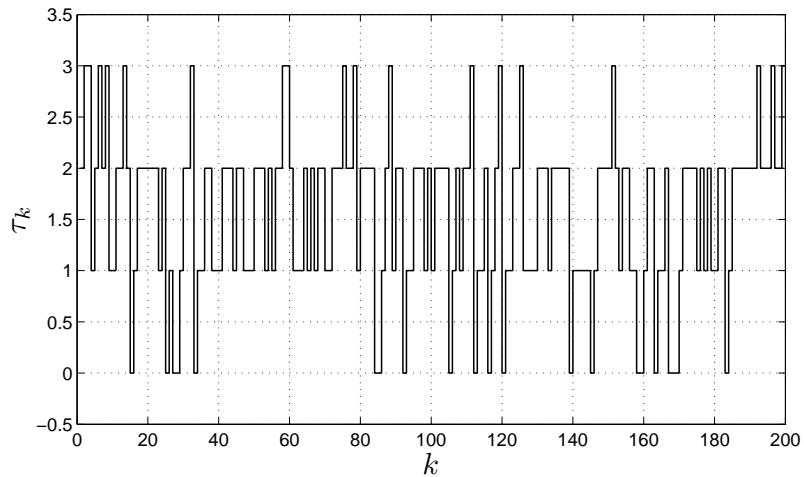
Figure 4.5: S-C delays τ_k governed by (4.37).

Simulation 3: M-GPC for networked HPCS tracking control. To verify the effectiveness of the proposed compensation schemes for S-C and C-A delays, the developed M-GPC is applied to the networked HPCS with identical pre-set parameters and the same network conditions as in Simulation 2. According to Theorem 4.1, theoretically the stochastic stability is guaranteed through checking the feasibility of a set of LMIs. This fact can also be observed and verified from the tracking performance shown in Figure 4.8. From the Figure 4.8, the system is stable and exhibits acceptable tracking performance.
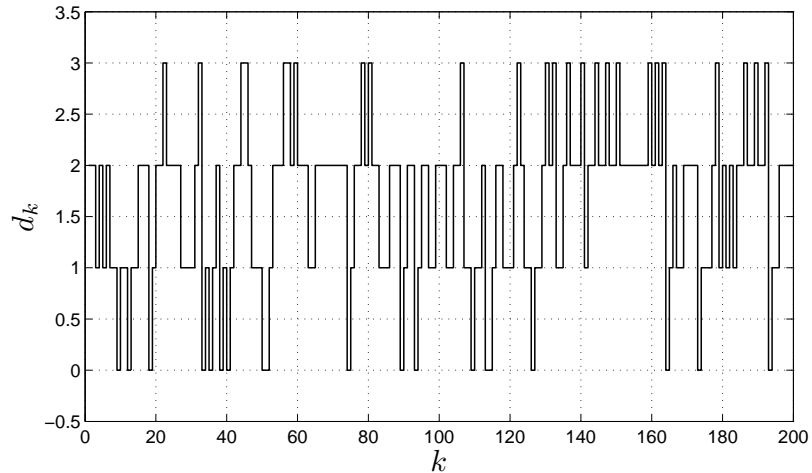
Figure 4.6: C-A delays d_k governed by (4.37).

4.4.2 Experimental tests

After the simulation studies for the controller design, the hardware-in-the-loop (HIL) test is conducted: The developed M-GPC is applied to an experimental HPCS shown in Figure 4.3. The network-induced delays are simulated and modeled as Markov chains in the control computer using the same parameters as in the simulation studies.

Figure 4.9 shows the experimental response of the system using conventional GPC for a local control setup without delays. Figure 4.10 shows the experimental response of directly applying the conventional GPC in the NCS with time delays governed by (4.37). It is clear that the system becomes unstable. By applying the M-GPC method, the results are shown in Figure 4.11. It is observed that the system is stable. The output can track the desired input and the M-GPC guarantees the stability. Note that the difference between the experimental and simulation results is mainly due to the modeling error and disturbance in the experiments. Through the experimental tests, it is clearly observed that the proposed M-GPC is effective in compensating for both S-C and C-A delays.

4.5 Conclusion

This chapter investigates the predictive controller design problem for NCSs with time delays. Both the S-C and C-A time delays are random and modeled by Markov chains. The M-GPC method is proposed to compensate for the time delays in both links. The closed-loop system is formulated to be a special jump linear system. The sufficient and necessary condition for stochastic stability is provided in terms of LMIs, which can be conveniently checked. The proposed design method is further tested on an experimental networked HPCS. The experimental results indicate that the
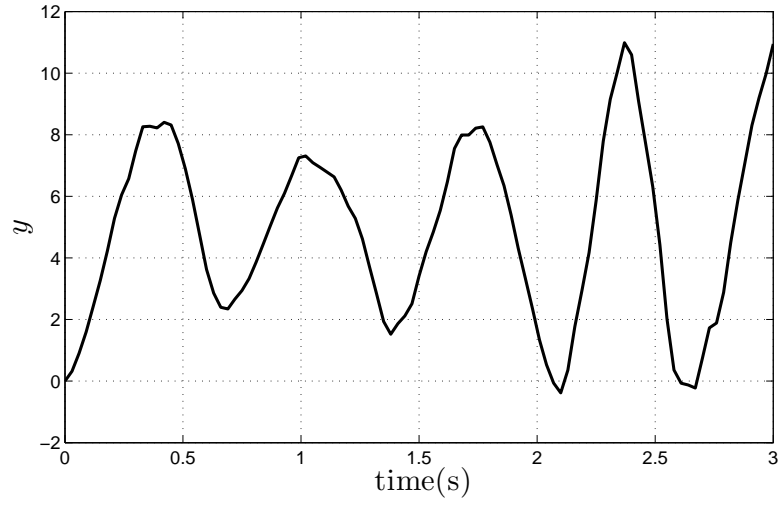
Figure 4.7: Simulation 2: Tracking performance of conventional GPC applied to the networked HPCS with delays governed by (4.37).

proposed theoretical tools can be useful in real NCSs. Important issues such as robust G-MPC design against model uncertainties, disturbance attenuation, and tracking performance improvement need further study.
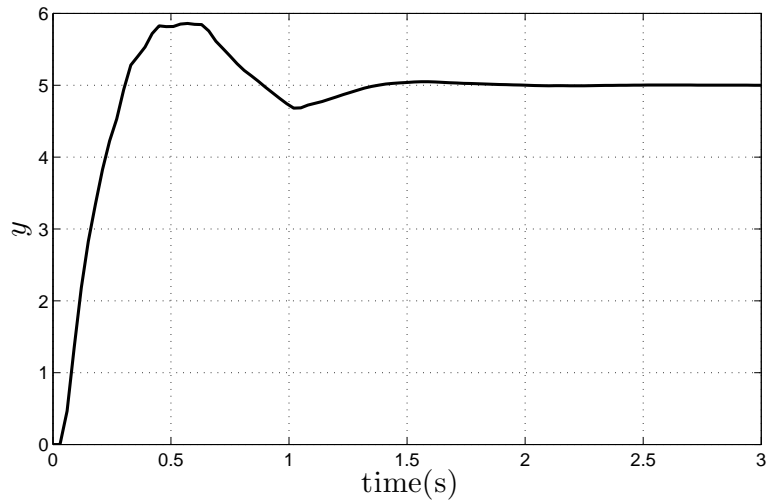
Figure 4.8: Simulation 3: Tracking performance of the M-GPC applied to the networked HPCS with delays governed by (4.37).
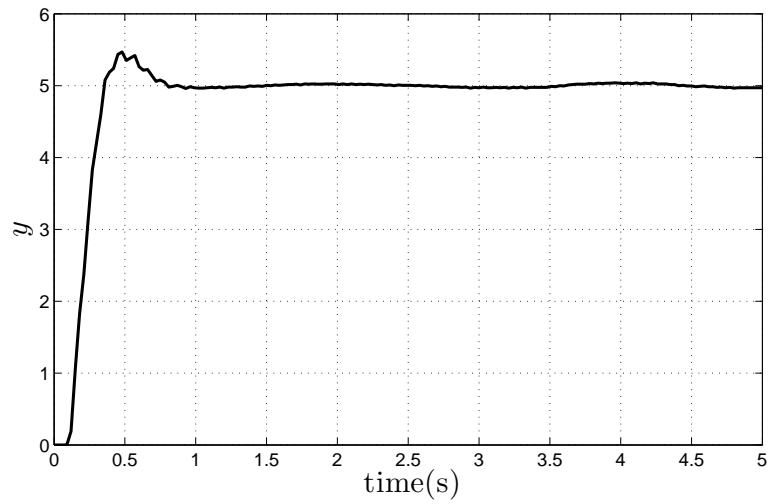
Figure 4.9: Experimental result: Tracking performance of conventional GPC applied to the local HPCS.
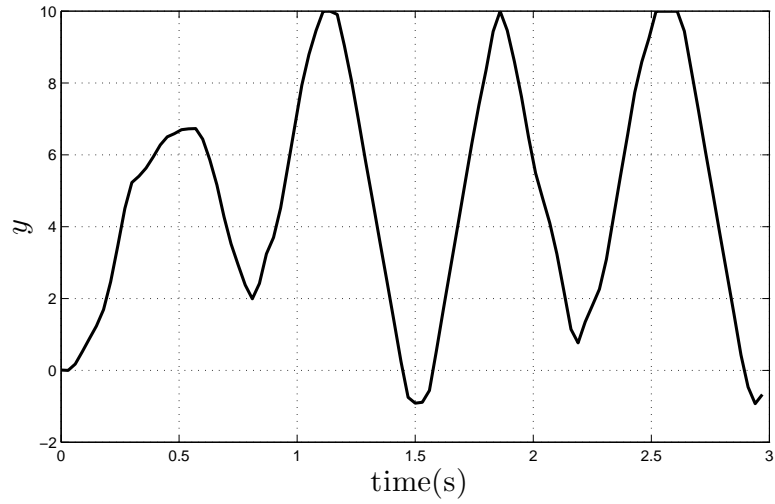
Figure 4.10: Experimental result: Tracking performance of conventional GPC applied to the networked HPCS with delays governed by (4.37).
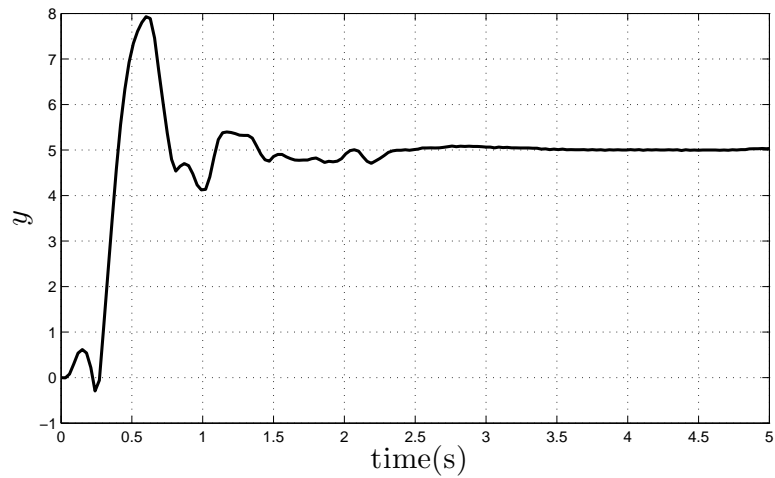
Figure 4.11: Experimental result: Tracking performance of M-GPC applied to the networked HPCS with delays governed by (4.37).

CHAPTER 5

$l_2 - l_\infty$ FILTERING FOR MULTIRATE SYSTEMS

5.1 Introduction

Multirate systems are common in chemical [51], mechanical [84], aeronautic [37], and communication [105, 107, 108] applications. In some complex systems, it is unrealistic and uneconomical, or sometimes impossible to sample all the physical signals uniformly at one single rate. Multirate systems arise when the components of the same system have several different sampling rates. A special and simple case of multirate systems is the dual-rate system where the input and states are updated at a fast rate and the output is sampled at a slow rate. In such dual-rate systems, a challenge for filtering is how to obtain fast-rate information, e.g., fast-rate states, from the slow sampled output measurements.

The filtering problem is to estimate the states or a linear combination of the states of a system based on the available measurements. The well-known Kalman filter provides a recursive algorithm to minimize the variance of the state estimation error when the power spectral densities of the process and the measurement noise are known [109, 112]. When the *a priori* information is not precisely known, the celebrated Kalman filter is not applicable. In such cases, filters based on alternative performance criteria have been developed and attracted much attention in the past several decades. One of these is the H_2 filtering which minimizes the H_2 norm of the transfer function from the process noise to the estimation error, see, e.g., [43, 44] and the references therein. Another is the H_∞ filtering which minimizes the H_∞ norm of the transfer function from the process noise to the estimation error [25, 43, 94, 137]. Recently, Sheng *et al.* extended the H_2 and H_∞ design methods to multirate systems [101, 102]. On the other hand, the $l_2 - l_\infty$ filtering design problems have received relatively less attention. The objective of $l_2 - l_\infty$ filtering is to design stable filters minimizing the peak value of the estimation error for all possible energy bounded disturbance, therefore it is also called energy-to-peak filtering. The $l_2 - l_\infty$ filtering design problems for single-rate systems have been studied, see, e.g., [42, 50] and the references therein. For multirate systems, however, the $l_2 - l_\infty$ filtering problem has not been fully investigated in the literature, which is still open and remains unsolved.

In this chapter, the approach to solve multirate filtering problems in the $l_2 - l_\infty$ setting is

proposed. Similar to the H_2 and/or H_∞ filtering [101, 102], while using the LMI machinery to solve $l_2 - l_\infty$ filtering problems, there is an unavoidable nonconvex constraint which is due to the particular structure of the designed filters. This technical difficulty can be handled by the product reduction algorithm (PRA) [24].

The rest of this chapter is organized as follows. In Section 5.2, multirate systems and lifted systems are introduced, and then the objective of multirate filtering problems in the $l_2 - l_\infty$ setting is stated. Furthermore, using the lifting technique, the proposed design is reformulated as a linear time-invariant $l_2 - l_\infty$ filtering problem. The main results involving LMI conditions with a nonconvex constraint are shown in Section 5.3. Also, the procedure to compute solutions by the PRA is presented. In Section 5.4, illustrative examples are provided. Finally, some concluding remarks are addressed in Section 5.5.

For simplicity, this chapter focuses on single-input single-output (SISO) multirate systems. The extension to multi-input multi-output multirate systems can be made following a similar line. The notation used throughout this chapter is fairly standard. The superscript ᵀ stands for the matrix transposition and the notation $P > 0$ means that P is symmetric and positive definite. In addition, diag{.} is used for a block-diagonal matrix. For a discrete-time vector-valued signal $f(k)$, the l_2 norm is $\|f\|_2 = \{\sum_0^\infty f(k)^\mathrm{T} f(k)\}^{1/2}$ and the l_∞ norm is $\|f\|_\infty = \sup_k \{f(k)^\mathrm{T} f(k)\}^{1/2}$.

5.2   Preliminaries and Problem Formulation

In this section, some preliminary knowledge about multirate systems will be given first, and then the objective of the $l_2 - l_\infty$ filtering design problem for multirate systems will be stated, and further the multirate filtering design problem will be converted to the filtering of a linear time-invariant (LTI) single rate system using the lifting technique [20, 102]. It is also worth noting that although the chapter deals with a special kind of dual-rate system for simplicity, more general treatment can be achieved by following the similar line.

Consider the multirate (specially dual-rate) sampled-data system in Figure 5.1. The input ω is updated at the fast period h, and the output y is sampled at the slow period nh, with n (the down-sampling ratio) being a positive integer; P_h is a discrete-time model with discretization period h; S_n is the discrete-time downsampler defined by

$$y = S_n v \Longleftrightarrow y[k] = v[kn], k = 0, 1, 2, ...$$

In Figure 5.1, the high-frequency dots stand for the fast-rate signal while the slow-frequency dots represent the slow-rate signal. The dual-rate system is time-varying. By applying the lifting technique [20], the lifted model $\underline{P} = S_n P_h L_n^{-1}$ can be obtained. Here, L_n and L_n^{-1} are the lifting and inverse lifting operators. For an integer $n > 0$, define the discrete lifting operator L_n via
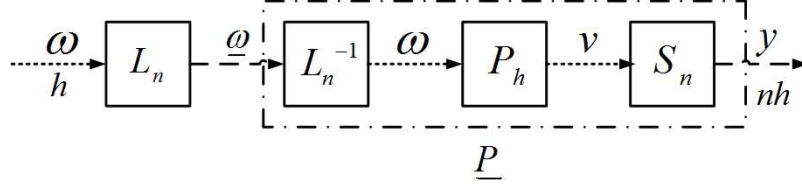
Figure 5.1: SISO dual-rate discrete-time system with lifting and inverse lifting operators.

$\underline{v} = L_n v,$

$$\left\{ v(0), \quad v(1), \quad \cdots \right\} \mapsto \left\{ \begin{bmatrix} v(0) \\ \vdots \\ v(n-1) \end{bmatrix}, \begin{bmatrix} v(n) \\ \vdots \\ v(2n-1) \end{bmatrix}, \quad \cdots \right\}.$$

The definition of inverse lifting operator is the reversion of the lifting operation. The input of the lifted model is the lifted signal $\underline{\omega}$ and its output is still y. Hence, $\underline{P}$ can be regarded as a single-rate multi-input single-output system with underlying period nh; furthermore, it is time-invariant.

5.2.1 Design objectives

Assume the discrete-time model P_h is known

$$x[k+1] \quad = \quad Ax[k] + B\omega[k], \tag{5.1a}$$

$$v[k] \quad = \quad Cx[k] + D\omega[k], \tag{5.1b}$$

$$z[k] \quad = \quad Fx[k]. \tag{5.1c}$$

Here, $x[k]$ is the state vector, $\omega[k]$ is the exogenous input, $v[k]$ is the fast-rate output, and $z[k]$ is the linear combination of the states to be estimated. The matrices A, B, C, and D are of appropriate dimensions.

Then, the lifted model $\underline{P}$ can be obtained as follows [20]:

$$\underline{x}[k+1] \quad = \quad \underline{A}\,\underline{x}[k] + \underline{B}\,\underline{\omega}[k], \tag{5.2a}$$

$$y[k] \quad = \quad \underline{C}\,\underline{x}[k] + \underline{D}\,\underline{\omega}[k]. \tag{5.2b}$$

Here,

$\underline{A} = A^n, \quad \underline{B} = [A^{n-1}B \ \ A^{n-2}B \ \ \cdots \ \ B], \quad \underline{C} = C, \quad \underline{D} = [D \ \ 0 \ \ \cdots \ \ 0],$

and $\underline{x}[k] = x[kn], y[k] = v[kn], \underline{\omega} = L_n\omega = [\omega[kn] \ \ \omega[kn+1] \ \ \cdots \ \ \omega[kn+n-1]]^{\mathrm{T}}$. Note that the lifting operator is *norm-preserving* [20]. For the case of l_2 norm, $\|\underline{\omega}\|^2 = \|\omega\|^2$.

The filtering error dynamics are illustrated in Figure 5.2, where S_1 is the sampler with sampling period h. The filter to be designed is time-varying: It will generate the state estimation $\hat{x}$ and the corresponding $\hat{z}$ every fast period h based on the measured y, which is only available at the slow period nh. During the kth frame period $[knh, (k+1)nh]$, at every intersample time instant $knh+ih$,

68
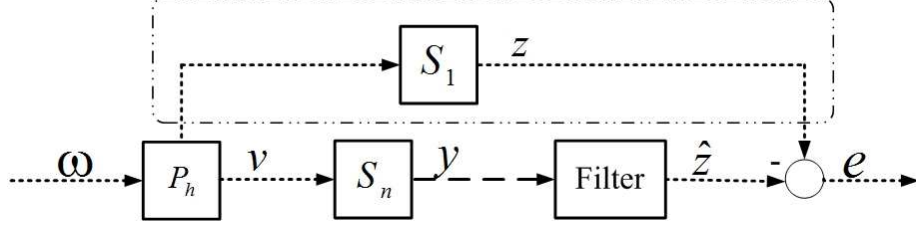
Figure 5.2: Filtering error dynamics for time-varying dual-rate systems.

the filter will use the most recent measured output $y[knh]$ to estimate the state $\hat{x}[knh + ih]$, $(i = 1, \ldots, n)$ and the corresponding $\hat{z}[knh + ih]$.

The observer has the following form:

$$\hat{x}[k + 1] = A\hat{x}[k] + K(y[k] - C\hat{x}[k]),$$

where K is the filter gain to be designed based on some system performance criterion. Considering that the dual-rate system is periodically time-varying, the similar structure is adopted and the gain K is periodically time-varying. That means at the intersample estimation time instant $knh + ih$, $K = L(i)$, $i = 1, 2, \ldots, n$. How to design this series of gains in the $l_2 - l_\infty$ settings is the focus of this chapter. To summarize, the objective of the multirate filtering design problem is:

Given $\gamma > 0$, find a series of filter gains $L(i)$ $(i = 1, \ldots, n)$, so that

1. The filter error system is asymptotically stable;

2. The $l_2 - l_\infty$ gain of the error system satisfies $\frac{\|e\|_\infty}{\|\omega\|_2} < \gamma$ (γ-suboptimal $l_2 - l_\infty$ filtering).

5.2.2 Lifted error system

Applying the lifting technique [20], the design problem will be converted into an LTI equivalent one following the similar line in [101, 102]. Define $\tilde{y}[kn] = v[kn] - \underline{C}\hat{x}[kn]$, the to-be-designed multirate filtering during the nth frame period can be written as follows:

$$\hat{x}[kn + i + 1] = A^{i+1}\hat{x}[kn] + [A^i L(1) + \cdots + L(i + 1)]\tilde{y}[kn], \quad (5.3a)$$

$$\hat{z}[kn + i] = F\hat{x}[kn + i], \quad (5.3b)$$

where $i = 0, 1, \ldots, n - 1$.

Let $e[kn] = z[kn] - \hat{z}[kn]$ and $x_e[kn] = x[kn] - \hat{x}[kn]$, it is straightforward to obtain

$$e[kn + i] = F[A^i - MLC] x_e[kn] - F[N - MLD] \underline{\omega}[k], \quad (5.4)$$

where

$$M = [\overbrace{A^{i-1} \quad \cdots \quad I}^{i\ blocks} \quad \overbrace{0 \quad \cdots \quad 0}^{n-i\ blocks}],$$

69

$$\overbrace{\qquad}^{i\ blocks}\qquad\overbrace{\qquad}^{n-i\ blocks}$$

$$N = [\ A^{i-1}B\ \ \cdots\ \ B\ \ 0\ \ \cdots\ \ 0\ ],$$

$$L = \left[\ L(1)^{\mathrm{T}}\ \ L(2)^{\mathrm{T}}\ \ \cdots\ \ L(n)^{\mathrm{T}}\ \right]^{\mathrm{T}}.$$

Now, define the state estimation error $\underline{x}_e[k] = x_e[kn]$, and lift filtering errors in the kth frame period as

$$\underline{e}[k] = \left[\ e[kn]^{\mathrm{T}}\ \ e[kn+1]^{\mathrm{T}}\ \ \cdots\ \ e[kn+n-1]^{\mathrm{T}}\ \right]^{\mathrm{T}}.$$

The model for the lifted error dynamics is then

$$\underline{x}_e[k+1] = \tilde{A}\ \underline{x}_e[k] + \tilde{B}\ \underline{\omega}[k], \tag{5.5a}$$

$$\underline{e}[k] = \tilde{C}\ \underline{x}_e[k] + \tilde{D}\ \underline{\omega}[k], \tag{5.5b}$$

where

$$\tilde{A} = A_0 - A_f L C_f,$$
$$\tilde{B} = B_0 - A_f L D_f,$$
$$\tilde{C} = C_0 - B_f L C_f,$$
$$\tilde{D} = D_0 - B_f L D_f,$$

with $A_0 = \underline{A}$, $B_0 = \underline{B}$, $C_0 = \begin{bmatrix} F \\ FA \\ \vdots \\ FA^{n-2} \\ FA^{n-1} \end{bmatrix}$, $D_0 = \begin{bmatrix} 0 & 0 & \cdots & \cdots & 0 \\ FB & 0 & \cdots & \cdots & 0 \\ FAB & FB & 0 & \cdots & 0 \\ \vdots & \ddots & \ddots & \ddots & 0 \\ FA^{n-2}B & \ddots & \ddots & FB & 0 \end{bmatrix}$,

and $A_f = \begin{bmatrix} A^{n-1} & A^{n-2} & \cdots & I \end{bmatrix}$, $B_f = \begin{bmatrix} 0 & 0 & \cdots & \cdots & 0 \\ F & 0 & \cdots & \cdots & 0 \\ FA & F & 0 & \cdots & 0 \\ \vdots & \ddots & \ddots & \ddots & 0 \\ FA^{n-2} & \ddots & \ddots & F & 0 \end{bmatrix}$, $C_f = \underline{C}$, $D_f = \underline{D}$.

Notice that the lifted error dynamics with input $\underline{\omega}$ and output $\underline{e}$ in (5.5) are time-invariant [20]. Therefore, the original multirate filtering problems can be converted to the $l_2 - l_\infty$ filter design for a single-rate LTI system.

5.3 $l_2 - l_\infty$ Multirate Filtering Design

In this section, the multirate filtering design problem is solved in the framework of LMI machinery under the $l_2 - l_\infty$ setting. The following lemma provides the relationship of the $l_2 - l_\infty$ performance between the original and the lifted error system.

Lemma 5.1. The γ-suboptimal $l_2 - l_\infty$ filtering problem is equivalent to finding a vector L so that the lifted filter error system is asymptotically stable and the $l_2 - l_\infty$ gain from $\underline{\omega}$ to $\underline{e}$ in (5.5) satisfies $\frac{\|\underline{e}\|_\infty}{\|\underline{\omega}\|_2} < \gamma$.

Proof. The result can be obtained by considering the norm preserving property of the lifting operator:

$$\|\underline{\omega}\|_2 = \|\omega\|_2,$$

$$\|\underline{e}\|_\infty = \|e\|_\infty.$$

Therefore,

$$\frac{\|\underline{e}\|_\infty}{\|\underline{\omega}\|_2} = \frac{\|e\|_\infty}{\|\omega\|_2}.$$

This proves Lemma 5.1. □

The following lemma gives the traditional $l_2 - l_\infty$ performance condition.

Lemma 5.2. [50] Suppose $(\tilde{A},\ \tilde{B},\ \tilde{C},\ \tilde{D})$ is arbitrary but fixed and let $\gamma > 0$ be given. Then the filtering error system is stable with an $l_2 - l_\infty$ disturbance attenuation level γ if and only if there exists a matrix $P > 0$ satisfying

$$\tilde{C}P\tilde{C}^{\mathrm{T}} + \tilde{D}\tilde{D}^{\mathrm{T}} < \gamma^2 I, \tag{5.6a}$$

$$\tilde{A}P\tilde{A}^{\mathrm{T}} - P + \tilde{B}\tilde{B}^{\mathrm{T}} < 0. \tag{5.6b}$$

Inequalities (5.6) contain the multiplication of two variables. Hence, they cannot be easily solved by the LMI solvers because they are nonlinear. In order to handle this difficulty, a new performance condition is derived, which is equivalent to Lemma 5.2.

Theorem 5.1. Given $\gamma > 0$, the multirate γ-suboptimal $l_2 - l_\infty$ filtering problem has a solution (L) if and only if there exists a matrix $P > 0$ satisfying

$$\begin{bmatrix} \gamma^2 I & \tilde{C}P & \tilde{D} \\ P\tilde{C}^{\mathrm{T}} & P & 0 \\ \tilde{D}^{\mathrm{T}} & 0 & I \end{bmatrix} > 0, \tag{5.7a}$$

$$\begin{bmatrix} P & \tilde{A}P & \tilde{B} \\ P\tilde{A}^{\mathrm{T}} & P & 0 \\ \tilde{B}^{\mathrm{T}} & 0 & I \end{bmatrix} > 0. \tag{5.7b}$$

Proof. Inequality (5.6a) can be rewritten as

$$(\gamma^2 I - \tilde{D}\tilde{D}^{\mathrm{T}}) - (\tilde{C}P)(P^{-1})(P\tilde{C}^{\mathrm{T}}) > 0.$$

Using Schur complement [8], the inequality above is equivalent to

$$\begin{bmatrix} \gamma^2 I - \tilde{D}\tilde{D}^{\mathrm{T}} & \tilde{C}P \\ P\tilde{C}^{\mathrm{T}} & P \end{bmatrix} > 0. \tag{5.8}$$

Furthermore, (5.8) can be written as

$$
\begin{bmatrix} \gamma^2 I & \tilde{C}P \\ P\tilde{C}^{\mathrm{T}} & P \end{bmatrix} - \begin{bmatrix} \tilde{D} \\ 0 \end{bmatrix} (I) \begin{bmatrix} \tilde{D}^{\mathrm{T}} & 0 \end{bmatrix} > 0.
$$

Using Schur complement [8] again, the inequality (5.7a) can be obtained. By following the similar procedure, the inequality (5.7b) can be derived from inequality (5.6b). This proves Theorem 5.1. $\square$

Notice that $(\tilde{A}, \ \tilde{B}, \ \tilde{C}, \ \tilde{D})$ are all affine in the unknown vector L, the two inequalities (5.7a) and (5.7b) are thus nonlinear and cannot be easily solved by the LMI solvers. But it can be converted to the LMI problems with a nonconvex constraint, as stated in the following theorem.

Theorem 5.2. Given $\gamma > 0$, the multirate γ-suboptimal $l_2 - l_\infty$ filtering problem has a solution (L) if and only if there exist matrices $P > 0$ and $W > 0$ satisfying

$$
\begin{bmatrix} \gamma^2 I & \tilde{C} & \tilde{D} \\ \tilde{C}^{\mathrm{T}} & W & 0 \\ \tilde{D}^{\mathrm{T}} & 0 & I \end{bmatrix} > 0, \tag{5.9a}
$$

$$
\begin{bmatrix} P & \tilde{A} & \tilde{B} \\ \tilde{A}^{\mathrm{T}} & W & 0 \\ \tilde{B}^{\mathrm{T}} & 0 & I \end{bmatrix} > 0, \tag{5.9b}
$$

with the new variable W and constraint $PW = I$.

Proof. Inequalities (5.9a) and (5.9b) can be derived from (5.7a) and (5.7b) by performing the congruence transformation with $\mathrm{diag}\{I, P^{-1}, I\}$, respectively. $\blacksquare$

All inequalities in Theorem 5.2 now appear in linear forms, with the constraint $PW = I$. However, this condition is nonconvex. This is due to the filter structure chosen in this work. This nonconvex constraint cannot be eliminated by using the linearizing change of variables in [42, 43]. This problem can be solved by some LMI-based algorithms, such as, alternating projections method, min-max algorithm, XY-centering algorithm, and PRA. In [24], the above mentioned algorithms are compared, and numerical experiments show that the PRA is the best since it is simple and very efficient in numerical implementation, and seldom fails to find a global optimum.

The PRA is based on the fact that for any matrices $X > 0$, $Y > 0$ and $X, \ Y \in R^{n \times n}$, if the LMI

$$
\begin{bmatrix} X & I \\ I & Y \end{bmatrix} \geq 0
$$

is feasible, then $\mathrm{trace}(XY) \geq n$, and $\mathrm{trace}(XY) = n$ if and only if $XY = I$. Hence, a feasible solution of Theorem 5.2 can be obtained from the solution of the following nonconvex optimization

problem:

$$\text{minimize trace}(PW) \text{ subject to } \begin{bmatrix} P & I \\ I & W \end{bmatrix} \geq 0 \text{ and inequalities (5.9a) and (5.9b).} \qquad (5.10)$$

It can be seen that if the optimal solution of (5.10) satisfies $\text{trace}(PW) = n$, then the filter design problem is solved; otherwise, the problem is infeasible. Hence, the filter design problem is converted to finding a global solution of the minimization problem. This, however, still a difficult problem since the objective function is nonconvex. The PRA can find the global solutions of this kind iteratively to most of the time [24].

Based on the PRA, the multirate $l_2 - l_\infty$ filter design problems can be solved by the following procedure. Given certain fixed γ, then use PRA to solve P, W, and L iteratively as follows:

(1) Start from P_0 and W_0 satisfying $\begin{bmatrix} P & I \\ I & W \end{bmatrix} \geq 0$ and inequalities (5.9).

(2) Define the linear objective function $f_k(P, W) := \text{trace}(W_k P + P_k W)$.

(3) Solve for (P_{k+1}, W_{k+1}) the convex optimization

$$\text{minimize } f_k \text{ subject to } \begin{bmatrix} P & I \\ I & W \end{bmatrix} \geq 0 \text{ and inequalities (5.9).}$$

(4) If f_k converges, then exit; otherwise, then repeat the procedure from step 2).

From the steps (2) and (3), the problem is converted to a linear convex optimization problem, which is easy to solved by the LMI toolbox softwares. As the objective is to find the minimum value of γ, if P, W, and L are feasible by using the above PRA, try a smaller γ and repeat the steps (1) – (4). This way the suboptimal γ and the corresponding gain L will be obtained.

5.4   Numerical Examples

In this section, filtering design examples about the state estimator design $(F = I)$ for dual-rate systems are given to illustrate the effectiveness of the proposed method.

Example 1: Consider a system [102] where the output can only be sampled at a fixed period $T = 1$ s, but the state estimation is required every $h = 0.25$ s. Assume P_h in Figures 5.1 with

$$A = \begin{bmatrix} 1.0168 & 0.2059 \\ -1.8117 & 0.3991 \end{bmatrix} \quad , \quad B = \begin{bmatrix} 0.0317 \\ 0.0111 \end{bmatrix},$$

$$C = \begin{bmatrix} -0.8 & 0.6 \end{bmatrix} \quad , \quad D = 1.5.$$

Using the LMI machinery, a slow single-rate (SSR) $l_2 - l_\infty$ state filtering is first designed to estimate the states every period T in accordance with the output availability. The performance of the SSR

$l_2 - l_\infty$ state filtering is shown in Figures 5.3 and 5.4 for states x_1 and x_2, respectively, where the solid lines represent the real states and the dash lines stand for the SSR $l_2 - l_\infty$ estimation.
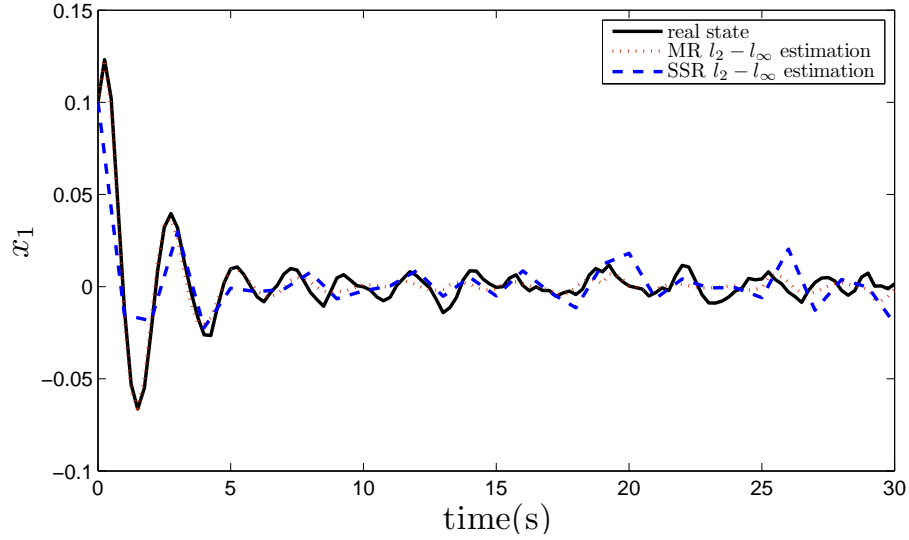
Figure 5.3: State estimation (x_1).
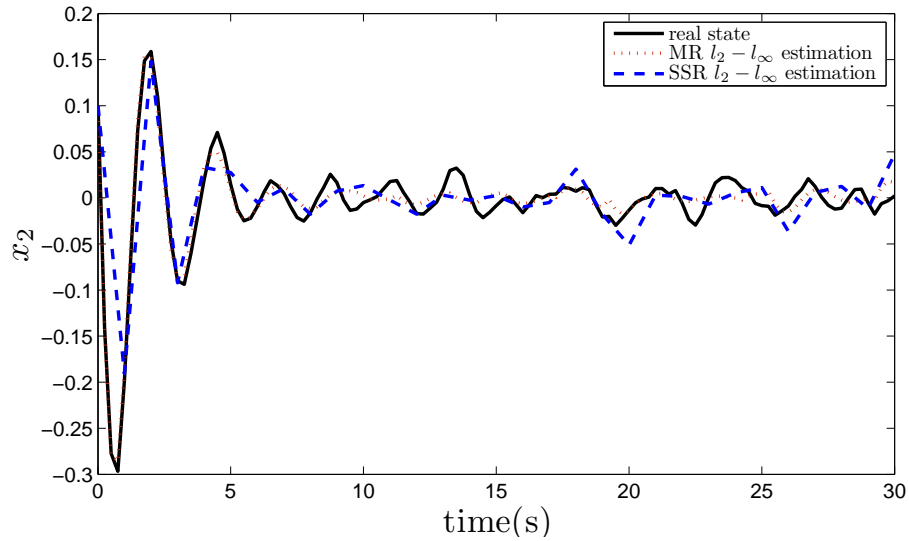
Figure 5.4: State estimation (x_2).

From the figures, it is clear that the SSR $l_2 - l_\infty$ design cannot provide satisfactory estimation performance because the period T is too large to capture the system information at the intersample instants. To consider the intersample estimation, the multirate $l_2 - l_\infty$ design in Section 5.3 is applied. Here, $n = T/h = 4$, and a series of 4 gain vectors $L(i)$, $i = 1, 2, 3, 4$, are designed.

Starting from certain large value of γ and trying smaller values step by step, it is finally found that the minimum value of γ to guarantee the feasibility of the optimization problem is 0.2458,

by using the PRA. Hence, the smallest $l_2 - l_\infty$ level is $\gamma = 0.2458$ and the corresponding L can be obtained accordingly. The simulation time is $30s$; the initial values are $x_1(0) = x_2(0) = 0.1$, and the exogenous input ω is a random signal with zero mean and variance 0.04. The response of x_1 and x_2 are shown in Figures 5.3 and 5.4 for comparison, where the dotted lines represent the multirate $l_2 - l_\infty$ state estimation. The $l_2 - l_\infty$ gain of this simulation is calculated as

$$\frac{\|e\|_\infty}{\|\omega\|_2} = 0.0569 < 0.2458.$$

From the figures and calculation, it is observed that the $l_2 - l_\infty$ multirate filter designed gives much better state estimation than the SSR design at the intersample instants based on the most recent available output, although the current output may not be available. It also provides very good state estimation compared with the real states.

Example 2: Analysis and comparisons with H_2 and H_∞ filters.
The famous Kalman filter has a minimum mean squared error type performance for linear system with the noise input of a known power spectral density. However, it does not work well for the uncertainty and nonstochastic input situations. The H_2 filter has a minimum error energy type performance for linear systems. The H_∞ filter places a boundary on the energy gain from the input to the filter error. The objective of H_∞ filtering is to minimize the energy of the estimation error for the worst possible bounded energy disturbance. The $l_2 - l_\infty$ filter guarantees a boundary on the energy-to-peak gain from the input to the filter error. The objective of $l_2 - l_\infty$ filtering is to minimize the peak value of the estimation error for the worst possible input (or disturbance) with bounded energy. The different performance criteria are shown in the following table.

Table 5.1: Filter performance criteria

Filter	Performance	Mathematic Description
Kalman	Mean Squared Error	$\min(E\|e\|_2^2)$
H_2	Least Squared Error	$\min(\|e\|_2^2)$
H_∞	Maximal Energy Gain	$\|G_{e\omega}\|_\infty^2 < \gamma^2$ or $\sup \frac{\|e\|_2}{\|\omega\|_2} < \gamma$
$l_2 - l_\infty$	Maximal Energy-to-peak Gain	$\sup \frac{\|e\|_\infty}{\|\omega\|_2} < \gamma$

Hence, if the design objective is focused on the energy of the filter error, the H_2 filter method should be employed. If the concern is on the energy gain from input to filter error, the H_∞ design scheme should be used. If the design objective is focused on energy-to-peak gain, the $l_2 - l_\infty$ is a better choice.

In the following, the results of the $l_2 - l_\infty$ filtering method with H_2 filter and H_∞ filter [102] are first compared in terms of $\|e\|_2$ and $\|e_\infty\|$ with the same input. The simulation time is $50s$; the initial values are $x_1(0) = x_2(0) = 0.1$, and the exogenous input ω is a random signal with zero mean and variance 0.04. The comparison is listed in Table 5.2. It is shown that $\|e\|_\infty$ of the $l_2 - l_\infty$

filter is smaller than both the H_2 filter and the H_∞ filter; however, the $\|e\|_2$ of the $l_2 - l_\infty$ filter is a bit larger in this example.

Table 5.2: Performance comparison ($\|e\|_2$ and $\|e\|_\infty$) for three filters with same inputs

Filter	$\|e\|_2$	$\|e\|_\infty$
H_2 Filter [102]	0.15256	0.024975
H_∞ Filter [102]	0.15260	0.024872
$l_2 - l_\infty$ Filter	0.15300	0.024525

Further, the ∞-norm of the filtering error signal ($\|e\|_\infty$) is compared for three types of filters with two different inputs: Unit impulse and white noise with the power of 1. The simulation time is $5000s$. The results are shown in Table 5.3. It is observed that for both input signals used in the experiment, the $l_2 - l_\infty$ filter results in smaller $\|e\|_\infty$ than both H_2 filter and H_∞ filter do.

Table 5.3: Performance comparison ($\|e\|_\infty$) for three filters with different inputs

Filter	Impulse input	White noise input
H_2 Filter [102]	0.019713	1.3005
H_∞ Filter [102]	0.018316	1.2991
$l_2 - l_\infty$ Filter	0.012941	1.2845

5.5   Conclusion

In this chapter, the $l_2 - l_\infty$ filter design problems for a special kind of multirate systems are considered where the output sampling period is an integer multiple of the input updating period. With the design of a periodically time-varying filter, a good estimation of the state at the fast rate can be obtained by using the slow output information. The proposed $l_2 - l_\infty$ multirate filter design problems are solved based on the lifting and LMI techniques. The nonconvex constraint is handled by the PRA. Several design examples are given to demonstrate the effectiveness of the method.

IDENTIFICATION OF HAMMERSTEIN OUTPUT-ERROR SYSTEMS WITH TWO-SEGMENT NONLINEARITIES BASED ON NEW SWITCHING SEQUENCES

6.1 Introduction

Industrial processes usually contain complex nonlinearities, which can be represented by some nonlinear mathematical models, e.g., Hammerstein and Weiner systems. The Hammerstein model consists of a static nonlinear block followed in series by a linear dynamic system. The identification of Hammerstein systems has been an active research area in the past years as it can find many engineering applications, e.g., biomedical engineering [114], power systems [1], chemical processing [36, 110] and communication systems [59], to name a few. Bai proposes an optimal two-stage method for Hammerstein-Wiener systems based on the recursive least square and singular value decomposition [3]; further, an iterative identification method is studied for Hammerstein systems with piecewise-linear nonlinearities in [75]. An identification method for MIMO Hammerstein models based on least square support vector machines is studied in [45]. In [150], a nonparametric approach is employed, and recursive algorithms are proposed for Hammerstein systems where the linear part is an ARX subsystem and the nonlinear function is not parameterized and no assumption is made on the structure of it. To analyze the convergence property of identification algorithms for Hammerstein systems is important. In [5], a detailed study on the convergence of the iterative algorithm is carried out and various convergence properties of the iterative algorithm are derived. Recently, iterative and recursive identification algorithms for Hammerstein systems based on the idea of replacing unmeasurable noise terms in information vectors by their estimates have been presented and the convergence properties are also addressed [27, 29–31].

Many nonlinear characteristics can be approximated by polynomials over a restricted range in industrial applications. A large portion of existing literatures in Hammerstein modeling assume that the nonlinear function is analytic and might be represented by a single polynomial form. However, the single polynomial approximation may be inappropriate for the whole operating range

of nonlinear systems. The two-segment nonlinearity representation (shown in Figure 6.1) can find many applications in practice, and usually different characteristics are exhibited for the positive and negative inputs. One approach to deal with this is to introduce appropriate switching sequences to transform the two-segment nonlinearities into the single nonlinearity form, which has been used in parameter identification and adaptive control [66, 120]. Vörös proposes an iterative algorithm using the so-called key term separation principle [120], and extends it to systems with multi-segment nonlinearities, deadzones and time-varying piecewise-linear characteristics [121–124]. However, this type of switching sequence may result in some redundancy of parameters to be estimated.

In this chapter, new switching sequences are proposed, which can result in less parameters to be estimated for identification of Hammerstein models with two-segment nonlinearities. This leads to the development of an identification model parametrization using the proposed new switching sequences. Furthermore, stochastic gradient algorithms based on the idea of replacing unmeasurable terms in the information vectors by their estimates are applied to the identification model, and the convergence analysis of the proposed algorithm is carried out. A varying forgetting factor (VFF) scheme is further proposed to make a tradeoff between the convergence rate and estimation accuracy.

The remainder of this chapter is organized as follows. In Section 6.2, the characteristics of two-segment nonlinearities are studied and new switching sequences are proposed. The identification model is derived in Section 6.3 by applying the proposed switching sequences. Section 6.4 describes the stochastic gradient algorithms and carries out the convergence analysis. Section 6.5 provides several illustrative numerical examples to show the effectiveness of the proposed algorithms. As an application example, the method is applied to the distillation columns in Section 6.6. Finally, the conclusion is addressed in Section 6.7.

In this chapter, the following notations are used.

$$
\begin{array}{ll}
\lambda_{\max}(X)\ (\lambda_{\min}(X)): & \text{Maximum (Minimum) eigenvalue of } X; \\
|X| = \det(X): & \text{Determinant of a square matrix } X; \\
\|X\|^2 = \text{tr}(XX^{\text{T}}): & \text{Trace of } XX^{\text{T}}; \\
f(t) = O\left(g(t)\right): & \exists\ \delta_0 \in \text{R}^+ \text{ and } t_0 \in \text{Z}^+,\ |f(t)| \leq \delta_0 g(t) \text{ for } t \geq t_0; \\
f(t) = o\left(g(t)\right): & f(t)/g(t) \to 0 \text{ for } t \to \infty.
\end{array}
$$

6.2 Two-Segment Nonlinearity and New Switching Sequences

In literature, the nonlinear characteristics are usually approximated by proper polynomials. To achieve better accuracy, the higher order polynomials may be utilized. However, the identification of higher order polynomials is more difficult in general. Hence, a compromise can be adopted between the lower order and precision in using polynomials to approximate the nonlinearity. On

the other hand, the single polynomial is not accurate enough for the whole operating range of nonlinear systems if the characteristics differ significantly for different ranges. Thus, it is not advisable to use single polynomials. A solution for the aforementioned problems is to use the two-segment nonlinearity description [120].
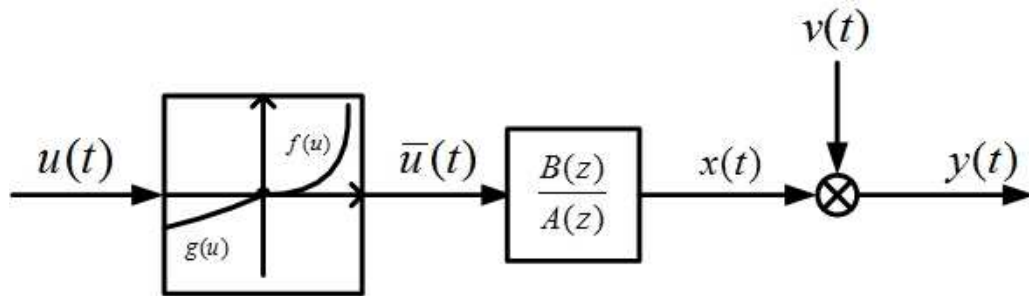
Figure 6.1: The Hammerstein output-error system with two-segment nonlinearities.

The nonlinearity $\bar{u}(t)$ in Figure 6.1 can be approximated by two different polynomials for positive and negative inputs $u(t)$, and expressed as

$$\bar{u}(t) = \begin{cases} f[u(t)], & \text{for } u(t) \geq 0, & (6.1a) \\ g[u(t)], & \text{for } u(t) < 0. & (6.1b) \end{cases}$$

Different from the switching sequence in [66, 120], the new switching sequences $h_1(t)$ and $h_2(t)$ are proposed in this chapter:

$$h_1(t) = h_1[u(t)] = \begin{cases} 1, & \text{for } u(t) \geq 0 \\ 0, & \text{for } u(t) < 0 \end{cases}, \qquad (6.2a)$$

$$h_2(t) = h_2[u(t)] = \begin{cases} 0, & \text{for } u(t) \geq 0 \\ 1, & \text{for } u(t) < 0 \end{cases}. \qquad (6.2b)$$

Then, the relation between the inputs $u(t)$ and outputs $\bar{u}(t)$ can be written as:

$$\bar{u}(t) = f[u(t)]h_1(t) + g[u(t)]h_2(t). \qquad (6.3)$$

Assume that the nonlinear parts $f(\cdot)$ and $g(\cdot)$ can be approximated by polynomials of known orders in the input, or, more generally, a nonlinear function of two different known basis $(f_1, f_2, \cdots, f_p)$ and $(g_1, g_2, \cdots, g_q)$:

$$f[u(t)] = \sum_{i=1}^{p} c_i f_i[u(t)], \qquad (6.4a)$$

$$g[u(t)] = \sum_{j=1}^{q} d_j g_j[u(t)]. \qquad (6.4b)$$

Then, (6.3) can be rewritten as:

$$\bar{u}(t) = \sum_{i=1}^{p} c_i f_i[u(t)]h_1(t) + \sum_{j=1}^{q} d_j g_j[u(t)]h_2(t). \qquad (6.5)$$

Table 6.1: Numbers of Parameters to Be Estimated in (6.5)

The proposed switching sequences (6.2)	The switching sequence (6.6) in [120]
$p + q$	$2 \times \max\{p, q\}$

Remark 6.1. The nonlinearity described in (6.1) could also be approximated by a single polynomial

$$\gamma[u(t)] = \sum_{k=1}^{R} \gamma_k u^k(t).$$

However, as mentioned above, to achieve the same level of accuracy, the orders p, q of $f(\cdot)$, $g(\cdot)$ may be lower than the order R of polynomial $\gamma(\cdot)$. This will reduce computational cost [120].

Remark 6.2. In [120], Vörös proposes a switching sequence

$$h(t) = h[u(t)] = \begin{cases} 0, & \text{for } u(t) \geq 0, \\ 1, & \text{for } u(t) < 0. \end{cases} \tag{6.6}$$

Compared with the switching sequence in [120], by using the proposed switching sequences in this chapter, less parameters in the identification of Hammerstein models are needed especially when the orders p and q differ a lot, and thus the computational cost for the same two-segment nonlinearities will be reduced. As shown in Table 6.1, numbers of parameters to be estimated are compared for these two types of switching sequences. Another advantage of the new sequences lies in that the base functions for representing $f(\cdot)$ and $g(\cdot)$ can be chosen separately, whereas they must be identical in [120].

6.3   Hammerstein Model with Two-segment Nonlinearities

Consider the Hammerstein output-error (OE) system shown in Figure 6.1 where the true output $x(t)$ (namely, the noise-free output) and the inner variable $\bar{u}(t)$ (namely, the output of the nonlinear block) are unmeasurable, $u(t)$ is the system input, $y(t)$ is the measurement of $x(t)$, $v(t)$ is an additive noise with zero mean. The nonlinear part of the system is given by (6.1). The Hammerstein output-error model in Figure 6.1 is then expressed as

$$x(t) = \frac{B(z)}{A(z)} \bar{u}(t), \tag{6.7a}$$

$$y(t) = x(t) + v(t). \tag{6.7b}$$

Here, $A(z)$ and $B(z)$ are polynomials in the shift operator $z^{-1} [z^{-1} y(t) = y(t-1)]$ with

$$
\begin{aligned}
A(z) &= 1 + a_1 z^{-1} + a_2 z^{-2} + \cdots + a_n z^{-n}, \\
B(z) &= b_1 z^{-1} + b_2 z^{-2} + b_3 z^{-3} + \cdots + b_n z^{-n}.
\end{aligned}
$$

Notice that for the Hammerstein model shown in Figure 6.1, $f(u)$, $g(u)$ and $G(z) := \frac{B(z)}{A(z)}$ are not unique. Any pair $(\alpha[f(u),\ g(u)],\ G(z)/\alpha)$ for some nonzero and finite constant α would produce identical input and output measurements. In other words, any identification scheme cannot distinguish between $(f(u), G(z))$ and $(\alpha[f(u),\ g(u)], G(z)/\alpha)$. Therefore, to get a unique parameterization, without loss of generality, one of the gains of $f(u)$, $g(u)$ and $G(z)$ has to be fixed. There are several ways to normalize the gains [3, 15]. Here, the assumption in [29] is adopted: The first coefficient of the function $f(\cdot)$ equals 1; i.e., $c_1 = 1$.

Equation (6.7a) can be rewritten as a recursive form

$$
\begin{aligned}
x(t) &= -\sum_{i=1}^{n} a_i x(t-i) + \sum_{i=1}^{n} b_i \bar{u}(t-i) \\
&= -\sum_{i=1}^{n} a_i x(t-i) + \sum_{i=1}^{n} b_i \left[\sum_{j=1}^{p} c_j f_j(t-i) h_1(t-i) + \sum_{j=1}^{q} d_j g_j(t-i) h_2(t-i) \right]. \quad (6.8)
\end{aligned}
$$

6.4 Identification Algorithm

6.4.1 Algorithm description

The purpose of parameter identification is to identify all the unknown parameters in the Hammerstein model merely based on the inputs $u(t)$ and outputs $y(t)$. The difficulty of identification is that the inner variables – $x(t)$ and $\bar{u}(t)$ are unmeasurable. The presented idea to handle this difficulty is to replace the unmeasurable terms $x(t)$ by their estimates based on the obtained parameter estimates. Define the information vector $\boldsymbol{\varphi}_0(t)$ (also called data vector) and parameter vector $\boldsymbol{\theta}$ as

$$
\begin{aligned}
\boldsymbol{\varphi}_0(t) &= [-x(t-1), \cdots, -x(t-n), \boldsymbol{\psi}_f^{\mathrm{T}}(t), \boldsymbol{\psi}_g^{\mathrm{T}}(t)]^{\mathrm{T}} \in \mathbb{R}^{(p+q+1)n}, \\
\boldsymbol{\theta} &= [\mathbf{a}^{\mathrm{T}}, c_1 \mathbf{b}^{\mathrm{T}}, c_2 \mathbf{b}^{\mathrm{T}}, \cdots, c_p \mathbf{b}^{\mathrm{T}}, d_1 \mathbf{b}^{\mathrm{T}}, d_2 \mathbf{b}^{\mathrm{T}}, \cdots, d_q \mathbf{b}^{\mathrm{T}}]^{\mathrm{T}} \in \mathbb{R}^{(p+q+1)n}, \\
\mathbf{a} &= [a_1, a_2, \cdots, a_n]^{\mathrm{T}} \in \mathbb{R}^{n}, \\
\mathbf{b} &= [b_1, b_2, \cdots, b_n]^{\mathrm{T}} \in \mathbb{R}^{n}, \\
\mathbf{c} &= [c_2, c_3, \cdots, c_p]^{\mathrm{T}} \in \mathbb{R}^{p-1}, \\
\mathbf{d} &= [d_1, d_2, \cdots, d_q]^{\mathrm{T}} \in \mathbb{R}^{q}, \\
\boldsymbol{\psi}_f(t) &= [\boldsymbol{\psi}_{f1}^{\mathrm{T}}(t), \boldsymbol{\psi}_{f2}^{\mathrm{T}}(t), \cdots, \boldsymbol{\psi}_{fp}^{\mathrm{T}}(t)]^{\mathrm{T}} \in \mathbb{R}^{pn}, \\
\boldsymbol{\psi}_g(t) &= [\boldsymbol{\psi}_{g1}^{\mathrm{T}}(t), \boldsymbol{\psi}_{g2}^{\mathrm{T}}(t), \cdots, \boldsymbol{\psi}_{gq}^{\mathrm{T}}(t)]^{\mathrm{T}} \in \mathbb{R}^{qn}, \\
\boldsymbol{\psi}_{fj}(t) &= [f_j(u(t-1))h_1(t-1), \cdots, f_j(u(t-n))h_1(t-n)]^{\mathrm{T}} \in \mathbb{R}^{n}, j = 1, 2, \cdots, p, \\
\boldsymbol{\psi}_{gj}(t) &= [g_j(u(t-1))h_2(t-1), \cdots, g_j(u(t-n))h_2(t-n)]^{\mathrm{T}} \in \mathbb{R}^{n}, j = 1, 2, \cdots, q.
\end{aligned}
$$

Then the identification model of the system is obtained:

$$
x(t) = \boldsymbol{\varphi}_0^{\mathrm{T}}(t)\boldsymbol{\theta}, \quad (6.9a)
$$

$$y(t) = \boldsymbol{\varphi}_0^{\mathrm{T}}(t)\boldsymbol{\theta} + v(t). \tag{6.9b}$$

The standard stochastic gradient algorithm

$$\hat{\boldsymbol{\theta}}(t) = \hat{\boldsymbol{\theta}}(t-1) + \frac{\boldsymbol{\varphi}_0(t)}{r(t)}[y(t) - \boldsymbol{\varphi}_0^{\mathrm{T}}(t)\hat{\boldsymbol{\theta}}(t-1)], \tag{6.10}$$

$$r(t) = r(t-1) + \|\boldsymbol{\varphi}_0(t)\|^2, \ r(0) = 1. \tag{6.11}$$

cannot be used directly to estimate the parameter vector $\boldsymbol{\theta}$ in (6.9) because the information vector $\boldsymbol{\varphi}_0(t)$ contains the unmeasured inner variable $x(t-i)$, $i = 1, 2, \cdots, n$. In order to solve this difficulty, the approach here is based on the hierarchical identification principle [28, 30]. Let $\hat{\boldsymbol{\theta}}(t)$ and $\hat{x}(t-i)$ be the estimates of $\boldsymbol{\theta}$ and $x(t-i)$, respectively. $\boldsymbol{\varphi}(t)$ denote the information vector $\boldsymbol{\varphi}_0(t)$ obtained by replacing $x(t-i)$ with $\hat{x}(t-i)$, i.e.,

$$\boldsymbol{\varphi}(t) = [-\hat{x}(t-1), -\hat{x}(t-2), \cdots, -\hat{x}(t-n), \boldsymbol{\psi}_f^{\mathrm{T}}(t), \boldsymbol{\psi}_g^{\mathrm{T}}(t)]^{\mathrm{T}}. \tag{6.12}$$

Replacing $\boldsymbol{\varphi}_0(t)$ and $\boldsymbol{\theta}$ in (6.9) with $\boldsymbol{\varphi}(t)$ and $\hat{\boldsymbol{\theta}}(t)$, respectively, the estimate $\hat{x}(t)$ can be computed by

$$\hat{x}(t) = \boldsymbol{\varphi}^{\mathrm{T}}(t)\hat{\boldsymbol{\theta}}(t). \tag{6.13}$$

Replacing the information vector $\boldsymbol{\varphi}_0(t)$ in (6.10) and (6.11) with $\boldsymbol{\varphi}(t)$, a recursive pseudo-linear stochastic gradient algorithm can be obtained:

$$\hat{\boldsymbol{\theta}}(t) = \hat{\boldsymbol{\theta}}(t-1) + \frac{\boldsymbol{\varphi}(t)}{r(t)}[y(t) - \boldsymbol{\varphi}^{\mathrm{T}}(t)\hat{\boldsymbol{\theta}}(t-1)], \tag{6.14a}$$

$$r(t) = r(t-1) + \|\boldsymbol{\varphi}(t)\|^2, \ r(0) = 1, \tag{6.14b}$$

$$\hat{x}(t) = \boldsymbol{\varphi}^{\mathrm{T}}(t)\hat{\boldsymbol{\theta}}(t), \tag{6.14c}$$

$$\boldsymbol{\varphi}(t) = [-\hat{x}(t-1), \cdots, -\hat{x}(t-n), \boldsymbol{\psi}_f^{\mathrm{T}}(t), \boldsymbol{\psi}_g^{\mathrm{T}}(t)]^{\mathrm{T}}. \tag{6.14d}$$

To initialize the algorithm, $\hat{\boldsymbol{\theta}}(0) = \hat{\boldsymbol{\theta}}_0$ is taken as some small real vector, e.g., $\hat{\boldsymbol{\theta}}(0) = 10^{-6}\mathbf{1}_n$ with $\mathbf{1}_n$ being an n-dimensional vector whose elements are all 1.

6.4.2 Convergence analysis

The convergence theorem can be proved by formulating a martingale process and using the martingale convergence theorem [19, 48].

It is assumed that $\{v(t), \mathcal{F}_t\}$ is a martingale difference sequence defined on a probability space $\{\Omega, \mathcal{F}, P\}$, where $\{\mathcal{F}_t\}$ is the σ algebra sequence generated by $\{v(t)\}$. The noise sequence $\{v(t)\}$ satisfies the following assumptions:

$(A1) \qquad \mathrm{E}[v(t)|\mathcal{F}_{t-1}] = 0, \ \text{a.s.};$

$(A2) \qquad \mathrm{E}[v^2(t)|\mathcal{F}_{t-1}] = \sigma_v^2(t) \le \bar{\sigma}_v^2 < \infty, \ \text{a.s.}.$

Theorem 6.1. For system in (6.9) and the stochastic gradient algorithm in (6.14), the parameter estimation vector $\hat{\boldsymbol{\theta}}(t)$ consistently converges to the true parameter vector $\boldsymbol{\theta}$ if $(A1)$, $(A2)$ and the following assumption $(A3)$ hold and $A(z)$ is strictly positive real.

$$(A3) \quad \limsup_{t \to \infty} \frac{r_0(t)}{\lambda_{\min}[\boldsymbol{R}_0(t)]} < \infty, \text{ a.s.,}$$

where

$$\boldsymbol{R}(t) \quad := \quad \sum_{i=1}^{t} \boldsymbol{\varphi}(i) \boldsymbol{\varphi}^{\mathrm{T}}(i),$$

$$\boldsymbol{R}_0(t) \quad := \quad \sum_{i=1}^{t} \boldsymbol{\varphi}_0(i) \boldsymbol{\varphi}_0^{\mathrm{T}}(i),$$

$$r_0(t) \quad := \quad \mathrm{tr}[\boldsymbol{R}_0(t)].$$

Proof. This theorem can be proved by following the similar way in [28–30, 33]. $\qquad \square$

Remark 6.3. Under the stochastic framework, the convergence analysis of least squares identification algorithms and gradient based algorithms has been discussed for ARMAX systems [19], Hammerstein ARMAX systems [29], dual rate systems [27, 30], to name a few. In Theorem 6.1, following the similar line, the results have been extended to the convergence properties of the stochastic gradient algorithm for Hammerstein OE systems with two-segment nonlinearities.

6.4.3 A varying forgetting factor scheme

The recursive stochastic gradient algorithm has low computational cost, but its convergence rate is relatively slow. In order to improve the performance of the algorithm, a forgetting factor $0 < \lambda < 1$ can be applied to obtain the recursive stochastic gradient algorithm with a forgetting factor:

$$\hat{\boldsymbol{\theta}}(t) \quad = \quad \hat{\boldsymbol{\theta}}(t-1) + \frac{\boldsymbol{\varphi}(t)}{r(t)}[y(t) - \boldsymbol{\varphi}^{\mathrm{T}}(t)\hat{\boldsymbol{\theta}}(t-1)], \tag{6.15a}$$

$$r(t) \quad = \quad \lambda\, r(t-1) + \|\boldsymbol{\varphi}(t)\|^2, \ r(0) = 1, \tag{6.15b}$$

$$\hat{x}(t) \quad = \quad \boldsymbol{\varphi}^{\mathrm{T}}(t)\hat{\boldsymbol{\theta}}(t), \tag{6.15c}$$

$$\boldsymbol{\varphi}(t) \quad = \quad [-\hat{x}(t-1), \cdots, -\hat{x}(t-n), \boldsymbol{\psi}_f^{\mathrm{T}}(t), \boldsymbol{\psi}_g^{\mathrm{T}}(t)]^{\mathrm{T}}. \tag{6.15d}$$

To make a tradeoff between the convergence rate and estimation accuracy, a varying forgetting factor (VFF) scheme is proposed: A smaller forgetting factor is specified at the initial period of estimation process, and then let the forgetting factor gradually increase with t, so that more accurate parameter estimates could be obtained.

Note $c_1 = 1$, the estimates $\hat{\mathbf{a}} = [\hat{a}_1, \hat{a}_2, \cdots, \hat{a}_n]^{\mathrm{T}}$ and $\hat{\mathbf{b}} = [\hat{b}_1, \hat{b}_2, \cdots, \hat{b}_n]^{\mathrm{T}}$ of $\mathbf{a}$ and $\mathbf{b}$ can be read from the first and second n entries of $\hat{\boldsymbol{\theta}}$, respectively. The estimates of c_j may be calculated as

$$\hat{c}_j = \frac{\hat{\theta}_{jn+i}}{\hat{b}_i}, \ j = 2, 3, \cdots, p; \ i = 1, 2, \cdots, n.$$

Also, the estimate of d_j can be obtained, i.e.,

$$\hat{d}_j = \frac{\hat{\theta}_{(p+j)n+i}}{\hat{b}_i}, \ j = 1, 2, \cdots, q; \ i = 1, 2, \cdots, n.$$

Since such n estimates of $\hat{c}_j$ and $\hat{d}_j$ are not needed, one way is to take their average as their estimates, i.e.,

$$\hat{c}_j = \frac{1}{n} \sum_{i=1}^{n} \frac{\hat{\theta}_{jn+i}}{\hat{b}_i}, \ j = 2, 3, \cdots, p.$$

$$\hat{d}_j = \frac{1}{n} \sum_{i=1}^{n} \frac{\hat{\theta}_{(p+j)n+i}}{\hat{b}_i}, \ j = 1, 2, \cdots, q.$$

6.5   Numerical Examples

Several examples are given to illustrate the effectiveness of the proposed algorithms and show the faster convergence rate.

Example 1: Consider a system described by

$$
\begin{aligned}
y(t) &= \frac{B(z)}{A(z)} \bar{u}(t) + v(t), \\
A(z) &= 1 + a_1 z^{-1} + a_2 z^{-2} = 1 - 0.20 z^{-1} + 0.35 z^{-2}, \\
B(z) &= b_1 z^{-1} + b_2 z^{-2} = z^{-1} + 0.50 z^{-2}, \\
\bar{u}(t) &= \begin{cases} f[u(t)] = u(t) - 0.3 u^2(t) - 0.1 u^3(t), & t \geq 0 \\ g[u(t)] = -1.1 u(t), & t < 0. \end{cases} \\
\boldsymbol{\theta}_s &= [a_1, \ a_2, \ b_1, \ b_2, \ c_2, \ c_3, \ d_1]^{\mathrm{T}}, \\
\delta &= \|\hat{\boldsymbol{\theta}}(t) - \boldsymbol{\theta}\| / \|\boldsymbol{\theta}\| \\
\delta_s &= \|\hat{\boldsymbol{\theta}}_s(t) - \boldsymbol{\theta}_s\| / \|\boldsymbol{\theta}_s\|,
\end{aligned}
$$

where $\hat{\boldsymbol{\theta}}_s(t)$ is the estimate of $\boldsymbol{\theta}_s$, δ and δ_s are the parameter estimate errors of $\boldsymbol{\theta}$ and $\boldsymbol{\theta}_s$, respectively. In the simulation, $\{u(t)\}$ is taken as a persistent excitation signal sequence with zero mean and unit variance $\sigma_u^2 = 1.00^2$, and $\{v(t)\}$ as a white noise sequence with the power of $\sigma_v^2 = 0.05^2$. The initial values of parameters are 1.

The parameter estimates $\boldsymbol{\theta}$ and $\boldsymbol{\theta}_s$ and their errors with different forgetting factors $\lambda = 0.3$ and $\lambda = 0.5$ are shown in Tables 6.2–6.5. The parameter errors δ and δ_s vs. t are shown in Figures 6.2 and 6.3. From the Tables 6.2–6.5 and Figures 6.2 and 6.3, it is observed that that increasing the data length generally leads to smaller parameter estimation errors. This confirms the proposed theorem.

Example 2: Comparisons. Here, the proposed algorithm is compared with that using the switching sequence in [66, 120]. If using the switching sequence (6.6) proposed in [120], a similar recursive stochastic algorithm for the same Hammerstein OE model can be derived, which contains
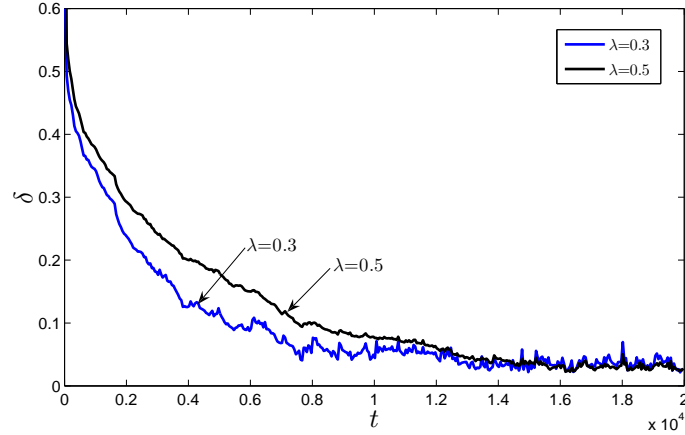
Figure 6.2: The parameter estimation errors $\boldsymbol{\delta}$ vs. t.
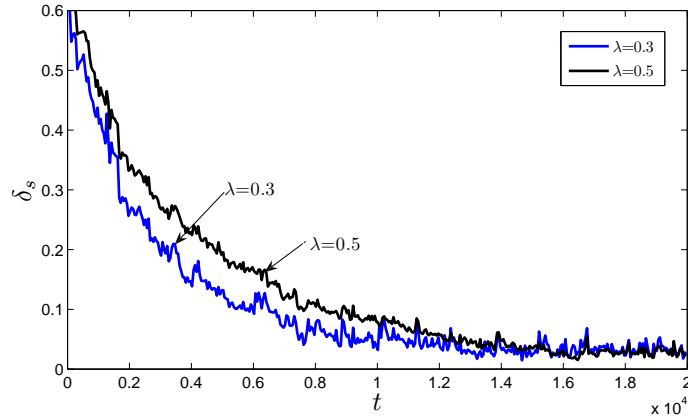
Figure 6.3: The parameter estimation errors $\boldsymbol{\delta}_s$ vs. t.

more parameters to be estimated. Now, the identification algorithms using the existing switching sequence (6.6) and the new switching sequences in this work are compared. To estimate the same parameters in the same Hammerstein OE model, the parameter vector and estimation error are

$$\boldsymbol{\theta}_s = [a_1,\ a_2,\ b_1,\ b_2,\ c_2,\ c_3,\ d_1]^{\mathrm{T}},$$
$$\delta_s = \|\hat{\boldsymbol{\theta}}_s(t) - \boldsymbol{\theta}_s\| / \|\boldsymbol{\theta}_s\|.$$

To start the algorithm, the initial values of the parameter are 1. The forgetting vectors are both 0.5. $\{u(t)\}$ is both taken as a persistent excitation signal sequence with zero mean and unit variance $\sigma_u^2 = 1.00^2$, and $\{v(t)\}$ as a white noise sequence with the power of $\sigma_v^2 = 0.05^2$. The trend of parameter estimation errors is shown in Figure 6.4. From this figure, it is clearly observed that the identification algorithm proposed in this chapter has faster convergence rate.

Table 6.2: The estimates of $\boldsymbol{\theta}$ ($\lambda = 0.30$)

t	θ_1	θ_2	θ_3	θ_4	θ_5	θ_6	θ_7	θ_8	θ_9	θ_{10}	δ (%)
1000	-0.1313	0.3263	0.7377	0.4165	0.1296	0.0862	-0.2739	-0.1487	-1.0891	-0.5750	34.458
2000	-0.1979	0.3502	0.8453	0.4383	-0.0062	0.0248	-0.2513	-0.1141	-1.0873	-0.5552	23.733
3000	-0.2176	0.3623	0.8816	0.4763	-0.0815	-0.0159	-0.1846	-0.1330	-1.1142	-0.5334	17.675
4000	-0.1560	0.4018	0.9208	0.4321	-0.1517	-0.0483	-0.1447	-0.1008	-1.0679	-0.4985	13.562
5000	-0.1641	0.3088	0.9691	0.5077	-0.1626	-0.0326	-0.1447	-0.0958	-1.0741	-0.5884	11.861
6000	-0.1708	0.3876	0.9082	0.4774	-0.2083	-0.0835	-0.1416	-0.0651	-1.0943	-0.5596	9.2531
7000	-0.1931	0.3574	0.9826	0.4786	-0.2129	-0.0963	-0.1264	-0.0700	-1.1204	-0.5566	6.5003
8000	-0.1893	0.3456	0.9433	0.4850	-0.2551	-0.1111	-0.1386	-0.0518	-1.0544	-0.5474	5.9188
9000	-0.1812	0.3432	0.9580	0.4942	-0.2313	-0.1405	-0.1153	-0.0430	-1.0712	-0.6083	6.1432
10000	-0.2020	0.3565	0.9729	0.5109	-0.2391	-0.1457	-0.1252	-0.0590	-1.1120	-0.5511	4.2427
15000	-0.1949	0.3559	0.9983	0.5110	-0.2655	-0.1454	-0.1002	-0.0742	-1.0980	-0.5549	2.5670
20000	-0.1885	0.3489	0.9854	0.4901	-0.2903	-0.1630	-0.0983	-0.0447	-1.1337	-0.5417	2.5260
True values	-0.2000	0.3500	1.0000	0.5000	-0.3000	-0.1500	-0.1000	-0.0500	-1.0000	-0.5500	

Table 6.3: The estimates of (a_i, b_i, c_i, d_i) ($\lambda = 0.30$)

t	a_1	a_2	b_1	b_2	c_2	c_3	d_1	δ_s (%)
1000	-0.13125	0.32632	0.73768	0.41653	0.19128	-0.36412	-1.4284	42.857
2000	-0.19785	0.35015	0.84530	0.43826	0.02458	-0.27879	-1.2765	26.848
3000	-0.21761	0.36233	0.88158	0.47634	-0.06290	-0.24425	-1.1918	19.213
4000	-0.15596	0.40178	0.92079	0.43212	-0.13822	-0.19512	-1.1567	14.076
5000	-0.16406	0.30878	0.96913	0.50768	-0.11597	-0.16901	-1.1337	12.679
6000	-0.17078	0.38757	0.90817	0.47742	-0.20217	-0.14613	-1.1885	10.626
7000	-0.19305	0.35739	0.98257	0.47859	-0.20900	-0.13742	-1.1517	6.9670
8000	-0.18926	0.34563	0.94329	0.48504	-0.24971	-0.12683	-1.1232	5.1991
9000	-0.18123	0.34324	0.95796	0.49418	-0.26290	-0.10370	-1.1746	5.7973
10000	-0.20200	0.35653	0.97293	0.51087	-0.26542	-0.12206	-1.1109	3.1485
15000	-0.19492	0.35593	0.99833	0.51100	-0.27521	-0.12281	-1.0929	2.2435
20000	-0.18854	0.34894	0.98535	0.49012	-0.31363	-0.09544	-1.1279	2.2931
True values	-0.20000	0.35000	1.00000	0.50000	-0.30000	-0.10000	-1.1000	

6.6 Identification of Distillation Columns

Most physical devices have nonlinear characteristics outside a limited linear range. In [36], the Hammerstein model was applied to the distillation columns. Distillation is one of the most important processes in the chemical industries, and its modeling and control have been a challenge for engineers. The dynamics of the distillation columns become more nonlinear and more difficult to control with the increase of demanded purities. There are several approaches to model the distillation column in the literature, e.g., linearization of the equations describing the behavior of the columns.

The purpose of the distillation column [110] in Figure 6.5 is to separate the Feed F, a mixture of a light and a heavy component, into a distillation product D, which contains most of the light component, and a bottom product B, which contains most of the heavy component. The driving force for this separation is the difference in volatility between the light and heavy component. The distillation column mentioned above has five controlled variables:

- vapor holdup (p)

Table 6.4: The estimates of $\boldsymbol{\theta}$ ($\lambda = 0.50$)

t	θ_1	θ_2	θ_3	θ_4	θ_5	θ_6	θ_7	θ_8	θ_9	θ_{10}	δ (%)
1000	-0.1317	0.3340	0.6959	0.4337	0.1762	0.1058	-0.2726	-0.1625	-1.0870	-0.5959	37.925
2000	-0.1975	0.3407	0.7879	0.4257	0.0747	0.0410	-0.2675	-0.1207	-1.0765	-0.5629	29.269
3000	-0.2162	0.3586	0.8165	0.4558	0.0062	0.0074	-0.2192	-0.1349	-1.1141	-0.5445	24.032
4000	-0.1795	0.3528	0.8506	0.4360	-0.0440	-0.0175	-0.1945	-0.1086	-1.0931	-0.5333	20.050
5000	-0.1766	0.3190	0.8976	0.4817	-0.0540	-0.0176	-0.1747	-0.0974	-1.0805	-0.5689	18.011
6000	-0.1843	0.3675	0.8678	0.4573	-0.1147	-0.0583	-0.1723	-0.0742	-1.1009	-0.5664	15.008
7000	-0.1869	0.3473	0.9205	0.4793	-0.1439	-0.0762	-0.1445	-0.0813	-1.1118	-0.5551	11.434
8000	-0.1886	0.3472	0.9028	0.4696	-0.1921	-0.0886	-0.1478	-0.0612	-1.0656	-0.5494	9.8403
9000	-0.1880	0.3421	0.9314	0.4725	-0.1892	-0.1040	-0.1344	-0.0521	-1.0746	-0.5971	8.8923
10000	-0.1957	0.3442	0.9377	0.4907	-0.2022	-0.1076	-0.1361	-0.0729	-1.1124	-0.5539	7.5508
15000	-0.2025	0.3577	0.9804	0.5060	-0.2535	-0.1317	-0.1028	-0.0804	-1.0932	-0.5518	3.6073
20000	-0.1954	0.3477	0.9780	0.4875	-0.2795	-0.1482	-0.1060	-0.0570	-1.1258	-0.5420	2.4978
True values	-0.2000	0.3500	1.0000	0.5000	-0.3000	-0.1500	-0.1000	-0.0500	-1.1000	-0.5500	

Table 6.5: The estimates of (a_i, b_i, c_i, d_i) ($\lambda = 0.50$)

t	a_1	a_2	b_1	b_2	c_2	c_3	d_1	δ_s (%)
1000	-0.13168	0.33398	0.69588	0.43371	0.24850	-0.38317	-1.4680	47.654
2000	-0.19754	0.34067	0.78790	0.42572	0.09562	-0.31149	-1.3443	33.826
3000	-0.21622	0.35864	0.81645	0.45582	0.01188	-0.28223	-1.2795	27.015
4000	-0.17954	0.35283	0.85059	0.43595	-0.04596	-0.23883	-1.2542	22.222
5000	-0.17655	0.31903	0.89760	0.48171	-0.04832	-0.19845	-1.1924	18.572
6000	-0.18425	0.36753	0.86776	0.45733	-0.12983	-0.18044	-1.2536	17.022
7000	-0.18686	0.34729	0.92048	0.47927	-0.15762	-0.16329	-1.1831	11.831
8000	-0.18861	0.34723	0.90279	0.46960	-0.20068	-0.14703	-1.1751	10.182
9000	-0.18798	0.34209	0.93139	0.47251	-0.21164	-0.12728	-1.2087	9.7796
10000	-0.19572	0.34417	0.93765	0.49067	-0.21744	-0.14684	-1.1576	7.7510
15000	-0.20252	0.35768	0.98035	0.50604	-0.25943	-0.13188	-1.1028	3.4057
20000	-0.19538	0.34771	0.97804	0.48745	-0.29491	-0.11263	-1.1314	2.5991
True values	-0.20000	0.35000	1.00000	0.50000	-0.30000	-0.10000	-1.1000	

- liquid holdup in the accumulator (M_D)

- liquid holdup in the column base (M_B)

- top composition (y_D)

- bottom composition (x_B)

and five manipulated inputs:

- distillate flow (D)

- bottom flow (B)

- reflux (L)

- boilup (V)

- overhead vapor (V_T).

This distillation column is a multi-input-multi-output system. Different control configurations can be obtained by choosing different inputs. For simplicity, a simple and feasible Hammerstein model
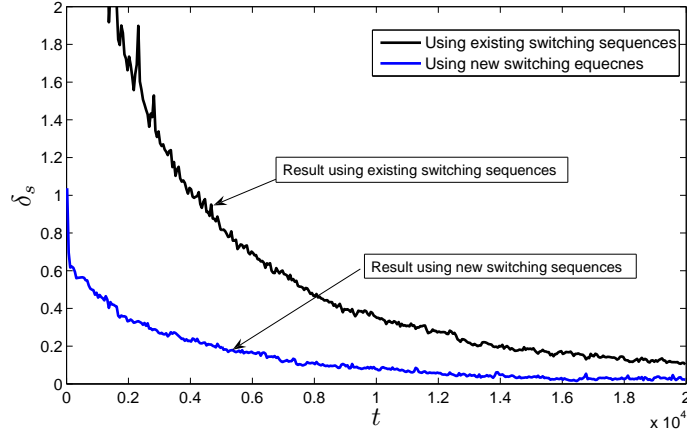
Figure 6.4: The comparison of parameter estimation errors $\boldsymbol{\delta}_s$ vs. t.

was obtained with the input as the reflux flow L, and the output as the top composition y_D in [36] stated as follows:

$$
\begin{aligned}
y_D(t) &= \tfrac{B(z)}{A(z)}\bar{u}(t) + v(t), \\
A(z) &= 1 + a_1 z^{-1} = 1 - 0.796 z^{-1}, \\
B(z) &= b_1 z^{-1} = 0.206 z^{-1}, \\
\bar{u}(t) &= f(L(t)) = c_1 L(t) + c_2 L^2(t) + c_3 L^3(t) \\
&= L(t) - 7.059 L^2(t) - 7.356 L^3(t), \\
\boldsymbol{\theta}_s &= [a_1, \ b_1, \ c_2, \ c_3]^{\mathrm{T}}.
\end{aligned}
\tag{6.16}
$$

It is worth noticing that the above Hammerstein model is with single-segment nonlinearity, which is a special case of the Hammerstein model with two-segment nonlinearities. The algorithm proposed in this chapter can be readily applied to this special case. $\{L(t)\}$ is taken as a persistent excitation signal sequence with zero mean and unit variance $\sigma_u^2 = 1.00^2$, and $\{v(t)\}$ as a white noise sequence with zero mean and constant variance $\sigma_v^2 = 0.01^2$. The recursive stochastic gradient algorithm is applied to estimate the parameters of this system. The parameter estimates $\boldsymbol{\theta} = [\theta_1, \theta_2, \cdots, \theta_4]^{\mathrm{T}}$ and $\boldsymbol{\theta}_s = [a_1, b_1, c_2, c_3]$ and their errors are shown in Tables 6.6 and 6.7, and two different parameter estimation error measures δ and δ_s versus t are shown in Figure 6.6. Here, $\delta = \|\hat{\boldsymbol{\theta}}(t) - \boldsymbol{\theta}\|/\|\boldsymbol{\theta}\|$, $\delta_s = \|\hat{\boldsymbol{\theta}}_s(t) - \boldsymbol{\theta}_s\|/\|\boldsymbol{\theta}_s\|$, $\hat{\boldsymbol{\theta}}_s(t)$ is the estimate of $\boldsymbol{\theta}_s$.

In this example, the VFF scheme is designed as: When $t < 500$, take $\lambda = 0.30$; when $t \geq 500$, take $\lambda = 0.80$. The parameter estimates are shown in Tables 6.8 and 6.9 and their estimation errors are shown in Figure 6.7. From the tables and figures, it is observed that the error curves in Figure 6.7 with the VFF scheme are smoother than the ones in Figure 6.6 with the fixed forgetting factor, and the VFF scheme has better convergence rate as well as acceptable stationarity in the estimation error.
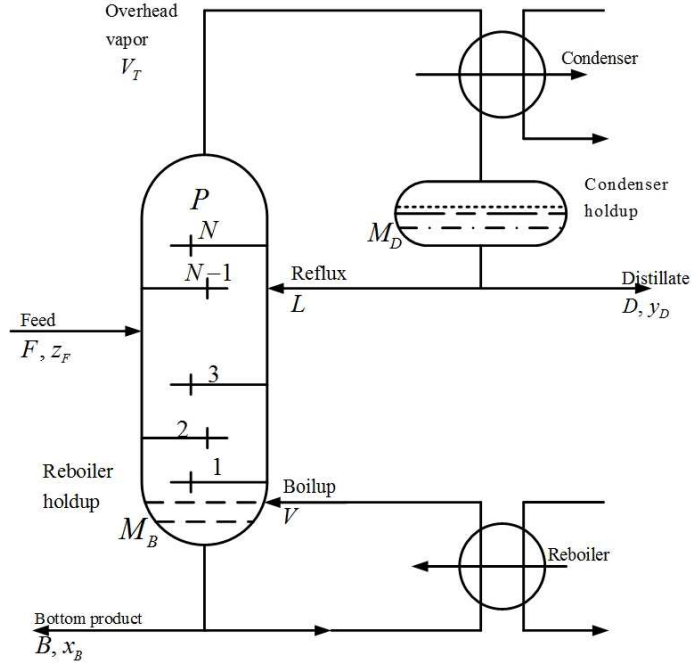
Figure 6.5: Two-product distillation column.

6.7 Conclusion

New switching sequences are proposed for the identification of two-segment Hammerstein output-error models. A recursive stochastic gradient algorithm based on replacing unavailable inner variables with their estimates is applied, and the convergence analysis is carried out. Simulation results show the effectiveness of the proposed algorithms. The proposed method is also applied to the distillation columns. It is worth mentioning that new switching sequences and the proposed algorithm can also be extended to systems with multisegment piecewise nonlinearities, deadzones, and time-varying piecewise-linear nonlinearities.

Table 6.6: The estimates of $\boldsymbol{\theta}$ (fixed forgetting factor: $\lambda = 0.30$)

t	θ_1	θ_2	θ_3	θ_4	δ (%)
100	-0.8017	0.3791	-1.3807	-1.6215	9.5747
200	-0.8178	0.2723	-1.4244	-1.5463	3.6328
300	-0.7967	0.2408	-1.4531	-1.5234	1.5849
400	-0.7959	0.2276	-1.4488	-1.5255	1.0855
500	-0.7933	0.2121	-1.4534	-1.5152	0.2998
600	-0.7948	0.2056	-1.4570	-1.5146	0.1400
700	-0.7991	0.2091	-1.4603	-1.5126	0.3558
800	-0.7961	0.2003	-1.4576	-1.5157	0.2980
900	-0.7963	0.2156	-1.4526	-1.5186	0.4575
1000	-0.7980	0.2133	-1.4507	-1.5199	0.4201
True values	-0.7960	0.2060	-1.4542	-1.5153	

Table 6.7: The estimates of (a_i, b_i, c_i) (fixed forgetting factor: $\lambda = 0.30$)

t	a_1	b_1	c_2	c_3	δ_s (%)
100	-0.8017	0.3791	-3.6426	-4.2777	44.9929
200	-0.8178	0.2723	-5.2314	-5.6794	24.2576
300	-0.7967	0.2408	-6.0345	-6.3267	14.2026
400	-0.7959	0.2276	-6.3653	-6.7023	9.3222
500	-0.7933	0.2121	-6.8508	-7.1422	2.9186
600	-0.7948	0.2056	-7.087	-7.3675	0.2958
700	-0.7991	0.2091	-6.9851	-7.2351	1.3856
800	-0.7961	0.2003	-7.2784	-7.5686	2.9877
900	-0.7963	0.2156	-6.7361	-7.0425	4.4015
1000	-0.7980	0.2133	-6.8019	-7.1263	3.3713
True values	-0.7960	0.2060	-7.0590	-7.3560	

Table 6.8: The estimates of $\boldsymbol{\theta}$ (VFF Scheme: $\lambda = 0.30, \quad t \leq 500; \quad \lambda = 0.80, \quad t > 500$)

t	θ_1	θ_2	θ_3	θ_4	δ (%)
100	-0.8017	0.3791	-1.3807	-1.6215	9.5747
200	-0.8178	0.2723	-1.4244	-1.5463	3.6328
300	-0.7967	0.2408	-1.4531	-1.5234	1.5849
400	-0.7959	0.2276	-1.4488	-1.5255	1.0855
500	-0.7933	0.2121	-1.4534	-1.5152	0.2998
600	-0.7960	0.2105	-1.4543	-1.5167	0.2081
700	-0.7958	0.2100	-1.4547	-1.5164	0.1872
800	-0.7937	0.2092	-1.4546	-1.5164	0.1823
900	-0.7961	0.2096	-1.4564	-1.5167	0.1976
1000	-0.7960	0.2094	-1.4552	-1.5168	0.1714
True values	-0.7960	0.2060	-1.4542	-1.5153	

Table 6.9: The estimates of (a_i, b_i, c_i) (VFF Scheme: $\lambda = 0.30, \quad t \leq 500; \quad \lambda = 0.80, \quad t > 500$)

t	a_1	b_1	c_2	c_3	δ_s (%)
100	-0.8017	0.3791	-3.6426	-4.2777	44.9929
200	-0.8178	0.2723	-5.2314	-5.6794	24.2576
300	-0.7967	0.2408	-6.0345	-6.3267	14.2026
400	-0.7959	0.2276	-6.3653	-6.7023	9.3222
500	-0.7933	0.2121	-6.8508	-7.1422	2.9186
600	-0.7960	0.2105	-6.9087	-7.2053	2.0812
700	-0.7958	0.2100	-6.9257	-7.2196	1.8646
800	-0.7937	0.2092	-6.9520	-7.2472	1.4926
900	-0.7961	0.2096	-6.9474	-7.2351	1.6090
1000	-0.7960	0.2094	-6.9492	-7.2436	1.5369
True values	-0.7960	0.2060	-7.0590	-7.3560	
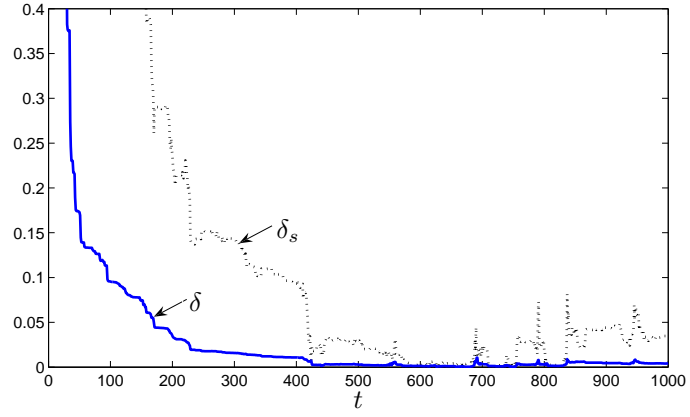
Figure 6.6: The parameter estimation errors (fixed forgetting factor scheme: $\lambda = 0.30$) – δ vs. t and δ_s vs. t.
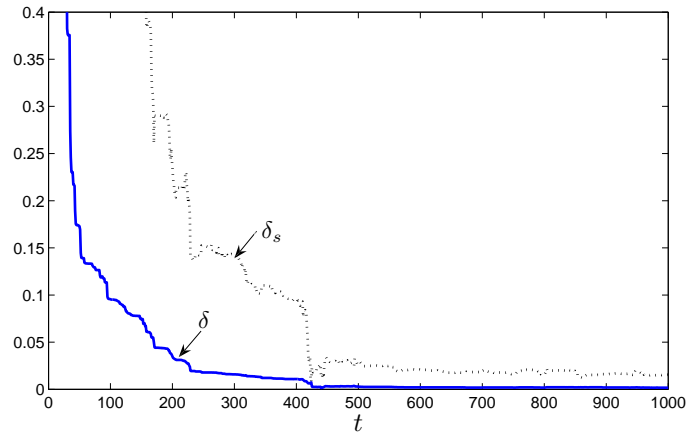

Figure 6.7: The parameter estimation errors (VFF scheme: $\lambda = 0.30$, $t \leq 500$; $\lambda = 0.80$, $t > 500$) – δ_s vs. t and δ_s vs. t.

Chapter 7

Conclusion and Future Work

This thesis has investigated the controller design for networked control systems (NCSs), $l_2 - l_\infty$ filtering for multirate systems, and identification of Hammerstein systems with two-segment nonlinearities. This chapter summarizes the results reported in the thesis, and proposes some possible future research directions.

7.1 Conclusion

The two-mode-dependent controller design problem for NCSs with time delays modeled by Markov chains has been studied. The work in this thesis is the first to incorporate the available information of both the sensor-to-controller and controller-to-actuator delays into the controller design. Compared with the existing mode-independent and one-mode-dependent controller, the two-mode-dependent controller can reduce the conservativeness as it can include them as special cases. Due to the introduction of the previous controller-to-actuator delay $(d_{k-\tau_k-1})$ in the controller, the closed-loop system was a special jump linear system. A proposition was further developed to characterize the stochastic properties of the multi-step jump of the delay. The sufficient and necessary conditions to guarantee the stochastic stability were obtained and further transformed to be a set of LMIs with nonconvex constraints, which can be efficiently solved by product reduction algorithm. The control synthesis problem of the system was further considered. The H_2 and H_∞ norms were defined for the special system and the robust mixed H_2/H_∞ control problem has been solved where the uncertainties of the plant were assumed to be norm-bounded.

The classical generalized predictive control (GPC) has been modified for the NCS design, and further a modified-GPC (M-GPC) method is proposed. The future control signals created by M-GPC are employed to compensate for the S-C and C-A delays. This method can be applied to NCSs with random delays and delays modeled by Markov chains. For the case with time delays modeled by Markov chains, the sufficient and necessary conditions to check the stochastic stability were provided. This method has been tested on an experimental hydraulic position control system.

Different from Kalman and H_∞ filtering, the $l_2 - l_\infty$ filtering provides an alternative performance index which minimizes the energy-to-peak gain from the external input to the error. The $l_2 - \infty$

filtering for multirate systems has been developed by using lifting and LMI techniques. The filtering design problem is finally formulated to be a series of LMIs with nonconvex constraints, which can be solved by the PRA.

Finally, the identification of Hammerstein systems with two-segment nonlinearities was investigated. A simple and efficient switching method was proposed to reduce the number of parameters to be estimated. Further, a stochastic gradient identification method was developed based on the idea of replacing the unmeasurable terms by their estimates. This method was verified through examples.

7.2   Future Work

Based upon the work presented in this thesis, some future research topics are proposed.

1. So far, most works on NCSs were developed either in the continuous-time domain or the discrete-time domain. However, in practical systems, an NCS is a sampled-data system. The model of the plant is continues-time and the controller to be designed is discrete-time. In this thesis, the controller for NCSs in the discrete-time domain has been developed. Two open problems are: (1) The intersample behaviors of the system are not considered; (2) the time delay is assumed to be integral multiple of the sampling time. Hence, to design a controller for NCSs modeled as sampled-data systems is worth further research.

2. Predictive control methodology is a promising approach to compensate for network-induced delays for NCSs. In existing works, the stochastic information of time delays, e.g., the probability transition matrix of Markov chains was not incorporated in the optimization process. To make full use of this information, powerful stochastic modeling and control tools can be used to predict the time delay likelihood in the near future. Base on such predictions, tools like stochastic predictive control can be used to plan the best likely control actions based on appropriate forecasts.

3. In the area of filtering design for multirate systems, the model of the plant is always assumed to be precisely known, because it is hard to explicitly deal with uncertainties during the lifting operation procedure. However, in real systems, the model uncertainty is unavoidable. Hence, it is desirable to develop the robust filtering schemes for multirate systems with polytopic or norm-bounded uncertainties.

References

[1] F. Alonge, F. D'Ippolito, F. M. Raimondi, and S. Tumminaro, "Nonlinear modeling of DC/DC converters using the Hammerstein's approach," *IEEE Transactions on Power Electronics*, vol. 22, no. 4, pp. 1210–1221, 2007.

[2] D. Andiusani and C.-F. Gau, "Estimation using a multirate filter," *IEEE Transactions on Automatic Control*, vol. 32, no. 7, pp. 653–656, July 1987.

[3] E.-W. Bai, "An optimal two-stage identification algorithm for Hammerstein-Wiener nonlinear systems," *Autoamtica*, vol. 34, no. 3, pp. 333–338, Mar. 1998.

[4] ——, "A blind approach to the Hammerstein-Wiener model identification," *Automatica*, vol. 38, no. 6, pp. 967–979, June 2002.

[5] E.-W. Bai and D. Li, "Convergence of the iterative Hammerstein system identification algorithm," *IEEE Transactions on Automatic Control*, vol. 49, no. 11, pp. 1929–1940, Nov. 2004.

[6] J. Baillieul and P. J. Antsaklis, "Control and communication challenges in networked real-time systems," *Proceedings of the IEEE*, vol. 95, no. 1, pp. 9–28, Jan. 2007.

[7] M. C. Berg, N. Amit, and J. D. Powell, "Multirate digital control system design," *IEEE Transactions on Automatic Control*, vol. 33, no. 12, pp. 1139–1150, Dec. 1988.

[8] S. Boyd, L. E. Ghaoul, E. Feron, and V. Balakrishnan, *Linear Matrix Inequalities in System and Control Theory*.   SIAM, 1994.

[9] M. S. Branicky, V. Liberatore, and S. M. Phillips, "Networked control system co-simulation for co-design," in *Proceedings of the American Control Conference*, vol. 4, Denver, CO, USA, June 2003, pp. 3341–3346.

[10] M. S. Branicky, S. M. Phillips, and W. Zhang, "Scheduling and feedback co-design for networked control systems," in *Proceedings of the 41st IEEE Conference on Decision and Control*, vol. 2, Las Vegas, NV, USA, Dec. 2002, pp. 1211–1217.

[11] G. Burdea, V. Popescu, V. Hentz, and K. Colbert, "Virtual reality-based orthopedic telerehabilitation," *IEEE Transactions on Rehabilitation Engineering*, vol. 8, no. 3, pp. 430–432, Sept. 2000.

[12] R. Burton, P. Ukrainetz, P. Nikiforuk, and G. Schoenau, "Neural networks and hydraulic control – from simple to complex applications," *Proceedings of the Institution of Mechanical Engineers, Part I: Journal of Systems and Control Engineering*, vol. 213, no. 5, pp. 349–358, Oct. 1999.

[13] E. F. Camacho and C. Bordons, *Model Predictive Control*.   Springer, 2000.

[14] D. Carnevale, A. R. Teel, and D. Nešić, "A Lyapunov proof of an improved maximum allowable transfer interval for networked control system," *IEEE Transactions on Automatic Control*, vol. 52, no. 5, pp. 892–897, May 2007.

[15] V. Cerone and D. Regruto, "Parameter bounds for discrete-time Hammerstein models with bounded output errors," *IEEE Transactions on Automatic Control*, vol. 48, no. 10, pp. 1855–1860, Oct. 2003.

[16] A. Cervin and J. Eker, "Control-scheduling codesign of real-time systems: The control server approach," *Journal of Embedded Computing*, vol. 1, no. 2, pp. 209–224, 2005.

[17] S. Chai, G.-P. Liu, D. Rees, and Y. Xia, "Design and practical implementation of internet-based predictive control of a servo system," *IEEE Transactions on Control Systems Technology*, vol. 16, no. 1, pp. 158–168, Jan. 2008.

[18] B.-S. Chen, C.-W. Lin, and Y.-L. Chen, "Optimal signal reconstruction in noisy filter bank systems: multirate Kalman synthesis filtering approach," *IEEE Transactions on Signal Processing*, vol. 43, no. 11, pp. 2496–2504, Nov. 1995.

[19] H.-F. Chen and L. Guo, *Identification and stochastic adaptive control.* Birkhauser Boston Inc., 1991.

[20] T. Chen and B. A. Francis, *Optimal Sampled-Data Control Systems.* Springer-Verlag, 1995.

[21] T. Chen and L. Qiu, "H_∞ design of general multirate sampled-data control systems," *Automatica*, vol. 30, no. 7, pp. 1139–1152, July 1994.

[22] O. L. V. Costa and R. P. Marques, "Mixed H_2/H_∞-control of discrete-time Markovian jump linear systems," *IEEE Transactions on Automatic Control*, vol. 43, no. 1, pp. 95–100, Jan. 1998.

[23] ——, "Robust H_2-control for discrete-time Markovian jump linear systems," *International Journal of Control*, vol. 73, no. 1, pp. 11–21, Jan. 2000.

[24] M. C. de Oliveira and J. C. Geromel, "Numerical comparison of output feedback design methods," in *Proceedings of the American Control Conference*, vol. 1, Albuquerque, NM, USA, June 1997, pp. 72–76.

[25] C. E. de Souza, R. M. Palhares, and P. L. D. Peres, "Robust H_∞ filter design for uncertain linear systems with multiple time-varying state delays," *IEEE Transactions on Signal Processing*, vol. 49, no. 3, pp. 569–576, May 2001.

[26] J. E. Deutsch, J. A. Lewis, and G. Burdea, "Technical and patient performance using a virtual reality-integrated telerehabilitation system: Preliminary finding," *IEEE Transactions on Neural Systems and Rehabilitation Engineering*, vol. 15, no. 1, pp. 30–35, Mar. 2007.

[27] F. Ding and T. Chen, "Combined parameter and output estimation of dual-rate systems using an auxiliary model," *Automatica*, vol. 40, no. 10, pp. 1739–1748, Oct. 2004.

[28] ——, "Hierarchical gradient-based identification of multivariable discrete-time systems," *Automatica*, vol. 41, no. 2, pp. 315–325, Feb. 2005.

[29] ——, "Identification of Hammerstein nonlinear ARMAX systems," *Automatica*, vol. 41, no. 9, pp. 1479–1489, Sept. 2005.

[30] ——, "Parameter estimation of dual-rate stochastic systems by using an output error method," *IEEE Transactions on Automatic Control*, vol. 50, no. 9, pp. 1436–1441, Sept. 2005.

[31] ——, "Performance analysis of multi-innovation gradient type identification methods," *Automatica*, vol. 43, no. 1, pp. 1–14, Jan. 2007.

[32] F. Ding, Y. Shi, and T. Chen, "Gradient-based identification methods for Hammerstein nonlinear ARMAX models," *Nonliner Dynamics*, vol. 45, no. 1-2, pp. 31–43, July 2006.

[33] ——, "Auxiliary model-based least-squares identification methods for Hammerstein output-error systems," *Systems & Control Letters*, vol. 56, no. 5, pp. 373–380, May 2007.

[34] N. Elia, "Remote stabilization over fading channels," *Systems & Control Letters*, vol. 54, no. 3, pp. 237–249, Mar. 2005.

[35] M. Embiruçu and C. Fontes, "Multirate multivariable generalized predictive control and its application to a slurry reactor for ethylene polymerization," *Chemical Engineering Science*, vol. 61, no. 17, pp. 5754–5767, Sept. 2006.

[36] E. Eskinat, S. H. Johnson, and W. L. Luyben, "Use of Hammerstein models in identification of nonlinear systems," *American Institute of Chemical Engineering Journal*, vol. 37, no. 2, pp. 255–268, 1991.

[37] D. Farret, G. Duc, and J. Harcaut, "Multirate LPV synthesis: A loop-shaping approach for missile control," in *Proceedings of the American Control Conference*, vol. 5, Anchorage, AK, USA, May 2002, pp. 4092–4097.

[38] X. N. Fernando and A. B. Sesay, "A Hammerstein-type equalizer for concatenated fiber-wireless uplink," *IEEE Transactions on Vehicular Technology*, vol. 54, no. 6, pp. 1980–1991, Nov. 2005.

[39] H. Gao and T. Chen, "H_∞ estimation for uncertain systems with limited communication capacity," *IEEE Transactions on Automatic Control*, vol. 52, no. 11, pp. 2070–2084, Nov. 2007.

[40] ——, "Network-based H_∞ output tracking control," *IEEE Transactions on Automatic Control*, vol. 53, no. 3, pp. 655–667, Apr. 2008.

[41] H. Gao, T. Chen, and J. Lam, "A new delay system approach to network-based control," *Automatica*, vol. 44, no. 1, pp. 39–52, Jan. 2008.

[42] H. Gao and C. Wang, "Robust energy-to-peak filtering with improved LMI representations," *IEE Proceedings - Vision, Image & Signal Processing*, vol. 150, no. 2, pp. 82–89, Apr. 2005.

[43] J. C. Geromel, J. Bernussou, G. Garcia, and M. C. de Oliveira, "H_2 and H_∞ robust filtering for discrete-time linear systems," *SIAM Journal on Control and Optimization*, vol. 38, no. 5, pp. 1353–1368, 2000.

[44] J. C. Geromel and M. C. de Oliveira, "H_2 and H_∞ robust filtering for convex bounded uncertain systems," *IEEE Transactions on Automatic Control*, vol. 46, no. 1, pp. 100–107, Jan. 2001.

[45] I. Goethals, K. Pelckmans, J. A. Suykens, and B. D. Moor, "Identification of MIMO Hammerstein models using least squares support vector machines," *Automatica*, vol. 41, no. 7, pp. 1263–1272, July 2005.

[46] E. N. Gonçalves, R. M. Palhares, and R. H. C. Takahashi, "H_2/H_∞ filter design for systems with polytope-bounded uncertainty," *IEEE Transactions on Signal Processing*, vol. 54, no. 9, pp. 3620–3626, Sept. 2006.

[47] G. C. Goodwin, H. Haimovich, D. E. Quevedo, and J. S. Welsh, "A moving horizon approach to networked control system design," *IEEE Transactions on Automatic Control*, vol. 49, no. 9, pp. 1427–1445, Sept. 2004.

[48] G. C. Goodwin and K. S. Sin, *Adaptive Filtering: Prediction and Control*. Prentice Hall, 1984.

[49] W. Greblicki, "Continuous-time Hammerstein system identification," *IEEE Transactions on Automatic Control*, vol. 45, no. 6, pp. 1232–1236, June 2000.

[50] K. M. Grigoriadis and J. T. Watson, "Reduced-order H_∞ and $L_2 - L_\infty$ filtering via linear matrix inequalities," *IEEE Transactions on Aerospace and Electronic Systems*, vol. 33, no. 4, pp. 1326–1338, Oct. 1997.

[51] R. D. Gudi, S. L. Shah, and M. R. Gray, "Adaptive multirate state and parameter estimation strategies with application to a bioreactor," *American Institute of Chemical Engineering Journal*, vol. 41, no. 11, pp. 2451–2464, 1995.

[52] V. Gupta, B. Hassibi, and R. M. Murray, "Optimal LQG control across packet-dropping links," *Systems & Control Letters*, vol. 56, no. 6, pp. 439–446, June 2007.

[53] Q. P. Ha, Q. H. Nguyen, D. C. Rye, and H. F. Durrant-Whyte, "Fuzzy sliding-mode controllers with applications," *IEEE Transactions on Industrial Electronics*, vol. 48, no. 1, pp. 38–46, Feb. 2001.

[54] J. P. Hespanha, P. Naghshtabrizi, and Y. Xu, "A survey of recent results in networked control systems," *Proceedings of the IEEE*, vol. 95, no. 1, pp. 138–162, Jan. 2007.

[55] D. Hristu-Varsakelis and W. S. Levine, *Handbook of Networked and Embedded Control Systems*. Birkhäuser, 2005.

[56] D. Huang and S. K. Nguang, "State feedback control of uncertain networked control systems with random time delays," *IEEE Transactions on Automatic Control*, vol. 53, no. 3, pp. 829–834, Apr. 2008.

[57] M. Huang and S. Dey, "Stability of Kalman filtering with Markovian packet losses," *Automatica*, vol. 43, no. 4, pp. 598–607, Apr. 2007.

[58] I. W. Hunter and M. J. Korenberg, "The identification of nonlinear biological systems: Wiener and Hammerstein cascade models," *Biological Cybernetics*, vol. 55, no. 2-3, pp. 135–144, Nov. 1986.

[59] M. Isaksson, D. Wisell, and D. Rönnow, "A comparative analysis of behavioral models for RF power amplifiers," *IEEE Transactions on Microwave Theory and Techniques*, vol. 54, no. 1, pp. 348–359, Jan. 2006.

[60] H. Ishii, "H_∞ control with limited communication and message losses," *Systems & Control Letters*, vol. 57, no. 4, pp. 322–331, Apr. 2008.

[61] S. Janardhanan and B. Bandyopadhyay, "Discrete sliding mode control of systems with unmatched uncertainty using multirate output feedback," *IEEE Transactions on Automatic Control*, vol. 51, no. 6, pp. 1030–1035, June 2006.

[62] Y. Ji and H. J. Chizeck, "Controllability, observability and discrete-time Markovian jump linear quadratic control," *International Journal of Control*, vol. 48, no. 2, pp. 481–498, Aug. 1988.

[63] Q. Jia, "A new method of multirate state feedback control with application to an HDD servo system," *Mechatronics*, vol. 18, no. 1, pp. 13–20, Feb. 2008.

[64] P. A. Kawka and A. G. Alleyne, "An analysis framework for evaluating dropout compensation strategies in wireless servo systems," *ASME Journal of Dynamic Systems, Measurement, and Control*, vol. 130, no. 3, May 2008.

[65] W. Kim, K. Ji, and A. Ambike, "Networked real-time control strategy dealing with stochastic time delays and packet losses," *ASME Journal of Dynamic Systems, Measurement, and Control*, vol. 128, no. 3, pp. 681–685, Sept. 2006.

[66] M.-C. Kung and B. F. Womack, "Discrete time adaptive control of linear dynamic systems with a two-segment piecewise-linear asymmetric nonlinearity," *IEEE Transactions on Automatic Control*, vol. 29, no. 2, pp. 170–172, Feb. 1984.

[67] D.-J. Lee and M. Tomizuka, "Multirate optimal state estimation with sensor fusion," in *Proceedings of the American Control Conference*, vol. 4, Denver, CO, USA, June 2003, pp. 2887–2892.

[68] N. E. Leonard, D. A. Paley, F. Lekien, R. Sepulchre, D. M. Fratantoni, and R. E. Davis, "Collective motion, sensor networks, and ocean sampling," *Proceedings of the IEEE*, vol. 95, no. 1, pp. 48–74, Jan. 2007.

[69] F.-L. Lian, "Analysis, design, modeling, and control of networked control systems," Ph.D. Thesis, University of Michigan, 2001.

[70] D. Liberzon and J. P. Hespanha, "Stabilization of nonlinear systems with limited information feedback," *IEEE Transactions on Automatic Control*, vol. 50, no. 6, pp. 910–915, June 2005.

[71] Y. Lin, Y. Shi, and R. Burton, "Discrete-time H_2 optimal control for hydraulic position control systems," in *Proceedings of ASME International Mechanical Engineering Congress and Exposition*, Seattle, WA, USA, Nov. 2007.

[72] G.-P. Liu, J. Mu, D. Rees, and S. Chai, "Design and stability analysis of networked control systems withrandom communication time delay using the modified MPC," *International Journal of Control*, vol. 79, no. 4, pp. 288–297, Apr. 2006.

[73] G.-P. Liu, Y. Xia, J. Chen, D. Rees, and W. Hu, "Networked predictive control of systems with random network delays in both forward and feedback channels," *IEEE Transactions on Industrial Electronics*, vol. 54, no. 3, pp. 1282–1297, June 2007.

[74] G.-P. Liu, Y. Xia, D. Rees, and W. Hu, "Design and stability criteria of networked predictive control systems with random network delay in the feedback channel," *IEEE Transactions on Systems, Man, and Cybernetics—Part C: Applications and Reviews*, vol. 37, no. 2, pp. 173–184, Mar. 2007.

[75] Y. Liu and E.-W. Bai, "Iterative identification of Hammerstein systems with piecewise-linear nonlinearities," in *Proceedings of the American Control Conference*, Minneapolis, MN, USA,, June 2006.

[76] L. Lu, L. Xie, and W. Cai, "H_2 controller design for networked control systems," *Asian Journal of Control*, vol. 6, no. 1, pp. 88–96, Mar. 2004.

[77] N. Lu, Y. Yang, F. Gao, and F. Wang, "Multirate dynamic inferential modeling for multivariable processes," *Chemical Engineering Science*, vol. 59, no. 4, pp. 855–864, Feb. 2004.

[78] Z. Mao and B. Jiang, "Fault identification and fault-tolerant control for a class of networked control systems," *International Journal of Innovative Computing, Information and Control*, vol. 3, no. 5, pp. 1121–1130, 2007.

[79] I. Mizumoto, T. Chen, S. Ohdaira, M. Kumon, and Z. Iwai, "Adaptive output feedback control of general MIMO systems using multirate sampling and its application to a cart-crane system," *Automatica*, vol. 43, no. 12, pp. 2077–2085, Dec. 2007.

[80] L. A. Montestruque and P. Antsaklis, "Stability of model-based networked control systems with time-varying transmission times," *IEEE Transactions on Automatic Control*, vol. 49, no. 9, pp. 1562–1572, Sept. 2004.

[81] ——, "Static and dynamic quantization in model-based networked control systems," *International Journal of Control*, vol. 80, no. 1, pp. 87–101, Jan. 2007.

[82] J. R. Moyne and D. M. Tilbury, "The emergence of industrial control networks for manufacturing control, diagnostics, and safety data," *Proceedings of the IEEE*, vol. 95, no. 1, pp. 29–47, Jan. 2007.

[83] R. M. Murray, K. J. Åström, S. P. Boyd, R. W. Brockett, and G. Stein, "Future directions in control in an information-rich world," *IEEE Control Systems Magazine*, vol. 23, no. 2, pp. 20–33, Apr. 2003.

[84] M. Nemani, T.-C. Tsao, and S. Hutchinson, "Multi-rate analysis and design of visual feedback digital servo-control system," *ASME Journal of Dynamic Systems, Measurement, and Control*, vol. 116, no. 1, pp. 45–55, Mar. 1994.

[85] D. Nešić and A. R. Teel, "Input-output stability properties of networked control systems," *IEEE Transactions on Automatic Control*, vol. 49, no. 10, pp. 1650–1667, Oct. 2004.

[86] ——, "Input-to-state stability of networked control systems," *Automatica*, vol. 40, no. 12, pp. 2121–2128, Dec. 2004.

[87] J. Nilsson, "Real-time control systems with delays," Ph.D. Thesis, Lund Institute of Technology, Lund, Sweden, 1998.

[88] P. Ögren, E. Fiorelli, and N. E. Leonard, "Cooperative control of mobile sensor networks: Adaptive gradient climbing in a distributed environment," *IEEE Transactions on Automatic Control*, vol. 49, no. 8, pp. 1292–1302, Aug. 2004.

[89] S. Oh and S. Sastry, "Approximate estimation of distributed networked control systems," in *Proceedings of the American Control Conference*, New York City, USA, July 2007, pp. 997–1002.

[90] H. Ouyang, G.-P. Liu, D. Rees, and W. Hu, "Predictive control of networked non-linear control systems," *Proceedings of the Institution of Mechanical Engineers, Part I: Journal of Systems and Control Engineering*, vol. 221, no. 3, pp. 453–463, 2007.

[91] J. W. Overstreet and A. Tzes, "An Internet-based real-time control engineering laboratory," *IEEE Control Systems Magazine*, vol. 19, no. 5, pp. 19–34, Oct. 1999.

[92] R. M. Palhares and P. L. D. Peres, "Optimal filtering schemes for linear discrete-time systems: a linear matrix inequality approach," *International Journal of Systems Science*, vol. 29, no. 6, pp. 587–593, June 1998.

[93] ——, "Robust H_∞-filtering design with pole placement constraint via linear matrix inequalities," *Journal of Optimization Theory and Applications*, vol. 102, no. 2, pp. 239–261, Aug. 1999.

[94] P. Park and T. Kailath, "H_∞ filtering via convex optimization," *International Journal of Control*, vol. 66, no. 1, pp. 15–22, Jan. 1997.

[95] A. Ray, "Performance evaluation of medium access control protocols for distributed digital avionics," vol. 109, pp. 370–377, Dec. 1987.

[96] D. J. Reinkensmeyer, C. T. Pang, J. A. Nessler, and C. C. Painter, "Web-based telerehabilitation for the upper extremity after stroke," *IEEE Transactions on Neural Systems and Rehabilitation Engineering*, vol. 10, no. 2, pp. 102–108, June 2002.

[97] M. Sahebsara, T. Chen, and S. L. Shah, "Optimal H_2 filtering in networked control systems with multiple packet dropout," *IEEE Transactions on Automatic Control*, vol. 52, no. 8, pp. 1508–1513, Aug. 2007.

[98] ——, "Optimal H_2 filtering with random sensor delay, multiple packet dropout and uncertain observations," *International Journal of Control*, vol. 80, no. 2, pp. 292–301, Feb. 2007.

[99] P. Seiler and R. Sengupta, "A bounded real lemma for jump systems," *IEEE Transactions on Automatic Control*, vol. 48, no. 9, pp. 1651–1654, Sept. 2003.

[100] ——, "An H_∞ approach to networked control," *IEEE Transactions on Automatic Control*, vol. 50, no. 3, pp. 356–364, Mar. 2005.

[101] J. Sheng, "Optimal filtering for multirate systems based on lifted models," in *Proceedings of the American Control Conference*, vol. 5, Portland, OR, USA, June 2005, pp. 3459–3461.

[102] J. Sheng, T. Chen, and S. L. Shah, "Optimal filtering for multirate systems," *IEEE Transactions on Circuits and Systems—Part II: Analog and Digital Signal Processing*, vol. 52, no. 4, pp. 228–232, Apr. 2005.

[103] P. Shi and E.-K. Boukas, "H_∞-control for Markovian jumping linear systems with parametric uncertainties," *Journal of Optimization Theory and Applications*, vol. 95, no. 1, pp. 75–99, Oct. 1997.

[104] P. Shi, E.-K. Boukas, and R. K. Agarwal, "Control of Markovian jump discrete-time systems with norm bounded uncertainty and unknown delay," *IEEE Transactions on Automatic Control*, vol. 44, no. 11, pp. 2139–2144, Nov. 1999.

[105] Y. Shi and T. Chen, "2-norm-based iterative design of filterbank transceivers: A control perspective," *Journal of Control Science and Engineering*, vol. 2008, 2008, article ID 143085.

[106] Y. Shi and F. Ding, "Parameter identification for input nonlinear output-error systems using the unknown variable estimation," in *Proceedings of the American Control Conference*, New York City, USA, July 2007, pp. 118–121.

[107] Y. Shi, F. Ding, and T. Chen, "2-norm based recursive design of transmultiplexers with designable filter length," *Circuits, Systems, and Signal Processing*, vol. 25, no. 4, pp. 447–462, Aug. 2006.

[108] ——, "Multirate crosstalk identification in xDSL systems," *IEEE Transactions on Communications*, vol. 54, no. 10, pp. 1878–1886, Oct. 2006.

[109] G. M. Siouris, *An Engineering Approach to Optimal Control and Estimation Theory.* John Wiley & Sons, Inc., 1996.

[110] S. Skogestad, M. Morari, and J. C. Doyle, "Robust control of ill-conditioned plants: high-purity distillation," *IEEE Transactions on Automatic Control*, vol. 33, no. 12, pp. 1092–1105, Dec. 1988.

[111] S. C. Smith and P. Seiler, "Estimation with lossy measurements: jump estimators for jump systems," *IEEE Transactions on Automatic Control*, vol. 48, no. 12, pp. 2163–2171, Dec. 2003.

[112] H. W. Sorenson, *Kalman Filtering: Theory and Application.* IEEE Press, 1985.

[113] J. A. Sparks, "Low cost technologies for aerospace applications," *Microprocessors and Microsystems*, vol. 20, no. 8, pp. 449–454, Apr. 1997.

[114] S. Su, L. Wang, B. Celler, A. Savkin, and Y. Guo, "Identification and control for heart rate regulation during treadmill exercise," *IEEE Transactions on Biomedical Engineering*, vol. 54, no. 7, pp. 1238–1246, July 2007.

[115] Y. S. Suh, V. H. Nguyen, and Y. S. Ro, "Modified Kalman filter for networked monitoring systems employing a send-on-delta method," *Automatica*, vol. 43, no. 2, pp. 332–338, Feb. 2007.

[116] M. Tabbara, D. Nešić, and A. R. Teel, "Stability of wireless and wireline networked," *IEEE Transactions on Automatic Control*, vol. 52, no. 9, pp. 1615–1630, Sept. 2007.

[117] P. L. Tang and C. W. de Silva, "Compensation for transmission delays in an Ethernet-based control network using variable-horizon predictive control," *IEEE Transactions on Control Systems Technology*, vol. 14, no. 4, pp. 707–718, July 2006.

[118] S. Tatikonda and S. Mitter, "Control under communication constraints," *IEEE Transactions on Automatic Control*, vol. 49, no. 7, pp. 1056–1068, July 2004.

[119] Y. Tipsuwan and M.-Y. Chow, "Control methodologies in networked control systems," *Control Engineering Practice*, vol. 11, no. 10, pp. 1099–1111, Oct. 2003.

[120] J. Vörös, "Iterative algorithm for parameter identification of Hammerstein systems with two-segment nonlinearities," *IEEE Transactions on Automatic Control*, vol. 44, no. 11, pp. 2145–2149, Nov. 1999.

[121] ——, "Modeling and parameter identification of systems with multisegment piecewise-linear characteristics," *IEEE Transactions on Automatic Control*, vol. 47, no. 1, pp. 184–188, Jan. 2002.

[122] ——, "Recursive identification of Hammerstein systems with discontinuous nonlinearities containing dead-zones," *IEEE Transactions on Automatic Control*, vol. 48, no. 12, pp. 2203–2206, Jan. 2003.

[123] ——, "Parameter identification of Hammerstein systems with asymmetric dead-zones," *Journal of Electrical Engineering*, vol. 55, no. 1-2, pp. 46–49, 2004.

[124] ——, "Identification of Hammerstein systems with time-varying piecewise-linear characteristics," *IEEE Transactions on Circuits and Systems—Part II: Analog and Digital Signal Processing*, vol. 52, no. 12, pp. 865–869, Dec. 2005.

[125] G. C. Walsh, O. Beldiman, and L. G. Bushnell, "Asymptotic behavior of nonlinear networked control systems," *IEEE Transactions on Automatic Control*, vol. 46, no. 7, pp. 1093–1097, July 2001.

[126] G. C. Walsh and H. Ye, "Scheduling of networked control systems," *IEEE Control Systems Magazine*, vol. 21, no. 1, pp. 57–65, Feb. 2001.

[127] G. C. Walsh, H. Ye, and L. G. Bushnell, "Stability analysis of networked control systems," *IEEE Transactions on Control Systems Technology*, vol. 10, no. 3, pp. 438–446, May 2002.

[128] Y. Wang and Z. Sun, "H_∞ control of networked control system via LMI approach," *International Journal of Innovative Computing, Information and Control*, vol. 3, no. 2, pp. 343–352, 2007.

[129] J. M. Winters, "Telerehabilitation research: Emerging opportunities," *Annual Review of Biomedical Engineering*, vol. 4, pp. 287–320, Aug. 2002.

[130] J. Wu and T. Chen, "Design of networked control systems with packet dropouts," *IEEE Transactions on Automatic Control*, vol. 52, no. 7, pp. 1314–1319, July 2007.

[131] J. Wu, L. Zhang, and T. Chen, "An MPC approach to networked control design," in *Proceedings of the 26th Chinese Control Conference*, Zhangjiajie, Hunan, China, July 2007, pp. 10–14.

[132] F. Xia and Y. Sun, "Control-scheduling codesign: A perspective on integrating control and computing," *Dynamics of Continuous, Discrete and Impulsive Systems - Series B: Applications & Algorithms*, vol. 13, no. S1, pp. 1352–1358, 2006.

[133] L. Xiao, A. Hassibi, and J. P. How, "Control with random communication delays via a discrete-time jump system approach," in *Proceedings of the American Control Conference*, vol. 3, Chicago, IL, USA, June 2000, pp. 2199–2204.

[134] L. Xie, "Output feedback H_∞ control of systems with parameter uncertainty," *International Journal of Control*, vol. 63, no. 6, pp. 741–750, Mar. 1996.

[135] L. Xie, Y. C. Soh, and C. E. de Souza, "Robust Kalman filtering for uncertain discrete-time systems," *IEEE Transactions on Automatic Control*, vol. 39, no. 6, pp. 1310–1314, June 1994.

[136] J. Xiong and J. Lam, "Stabilization of linear systems over networks with bounded packet loss," *Automatica*, vol. 43, no. 1, pp. 80–87, Jan. 2007.

[137] S. Xu and T. Chen, "Reduced-order H_∞ filtering for stochastic systems," *IEEE Transactions on Signal Processing*, vol. 50, no. 12, pp. 2998–3007, Dec. 2002.

[138] S. Xu and J. Lam, "Reduced-order H_∞ filtering for singular systems," *Systems & Control Letters*, vol. 56, no. 1, pp. 48–57, Jan. 2007.

[139] F. Yang, Z. Wang, Y. S. Hung, and M. Gani, "H_∞ control for networked systems with random communication delays," *IEEE Transactions on Automatic Control*, vol. 51, no. 3, pp. 511–518, Mar. 2006.

[140] L. Yang and M. Tomizuka, "Short seeking by multirate digital controllers for computation saving with initial value adjustment," *IEEE/ASME Transactions on Mechatronics*, vol. 11, no. 1, pp. 9–16, Feb. 2006.

[141] S. Yang, X. Chen, L. Tan, and L. Yang, "Time delay and data loss compensation for Internet-based process control systems," *Transactions of the Institute of Measurement and Control*, vol. 27, no. 2, pp. 103–118, 2005.

[142] B. Yu and Y. Shi, "State feedback stabilization of networked control systems with random time delays and packet dropout," in *Proceedings of the 1st Dynamic Systems and Control Conference*, Ann Arbor, MI, USA, Oct. 2008.

[143] D. Yue, Q.-L. Han, and J. Lam, "Network-based robust H_∞ control of systems with uncertainty," *Automatica*, vol. 41, no. 6, pp. 999–1007, June 2005.

[144] D. Yue, Q.-L. Han, and C. Peng, "State feedback controller design of networked control systems," *IEEE Transactions on Circuits and Systems—Part II: Analog and Digital Signal Processing*, vol. 51, no. 11, pp. 640–644, Nov. 2004.

[145] L. Zhang and D. Hristu-Varsakelis, "Communication and control co-design for networked control systems," *Automatica*, vol. 42, no. 6, pp. 953–958, June 2006.

[146] L. Zhang, B. Huang, and J. Lam, "H_∞ model reduction of Markovian jump linear systems," *Systems & Control Letters*, vol. 50, no. 2, pp. 103–118, Oct. 2003.

[147] L. Zhang, Y. Shi, T. Chen, and B. Huang, "A new method for stabilization of networked control systems with random delays," *IEEE Transactions on Automatic Control*, vol. 50, no. 8, pp. 1177–1181, Aug. 2005.

[148] W. Zhang, M. S. Branicky, and S. M. Phillips, "Stability of networked control systems," *IEEE Control Systems Magazine*, vol. 21, no. 1, pp. 84–99, Feb. 2001.

[149] W.-A. Zhang and L. Yu, "output feedback stabilization of networked control systems with packet dropouts," *IEEE Transactions on Automatic Control*, vol. 52, no. 9, pp. 1705–1710, Sept. 2007.

[150] W.-X. Zhao and H.-F. Chen, "Recursive identification for Hammerstein system with ARX subsystem," *IEEE Transactions on Automatic Control*, vol. 51, no. 12, pp. 1966–1974, Dec. 2006.

[151] Y.-B. Zhao, G.-P. Liu, and D. Rees, "Integrated predictive control and scheduling co-design for networked control systems," *IET Control Theory & Applications*, vol. 2, no. 1, pp. 7–15, Jan. 2008.

[152] ——, "Networked predictive control systems based on the Hammerstein model," *IEEE Transactions on Circuits and Systems—Part II: Analog and Digital Signal Processing*, vol. 55, no. 5, pp. 469–473, May 2008.

[153] K. Zhou, J. C. Doyle, and K. Glover, *Robust and optimal control.* Prentice Hall, 1996.

[154] Y. Zhou and J. Li, "Reduced-order $L_2 - L_\infty$ filtering for singular systems: a linear matrix inequality approach," *IET Control Theory & Applications*, vol. 2, no. 3, pp. 228–238, Mar. 2008.

[155] K. Ziaei and N. Sepehri, "Design of a nonlinear adaptive controller for an electrohydraulic actuator," vol. 123, no. 3, pp. 449–456, Sept. 2001.